RESCUING A BROKEN HEART:

A TALE OF TWO MODELS OF NEURAL CREST DEFICIENCY AND ITS IMPACT ON *IN UTERO* HEART FUNCTION AND EMBRYONIC SURVIVAL VIA THE BETA-ADRENERGIC PATHWAY

Michael A. Olaopa

Submitted to the faculty of the University Graduate School
in partial fulfillment of the requirements
for the degree
Doctor of Philosophy
in the Department of Medical and Molecular Genetics
Indiana University

February 2011

Accepted by the Faculty of Indiana University, in partial
fulfillment of the requirements for the degree of Doctor of Philosophy

_____

Simon J. Conway, Ph.D., Chair

_____

Anthony B. Firulli, Ph.D.

Doctoral Committee

_____

Kenneth E. White, Ph.D.

November 3, 2010

_____

Simon J. Rhodes, Ph.D.

Dedication

To my parents, Gabriel and Sophia

My brother, Felix

My sisters, Myra and Juanita

And

Patients of congenital heart defects

All of whom have been my constant source of inspiration

Acknowledgements

I would like to thank my faculty advisor Dr. Simon J. Conway for his support, patience and scientific tutorship during my Ph.D. program. Your mentorship has helped shaped me into a scientist.

I would like to acknowledge the thoughtful and constructive criticism from my committee members: Dr. Anthony B. Firulli, Dr. Kenneth E. White and Dr. Simon J. Rhodes. Your expertise helped mold my thesis into both a successful and meaningful project.

I would like to also acknowledge Dr. R. Mark Payne and Dr. Loren J. Field. Your technical and scientific expertise was invaluable to my project. I also want to thank Dr. Kenneth B. Durgans and Dr. Brittney-Shea Herbert. Your invaluable mentorship and advice came at a time when it was most needed.

I would like to express my appreciation to the faculty and staff of the department of Medical and Molecular Genetics. Thank you for all your guidance and support. Also, I would like to give many thanks to the staff of the University Graduate School for all your assistance during my study.

I would also like to give special thanks to Jian Wang, Dr. Hong-Ming Zhou, Dr. Paige Snider and Mica Gosnell for their respective contributions to my project. Also, current colleagues – Olga Simmons and Rachel Walls – and former

colleagues in the Conway laboratory – Dr. Sunyong Tang, Rhonda Rogers, Goldie Lin, Dr. Kara Standley, Dr. Doug Metcalf and Rachel Young. Thank you all for your guidance, direction and friendship. I also want to give a special thanks to Mark Soonpaa in the Field laboratory for his patience and technical assistance with my project.

Finally, I would like to acknowledge my dear family: my father, Gabriel, for your incredible love, support and prayers; my siblings, Felix, Myra and Juanita, for allowing me to grow in a loving environment surrounded by constant support and trust. Thank you all for your unvarying love, encouragement and belief in my ability to be successful: without which I could not have come this far. I also want to especially remember my mother, Sophia, who is no longer here with us. You are the reason and source of everything good in me. Thank you for living a life that I could only dream to aspire to, and for your insurmountable sacrifice and love, you will always live on in my heart.

Abstract

Michael A Olaopa

RESCUING A BROKEN HEART:
A TALE OF TWO MODELS OF NEURAL CREST DEFICIENCY AND ITS IMPACT ON *IN UTERO* HEART FUNCTION AND EMBRYONIC SURVIVAL VIA THE BETA-ADRENERGIC PATHWAY

Congenital heart defects occur in approximately one percent of births every year, which makes it the most frequently occurring congenital defect in patients. The aim of this project was to use two mutant neural crest (NC) mouse models to study the mechanisms underlying congenital heart failure *in utero*. The first mouse model was a *Pax3* systemic knockout, which was lethal by mouse gestational day 14, and had appreciably reduced numbers of migratory NC cells. The second mouse model was a *Wnt1Cre*-mediated NC genetic cell ablation model, which was surprisingly viable and survived to birth, despite an apparent lack of migratory NC cells. The resultant data indicated that both mouse models had similar heart structural defects including persistent truncus arteriosus, which was due to fewer or no migratory cardiac NC cells. However, *in utero* heart function was appreciably perturbed in *Pax3* mutants when compared to that of the ablated mutant model. The loss of embryonic cardiac function in *Pax3* mutants was directly attributed to a substantial decrease in the activity of the

beta-adrenergic pathway. This was due to a lack of proper specification of trunk NC cells, leading to diminished levels of circulating catecholamine levels in the embryo. To definitively confirm this conclusion, poor cardiac function was successfully restored by pharmacological stimulation of the beta-adrenergic pathway via administration of isoproterenol and forskolin to pregnant dams, which led to embryonic survival of *Pax3* mutants to birth. By comparison of these two mutant mouse models, perturbation in the beta-adrenergic pathway was identified as the underlying mechanism responsible for *in utero* heart failure and lethality in *Pax3* mutant embryos. The results of this study are expected to be significant in developing future therapeutic targets for congenital heart failure in prenatal and newborn patients.

Simon J. Conway, Ph.D., Chair

Table of Contents

List of Tables and Schematics x

List of Figures xi

List of Abbreviations xiii

Chapter I: Introduction 1

1. Neural crest development 1

2. Cardiac neural crest development 4

3. Trunk neural crest development 9

4. *In utero* lethality due to defects in cardiac and trunk neural crests 15

5. Pax3: an important transcription factor 19

6. Hypothesis 23

Chapter II: Pax3 is required during very early neural crest formation and specification for normal cardiogenesis 26

1. Abstract 26

2. Introduction 28

3. Materials and Methods 31

4. Results 35

5. Discussion 44

Chapter III: Beta-adrenergic signaling is essential for maintaining embryonic cardiac output and *in utero* viability 68

1. Abstract 68

2. Introduction 70

3. Materials and Methods 73

4. Results 81

5. Discussion 90

Chapter IV: Discourse 109

1. Review 109

2. Other studies of relevance 111

3. Future studies 114

References 119

Curriculum Vitae

List of Tables and Schematics

Table 1. Measurement via HPLC of catecholamine levels 94

Table 2. Summary of number of pharmacologically rescued *Pax3*$^{d5/d5}$ embryos..... 95

Scheme 1. Cre-inducible lineage mapping using *ROSA26R-LACZ (R26R-lacZ)* reporter/promoter mice..... 48

Scheme 2. Cre-inducible genetic ablation using *ROSA26R-EGFP-DTA* (*R26R-DTA)* reporter/promoter mice 49

List of Figures

Figure 1. Cardiac and trunk NC subpopulations and their derivatives 24

Figure 2. Schematic representation of the sequential changes that occur during remodeling of aortic arch arteries 25

Figure 3. Catecholamine synthesis 25

Figure 4. Characterization of *Pax3*^{d5} allele 50

Figure 5. Ink injection analysis of aortic arch artery formation and remodeling during OFT morphogenesis 52

Figure 6. Lineage mapping of *lacZ* stained CNC and their derivatives (marked via *Wnt1Cre;R26R* reporter) 54

Figure 7. Lineage mapping of *lacZ* stained CNC and their derivatives (marked via *Ap2aCre;R26R* reporter) 56

Figure 8. Genetic ablation of NC lineage in *Wnt1Cre/DTA* mutants 58

Figure 9. NC lineage mapping and AAA analyses in *Wnt1Cre/DTA* mutants 60

Figure 10. *In situ* hybridization analysis of NC markers in *Wnt1Cre/DTA* mutants 62

Figure 11. Analysis of *Pax3*$^{f/d5}$*/Wnt1Cre* conditional knockout 64

Figure 12. Analysis of *Pax3*$^{f/d5}$*/AP2aCre* conditional knockout 66

Figure 13. Structural and molecular analyses of *Pax3*$^{d5/d5}$ mutants 96

Figure 14. *Pax3*$^{d5/d5}$ mutants display insufficient NC-derived PNS structures 98

Figure 15. Tyrosine hydroxylase is significantly reduced in *Pax3*$^{d5/d5}$ mutants but unaffected in *Wnt1Cre/DTA* embryos..... 101

Figure 16. Histological analyses show structural defects in *Pax3*$^{d5/d5}$ mutants remain after isoproterenol treatment 103

Figure 17. Echocardiography analyses show poor cardiac function in *Pax3*$^{d5/d5}$ mutants are rescued by isoproterenol treatment 105

Figure 18. Molecular analyses show molecular defects in *Pax3*$^{d5/d5}$ mutants are rescued by isoproterenol treatment 107

Figure 19: Critical temporal requirement of catecholamines during embryonic development..... 116

Figure 20: *Pax7* can substitute role of *Pax3* in suppression of *Msx2*..... 117

List of Abbreviations

α1c	alpha-1c subunit of the L-type calcium channel
αSMA	alpha-smooth muscle actin
AAA	aortic arch artery
AC5	adenylate cyclase V
ANF	atrial natriuretic factor
AP2a	activating protein type II alpha
B1ar	beta1-adrenergic receptor
B2ar	beta2-adrenergic receptor
BMP	bone morphogenetic protein
BrdU	bromodeoxyuridine
BSA	bovine serum albumin
cAMP	cyclic adenosine monophosphate
CHD	congenital heart defect
cDNA	complementary deoxyribonucleic acid
CNC	cardiac neural crest
d5	delta 5
dAo	dorsal aorta
Dbh	dopamine beta-hydroxylase
DNA	deoxyribonucleic acid
DOPA	3,4-dihydroxyphenylalanine
DORV	double-outlet right ventricle

Drg	dorsal root ganglia
DTA	diphtheria toxin fragment-A
EC	excitation-contraction coupling
EMT	epithelial-to-mesenchymal transformation
ERK	extracellular signal-regulated kinase
Ex	exencephaly
FGF	fibroblast growth factor
GAPDH	glyceraldehyde-3-phosphate dehydrogenase
H&E	haematoxylin-eosin staining
Insm1	insulinoma-associated 1
IRES	internal ribosome entry site
LA	left atria
LV	left ventricle
mRNA	messenger ribonucleic acid
NC	neural crest
Ncx1	sodium-calcium exchanger I
NT	neural tube
NTR	nuclear translocation region
OFT	outflow tract
Pax	paired box family
PBS	phosphate-buffered saline
PCR	polymerase chain reaction
p-erk	phosphorylated-erk

p-pln	phosphorylated-phospholamban
p-trop1	phosphorylated-troponin I
PKA	cAMP-dependent protein kinase A
PNS	peripheral nervous system
PTA	persistent truncus arteriosus
SNS	sympathetic nervous system
RT-PCR	reverse transcriptase polymerase chain reaction
RA	right atria
RV	right ventricle
Ryr2	ryanodine receptor II
Sb	spina bifida
SNS	sympathetic nervous system
Th	tyrosine hydroxylase
TNC	trunk neural crest
Wnt	wingless-type mmtv integration site family

Chapter I: Introduction

1. Neural crest development

Neural crest (NC) cells are a multipotent and transient migratory lineage originating from the neuroepithelium, which borders the surface ectoderm and gives rise to the embryonic neural tube. NC cells can give rise to an array of different cell types, tissues, and organs [1]. For this reason, they are often referred to as the fourth germ layer of the developing embryo, in addition to the ectoderm, endoderm and mesoderm cell lineages. The derivatives of NC are considerably diverse in both function and structure. From the cardiovascular to the peripheral nervous systems, NC cells have been shown to be absolutely essential at very early stages during development for normal organogenesis to occur. In addition, they are important during *in utero* craniofacial, melanocyte, and gastrointestinal development, as well as postnatally as NC stem cells [2].

Different subpopulations of NC have been identified based on their rostrocaudal position of origin along the axis of the developing embryo, their specific properties, and the nature of their derivatives. The developing neural tube extends in a rostral to caudal direction beginning at the mid-diencephalon. As a result, NC cells have been broadly subdivided into cranial, cardiac, trunk and sacral NC's. In mouse, the cranial and cardiac NC cells originate from the mid-diencephalon to the fifth somite [3, 4]. Furthermore, the trunk and sacral NC cells

begin from the fifth somite to the caudal region of the neural tube [5]. In addition to location, the cranial and trunk NC's also differ in functional properties. For instance, the cranial NC is ectomesenchymal, which means that it has the ability to give rise to mesenchymal derivatives, while the trunk NC does not. Alternatively, the trunk NC has the ability to regenerate, while the cranial NC does not. Interestingly, the cardiac NC originates from the mid-otic sulcus (the presumptive ear) to the third somite, which represents the caudal region of the cranial NC directly rostral to the beginning of the trunk NC [6]. As a result, the cardiac NC shares some properties of both cranial and trunk NC's, including their respective abilities to generate ectomesenchyme and regenerate [5]. This project focuses primarily on the roles of both cardiac and trunk NC's, and their importance to organ development. Specifically, I have explored their respective contributions to the cardiovascular and peripheral nervous systems, with emphasis on their functional and structural roles in cardiac and sympathoadrenal differentiation and stabilization (Figure 1).

1.1. Neural crest formation and specification

It is generally believed that the neural plate can induce formation of NC cells via interaction with the adjacent epidermis. Experiments done in avian embryos [7] demonstrated effectively that early or late stage neural plate tissue could give rise to NC cells. Furthermore, this induction occurred via interaction between the neural plate and the non-neural ectoderm. Although NC cells originate from a subpopulation of cells located between the developing neural and non-neural

ectoderm, studies have shown that these cells can give rise to other cell types as well, indicative of a higher developmental potential [8]. Thus, this suggests that signaling from the neural plate is important in initial induction and formation.

Several families of proteins have been shown to be important in initial NC formation, including the BMP, FGF and Wnt families. BMP4 is expressed within the epidermis at the border of the neural plate, and several studies have demonstrated that BMP4 is important in early NC induction. BMP4 has been shown to be absolutely required for cultured neural plates to induce NC, even in the absence of ectoderm [9]. In addition, beads soaked with noggin, (a BMP antagonist) when placed in the region of the epidermis that borders the neural plate, leads to its expansion [8]. In *Xenopus*, FGFs may be required to induce mesoderm, from which NC can be induced [10]. However, the exact role of FGF signaling in NC induction is still being determined. Some studies have suggested that FGF signaling acts directly through modulation of noggin in order for early NC induction to occur [11]. Furthermore, Wnt activity has been shown to play a role as well. In the absence of Wnt signaling in chick embryos, neural crest marker expression is diminished or completely eliminated [12]. It is believed that initial Wnt expression is required for NC induction, and then subsequent downregulation of Wnt must occur in order for the NC cells to delaminate from neural tube. This downregulation may also be regulated by a BMP-dependent pathway [13].

2. CNC development

The CNC is a subpopulation of NC that contributes to heart morphogenesis. In addition to providing all of the parasympathetic innervation of the heart [14], migratory CNC also contribute to the smooth muscle cells that surround the aortic arches and the mesenchymal cells that colonize the OFT. Thus, improper specification or migration of CNC can lead to abnormal regression/persistence of AAA's [5], which results in OFT defects such as PTA/VSD (Figure 1).

2.1. AAA asymmetric remodeling

Aortic arch arteries develop from endothelial strands within the arches, and connect the aortic sac and the dorsal aortas. In chick embryos, they begin as six symmetric pairs of arteries attached to the paired dorsal aorta. However, in mammals, there are only five symmetric pairs, which are remodeled to give rise to a separate ascending aorta [15]. Well-established reports [16] have clearly demonstrated that the cranial NC gives rise to $1^{st}/2^{nd}$ AAA, while CNC cells migrate and colonize $3^{rd}/4^{th}/6^{th}$ AAA [17]. This occurs on their way to colonizing the aorticopulmonary septum of the OFT, where they coalesce into ridges of connective tissue [6]. Interestingly, the CNC cells are not required for the initial formation of the aortic arches, but are important for their final patterning [18] and stabilization [19]. These CNC cells migrate into each arch as it successively forms and then surround the endothelial cells that form the emerging arches. The role of CNC in stabilizing the arches is a very important one. In fact, stability of

target tissues and vessels appears to be a common function of both cardiac and trunk NC.

In order for proper AAA remodeling to occur, the arteries must undergo a series of asymmetric regression and persistence (Figure 2). The 3rd arch arteries give rise to common carotid arteries, 4th arch arteries contribute to the formation of the distal part of the aortic arch, the brachiocephalic artery and a proximal part of the right subclavian artery, while the left 6th arch arteries contribute to the ductus arteriosus and the proximal parts of the pulmonary arteries [2]. In addition, the parathyroid and thyroid glands are derived from the endoderm of the third arches via interaction with cardiac NC cells [20]. Reciprocal interactions between the migratory cardiac NC cells and the surrounding endothelial cells of the arches have been shown to be important in arch artery remodeling as well. *Endothelin-1* (*ET-1*), which is expressed in the surrounding endothelial cells of the arches but not in the migratory CNC cells, has been shown to be involved in a complex signaling pathway that is required for normal arch remodeling to occur [21]. The migratory CNC cells are known to express *ET-A* (ET-1 receptor), and it is believed that proper signaling between the arches and the CNC cells as they migrate through them is important [5, 6] in order to have proper remodeling. Furthermore, mouse embryos which are deficient for either *ET-1* or *ET-A* display defects in arch remodeling and alignment. Specifically, there is regression of arches 4 and 6, and these mice eventually die from other heart-related defects.

Certain growth factors have also recently been implicated in the remodeling process. Specifically, endothelial-specific expression of platelet-derived growth factor alpha (PDGFα) and activated (phosphophorylated) vascular endothelial growth factor receptor 2 (VEGFr2) have been shown to be important in the cells surrounding the left 6th arch artery, which continues to persist even as the right 6^{th} arch regresses [22]. This expression of growth factors was shown to be maintained by unilateral distribution of blood flow. It is still unclear what role CNC cells may play in this signaling pathway. However, CNC cell-specific expression of platelet-derived growth factor receptor alpha (PDGFrα) has been shown to be important in regulating smooth muscle cell differentiation [23], which surround the arches and play an important stabilization role. In addition, asymmetric expression of *Pitx2* in the aortic arch mesoderm has been shown to be important for normal remodeling to occur. Loss of *Pitx2c* results in abnormal remodeling of the aortic arch vessels [24], due to poor communication between CNC cells and the endothelial cells surrounding the arteries. This provides another example of the importance of signaling between the CNC cells and the adjacent surrounding endothelial cells for proper AAA development and eventual OFT remodeling.

2.2. OFT formation and remodeling

The OFT is a common vessel exiting the heart, which during cardiac development is septated into the pulmonary artery and aorta. This leads to proper separation of pulmonic and systemic blood flow. Before septation, as a common vessel, it branches at the aortic sac into aortic arches 3, 4 and 6 [2, 5,

18]. CNC cells are known to play an important role in giving rise to the aorticopulmonary septum, which eventually divides the OFT. Extensive studies on the migration and colonization of the OFT by cardiac NC cells is now possible with the advent of transgenic mouse *Cre* lines, which allow *Cre/loxP*-mediated lineage traces to be performed. Several transgenic mouse *Cre* lines are now used to study cardiac NC cell migration, including the *P0-cre, Wnt1-cre*, *Pax3-cre*, and *PlexinA2-cre* lines [4, 25, 26]. Based on these studies, we now have a more comprehensive image of the structural contribution of CNC cells and their derivatives to the OFT.

The OFT cushions are initially acellular, and then become filled with cardiac jelly derived from a mixture of mesenchymal cells that migrate from the pharynx and endocardially-derived cells that have undergone epithelial to mesenchymal transformation. CNC cells also contribute to this mesenchymal population, by migrating via a pair of horseshoe-shaped prongs or condensed streams into the distal region of the OFT. In mouse, the CNC cells do so via a subendocardial route, and they continue all the way to the distal conus of the OFT [2, 5]. During development, this CNC cell-derived mesenchymal population is gradually replaced by myocardium in a process known as myocardialization [27]. Myocardialization of the proximal OFT is important to form the muscular outlet septum of the heart and the atrioventricular canal septum. This process is believed to be regulated by Wnt family of proteins [28] via the Wnt-PCP pathway. These studies demonstrated that growth factors such as Wnt5a and Wnt11 are

required to be expressed in the OFT cushion mesenchyme in order for normal myocardialization to occur [29]. In addition, to the Wnt family, BMP and FGF family of proteins have been shown to be required in conjunction with other factors to induce normal myocardialization [30].

The Wnt pathway has also been implicated in regulating the process of cell death of a subset of these CNC cells, which contribute to the conotruncal cushions. After septation is complete, they are believed to eventually undergo apoptosis [31]. These cells transiently express a Wnt receptor *Frizzled-2* [32], suggesting a role in remodeling and patterning during septation. However, it is believed that some CNC cells can persist even after birth [4, 33], despite the massive apoptosis and rearrangement of cardiomyocytes that occurs after septation and during myocardialization. In addition to septation of the OFT, cardiac NC cells are also important in its elongation and eventual looping and correct alignment. Besides providing a structural framework for the outflow septum, the cardiac NC cells are also believed to be important in regulating cell-cell signaling between the pharynx, during addition of cells derived from the anterior heart field (AHF) to the OFT. In conjunction with these AHF-derived cell lineages, cardiac NC cells play a role in OFT elongation [34]. The derivatives of the AHF give rise to the myocardial cuff of the OFT, while the CNC cells give rise to the mesenchymal cell population in the cushions. As cells continue to be added to the caudal end of the OFT, the endocardial cushions spiral, leading to rotation of the outflow

septum and eventual realignment of the aorta in a posteriolateral direction and the pulmonary artery in an anteriomedial direction [35].

Despite the significant progress that has been made regarding the structural and functional roles of cardiac NC cells in OFT remodeling, elongation and septation, still very little is known about what molecular factors are expressed within these cells post-migration as they undergo differentiation within the OFT cushions. The identification of a post-migratory marker of CNC cells will be both a significant and transformative discovery in the field of cardiovascular development. This could open the door to designing potential therapeutic targets for congenital heart defects and OFT remodeling anomalies associated with aberrant gene expression. Currently, there are several strategies being used to address this question, including the use of laser-capture and cell-sorting technologies to isolate and screen expression profiles of cells located in the cardiac crest-derived distal region of the OFT.

3. TNC development

The TNC cells, which give rise to elements of the sympathoadrenal lineage take the dorsoventral migration route, passing mainly through the anterior parts of the somites [36]. During their migration they are exposed to signals from the somites, the ventral neural tube and the notochord. They aggregate in the vicinity of the

dorsal aorta, where they form the so-called primary sympathetic ganglia and undergo neuronal and catecholaminergic differentiation

TNC cells encounter a variety of transient structures, which undergo their own remodeling, as the cells emigrate from the dorsal neural tube and migrate into the periphery. They do so in three stages – early, mid and late stage – and these are controlled by a tightly regulated expression of specific molecular factors [37, 38]. During the early stage of migration, NC cells emigrate ventrally between the neural tube and the somites along intersomitic vessels. At this stage, the NC cells express type2 neuropilin (Nrp2), while the presumptive dermomyotome within the somites express type3A semaphorin (Sema3A). As this occurs, the epithelial somites will dissociate to give rise to dermomyotome and the eventual sclerotome. This dissociation is believed to be caused by an upregulation of Nrp1 within the trunk NC [37, 39].

In the middle phase of migration, a subset of TNC cells migrate dorsolaterally or ventrolaterally (in mouse and chick, respectively) into the rostral sclerotome, while the remaining cells aggregate at the dorsal aortae. Low levels of Sema3A and Sema3F expression in the caudal sclerotome, but mainly Sema3A in the dermomyotome, are important in repelling the NC cells at this stage from the intersomitic space [40]. This leads to restriction of the NC cells to only the rostral sclerotome [41].

Finally, during late-stage migration, the subset of TNC cells that invaded the somites aggregate to form the segmented dorsal root ganglia. This is due to downregulation of Sema3F in the caudal sclerotome and a corresponding upregulation of Sema3A [42]. Alternatively, the subset of TNC cells that goes on to colonize the dorsal aortae is induced along the sympathoadrenal lineage, and begins to aggregate into the primary sympathetic ganglia.

3.1. Sympathetic nervous development

There are two major schools of thought regarding TNC induction and specification into the sympathoadrenal cell lineage. One proposal is that both the sympathetic precursors, which give rise to neurons in the sympathetic ganglia, and the chromaffin cells, which give rise to the adrenal lineage, originate from a the same homogenous population of cells. However, more recently, it has been proposed that these two lineages may originate from two different pools of precursors which determine which subpopulations of NC cells colonize the dorsal aorta and which ones migrate onwards into the adrenal anlage [43, 44].

A major player in TNC induction is the BMP family of proteins [43]. It is believed that as NC cells migrate pass the dorsal aorta, they are inducted by BMP signaling to develop into sympathoadrenal precursors. In addition to BMP signaling, expression of other factors such as Gata3, Phox2b and Mash1/2 have been shown to be important for proper specification of the NC along both the sympathetic and adrenal lineages [45]. However, in both cases, induction is

believed to occur both along the neural tube and migratory pathway, and finally at the site of colonization at the dorsal aortae. Despite the fact that adrenergic markers such as tyrosine hydroxylase (Th) are not seen to be expressed until the TNC colonize the dorsal aortae, the tissues lining the migratory pathway clearly play a role in inducing TNC along the sympathoadrenal lineage [46].

It is now believed that the notochord, ventral neural tube and somitic mesoderm are all important in inducing adrenergic differentiation in TNC cells. This was demonstrated by a number of explant experiments done in chick embryos [47] and ablation experiments involving the removal of both notochord and ventral tube, which inhibited differentiation of trunk NC cells into sympathetic ganglia [48]. According to other similar experiments, which also involved removal of notochord and neural tube, induction at the site of colonization of the dorsal aortae is still dependent on proper expression of earlier factors along the migratory pathway [46].

3.2. Sympathetic ganglia colonization

The formation and colonization of sympathetic ganglia occurs in three major stages – migration, desegmentation and resegmentation. Initially, migratory trunk NC cells migrate segmentally from the dorsal somite towards the dorsal aorta. They are guided by a complementary series of receptor expression and their corresponding ligands. Properly specified TNC cells will intrinsically express ErbB2, ErbB3 and CXCR4 receptors [37]. This is important in providing guidance

cues to the crest cells as they migrate through the dorsal somite, which expresses receptor-specific ligands such as neuregulin (ligand for ErbB2, ErbB3 receptors) and CXCL12 (ligand for CXCR4 receptor). In addition to these guidance cues, the dermomyotome and notochord also express Sema3A which is important in repelling TNC cells via signaling with Nrp1, which is expressed in the crest [40]. As a result of a combination of repulsion and attraction cues, the trunk NC cells are able to migrate through the dorsal somite toward the dorsal aorta.

The second and third stages occur at the site of the dorsal aorta, and involve the segmental state of the migratory TNC cells. As they colonize the aorta, they become desegmented, allowing them to diffuse along the outer wall. At this stage, segmental populations of trunk crest are indistinguishable from each other based solely on their location. However, once the crest cells are evenly dispersed along the aorta, they undergo resegmentation, allowing the formation of the metameric sympathetic ganglia [37].

3.3. Adrenal formation

In the mouse, adrenal development begins at E11.5, which is at least two days post-delamination of TNC from the neuroepithelium. The adrenal gland is formed from an adrenal primordium located along the urinogenital ridge of the developing embryo. TNC cells are important in forming the medulla of the adrenals, which is surrounded by a multilayered mesoderm-derived cortex. The

cortex is formed by budding from the coelomic epithelium between the mesogastrium and the urogenital fold. Alternatively, the medulla is composed of chromaffin cells and ganglion cells, which produce and circulate catecholamines respectively.

During development, TNC cells that have been fated to differentiate along the sympathoadrenal lineage migrate from the dorsal neural tube to the adrenal primordium. Certain transcription factors, such as those belonging to group E of the Sox protein family (SoxE), including Sox8, Sox9 and Sox10, may be important during the process of adrenal gland formation [44]. During migration from the neural tube, as described earlier, TNC pass by the anterior region of the somites and a subset of these cells will colonize the sympathetic ganglia located adjacent to the dorsal aorta. In the mouse, by E12.5, the trunk crest has already colonized the adrenal medulla, and formation of both the medulla and cortex is completed by E15 [49].

Expression of Sox8 and Sox9 begins before the TNC cells have delaminated from the neural tube, and it is believed to be important in early specification [50, 51]. However as they undergo delamination from the NT, Sox9 is downregulated in favor of induction of Sox10, which maintains expression throughout migration of the TNC and their eventual colonization of the adrenal medulla, where it is co-expressed with Sox8 [52, 53]. Recent studies suggest that Sox10 is very important for normal adrenal development [44]. Sox10-deficient mice did not form

an adrenal medulla, due to lack of TNC cells colonizing the adrenal anlage. These findings is consistent with earlier studies [54] showing that dominant-negative expression of Sox10 in mice resulted in no adrenal formation. Alternatively, despite expression of Sox8 within the medulla, Sox8-deficient mice did not have significant defects in adrenal formation, except when placed on a Sox10 hypomorphic background [44].

In addition to regulating TNC cell survival, Sox10 may also be important in their differentiation, as the reduced number cells in mutant mice around the dorsal aorta lacked proper specification and eventually underwent apoptosis. These cells lacked proper expression of Phox2b and Mash1, indicative of a previously suggested role of Sox10 in induction of molecular factors important in the establishing and maintaining the sympathoadrenal lineage [55, 56].

4. *In utero* lethality due to defects in cardiac and trunk neural crests

4.1. *In utero* lethality associated with CNC

Myocardial defects associated with CNC have been an interesting conundrum in the field of cardiovascular development. This is primarily because CNC cells are not believed to directly contribute to the myocardium of the developing heart. However, quite a few animal models of NC have been found to have problems with myocardial function. One of the earliest models was studied in chick embryos, in which the NC had been surgically ablated [14]. These embryos, in

addition to classic NC-related defects, also displayed signs of myocardial dysfunction and died before birth [57]. Specifically, they had depressed calcium transients, problems with excitation-contraction coupling and low ejection fraction.

In mouse, embryos homozygous for the *Splotch* (Sp^{2H}) mutation in the *Pax3* gene display similar conotruncal anomalies associated with cardiac NC malformations [58]. However, these embryos also die by mid-gestation due to apparent poor cardiac output [59, 60], and exhibit similar myocardial-related defects to the chick-ablation model. In *Splotch* embryos, there is a failure of CNC to populate the arches and OFT septum in proper numbers [19]. However, unlike the ablation model, there are still some CNC-derived cells that make it into the aorticopulmonary septum.

There has been some suggestion that CNC cells are required to mediate growth factor signaling between the OFT myocardium and the ventral pharyngeal endoderm. Specifically, studies have reported FGF signaling to be important for normal elongation and remodeling [61]. Continuous expression of FGF2 and FGF8 in the ventral pharyngeal endoderm can be detected as cardiac NC cells are still migrating and before they reach the OFT myocardium. In chick embryos, FGF upregulation occurs prior to the arrival of cardiac NC cells in the OFT. Conversely, haploinsufficiency of *FGF8* in embryonic mice also results in OFT alignment defects including PTA [62, 63] due partly to an increase in CNC cell

apoptosis. This suggests regulated FGF8 expression in the pharyngeal endoderm is important in both OFT development and perhaps myocardial stability. Interestingly, reduction of FGF signaling in chick embryos that have undergone CNC ablation is sufficient to normalize abnormal calcium transients reported earlier [61]. Furthermore, backtransplantation of CNC cells into NC-ablated chick embryos is able to normalize calcium transients and partially rescue the myocardial phenotype [5, 61]. To our knowledge, FGF signaling has not been comprehensively studied in the *Splotch* mouse model. However, it is believed that CNC cells are important in mediating signaling to the myocardium of the developing heart, which must be required for normal cardiac function and output.

4.2. *In utero* lethality associated with TNC

Similarly, there are a number of animal models of TNC that have been shown to be associated with myocardial defects. Perhaps, the most significant model reported is that of the *tyrosine hydroxylase* (*Th*) knockout mice. Tyrosine hydroxylase is an enzyme important in the catalytic conversion of L-tyrosine to DOPA (a catecholamine intermediate) in the catecholamine synthesis pathway (Figure 3) that leads to production of norepinephrine and epinephrine (adrenaline). *Th* null mice are embryonic lethal by E11-15 [64, 65]. Although they appear grossly normal, the embryos displayed congestion of blood in the liver and atrial wall thinning. Furthermore, they had slight bradycardia and disorganization of ventricular cardiomyocytes. Since TNC cells do not contribute

directly to the cardiomyocyte cell population, the observed cardiac defects proved to be an even more significant result. The authors postulated that the observed lethality was due to a catecholamine deficiency caused by failure of TNC to properly give rise to developing sympathetic neurons, adrenal chromaffin cells and enteric neurons. They confirmed this by feeding pregnant dams with L-DOPA and were able to rescue at least 50% of mutant embryos to term, even though the rescued mutants were severely runted and died within a few weeks after birth. They also observed similar results in *dopamine beta-hydroxylase* (*Dbh*) knockout mice. Dbh is also involved in later stages of catecholamine synthesis, by catalyzing conversion of dopamine to norepinephrine (Figure 3). However, since the observed lethality occurred before cathecolaminergic neurotransmission is completely established, the study postulated that catecholamines probably act in a paracrine manner at these early stages [64-66].

In addition to the *Th* knockout mice, the *Gata3* knockout mouse model has been quite informative in this regard. These mice are also embryonic lethal by mid-gestation, and display deficiencies in Th, Dbh and noradrenaline [67]. The mutants were also rescued to birth by administration of DOPS (a synthetic catecholamine intermediate) to the pregnant dams. Similar to the *Th* knockouts, these mutants were also reported to have loosely organized cardiomyocyte structure, as well as blood congestion in the heart, and had poorly developed neural crest-derived structures. However, the authors were unable to conclusively link the exact role of Gata3 in Th/Dbh activity and subsequent heart

failure in these mutants. Based on subsequent *in vitro* studies, it is now believed that Gata3 can directly bind to the *Th* promoter and regulate its transcription [68].

More recent studies, have suggested that while expression of Th and Gata3 within the TNC may be required for normal sympathetic neuron development, expression of much earlier molecular factors are important in determining their noradrenergic identity. Hand2 has been shown to be required for early specification of the noradrenergic cell lineage. Conditional deletion of Hand2 within the neural crest leads to embryonic lethality by mid-gestation and severe cardiovascular defects [69]. These mutants displayed reduced specific reduction in the expression of Th and Dbh. However, it concluded that Hand2 regulation of both Th and Dbh expression is independent of Gata2/3, Phox2a/b and Mash1, which are markers of sympathetic neuronal differentiation [70-72], but are all normally expressed in these mutants.

5. Pax3: an important transcription factor

Pax3 (paired box 3) is a transcription factor belonging to the Pax family of proteins. They get their name from the fact that all members contain a paired box domain and a paired-type homeodomain involved in DNA binding and regulation of downstream targets. A number of different syndromes in humans are implicated by mutations in *Pax3*. Two such syndromes are Waardenburg syndrome (WS) and DiGeorge syndrome (DGS).

Patients with WS have a range of features including sensorineural deafness, pigmentation anomalies (white forelock, forehead), and abnormalities in skeletal and neurological development [73, 74]. WS has a prevalence of 1 in 15000 within the general population, and it has been observed to be as high as 1 in 30 students in schools for the deaf. Although the *Pax3* gene is located on human chromosome 2q35 [75, 76], it has also been implicated in DGS. Patients with DGS display the CATCH 22 phenotype (cardiac defects, abnormal facies, thymic hypoplasia, cleft palate, hypocalcaemia; associated with microdeletion on chromosome 22q11). Cardiac defects include interrupted aortic arch, PTA, and other arch artery defects. There are a considerably high proportion of patients with these cardiac defects, who also carry the microdeletion [77]. The general prevalence is about 1 in 6000 births, which makes it a fairly common syndrome. The microdeletion varies from patient to patient, but can encompass as much as a 3-million base-pair deletion, and as many as 30 genes have currently been identified. *Pax3* is believed to have a cooperative or interactive role with some of these genes, and thus, patients with mutations in *Pax3* also display similar features of DGS.

5.1. Role as both an effector and regulator

Pax3 expression diminishes in a rostrocaudal direction along the axis of the neural tube and as NC cells begin to emigrate. Based on avian studies, this may be modulated by BMP4, which has been shown to be capable of maintaining

ectopic Pax3 expression at late post-delamination stages in the embryo [78]. Several models have been designed to further study the effects of BMP signaling on cardiac development. BMP2 and BMP4 have been shown to be important for neural crest induction, migration and differentiation. Mice deficient for *Bmpr1a* receptor within the NC display OFT and arch artery remodeling defects [79]. These mice also die mid-gestation due to apparent heart failure.

Another molecular factor that has recently been shown to be a direct downstream effector of *Pax3* within the NT is *Msx2* [80]. *Msx2* is a homeobox gene and is also involved in regulation of BMP signaling. Mice deficient for *Msx2* are viable, but have cranial defects including problems with skull ossification, calvarial bones, and teeth formation [81]. Interestingly, *Msx2* has been shown to be upregulated in *Splotch* mutants, and a loss of function *Msx2* mutation in the *Pax3* homozygote background rescues the previously described cardiac defects [80].

5.2. Role in NC and heart development

As a transcription factor, *Pax3* is involved in numerous developmental processes. In mice, *Pax3* expression begins by E8 [82]. It is expressed in the dorsal neural tube, including but not restricted to NC progenitors, and somites (musculature) of the developing embryo. It is involved in formation of myogenic precursors [83], peripheral nervous system and melanocyte differentiation [84], and most importantly, early CNC cell formation and delamination from the neural tube. Its

expression diminishes as the CNC cells colonize the arches and is completely gone in the OFT [85].

Splotch homozygote embryos display neural tube and NC-related defects, including PTA and accompanied interventricular septal defect [15, 58, 60, 85], but surprisingly die by embryonic day 14. However, it is unclear why *Pax3* mutant embryos fail to survive past the mid-gestation. As mentioned earlier, embryonic lethality had previously been postulated to be due to poor cardiac function and output secondary to myocardial defects [15, 59]. Transgenic rescue studies using a well-defined 1.6kb *Pax3*-promoter [86] showed restricted re-expression of *Pax3* in the NT and NC in a *Pax3* null background was sufficient to rescue the cardiac phenotype. Not only was PTA rescued, but these mice also survived to birth. However, they still had musculature defects and eventually died due to respiratory failure shortly after birth. From these studies, it is now clear that restricted *Pax3* expression within the NT and perhaps the NC specifically, may be important in maintaining normal cardiac function and output in the developing mouse embryo. However, the underlying cause of embryonic lethality in *Pax3* mutants is still unknown.

6. Hypothesis

The observed mid-gestation lethality in *Pax3* mutant embryos led me to examine the underlying cause of poor cardiac function and embryonic death. This was particularly because PTA/VSD (the major heart defect of *Pax3* mutants) is not sufficient to cause embryonic death, nor is Pax3 protein known to be expressed in the heart. Therefore, I proposed to compare the specific consequences of *Pax3*-deficient migratory NC cells on AAA and OFT remodeling and determine the secondary effects this may have on embryonic cardiac output. To do this, I used two mouse models of NC-deficiency. The first mouse model was a *Pax3*-deficient model, which was lethal by E14, and had appreciably reduced numbers of migratory NC cells. The second mouse model was a NC-ablated model, which was surprisingly viable and survived to birth, despite an apparent lack of migratory NC cells. I hypothesize that having *Pax3* mutant CNC, albeit in fewer numbers (as is the case in *Pax3*$^{-}$ mutants), is more detrimental than complete absence of wildtype CNC (as is the case in the NC-ablated model).

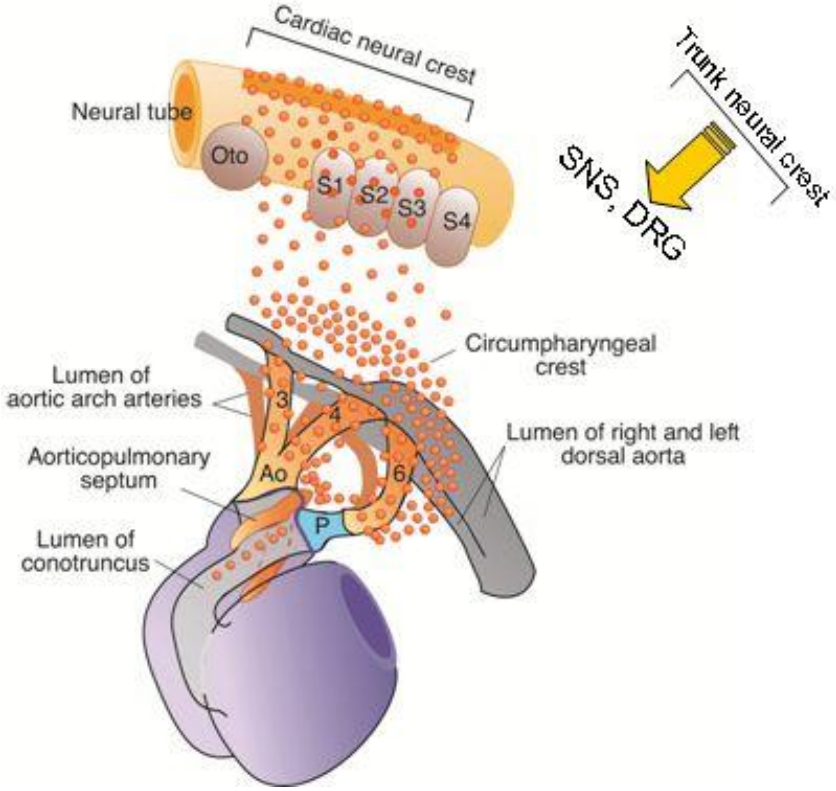

Figure 1: Cardiac and trunk NC subpopulations and their derivatives.

Adapted from [5].

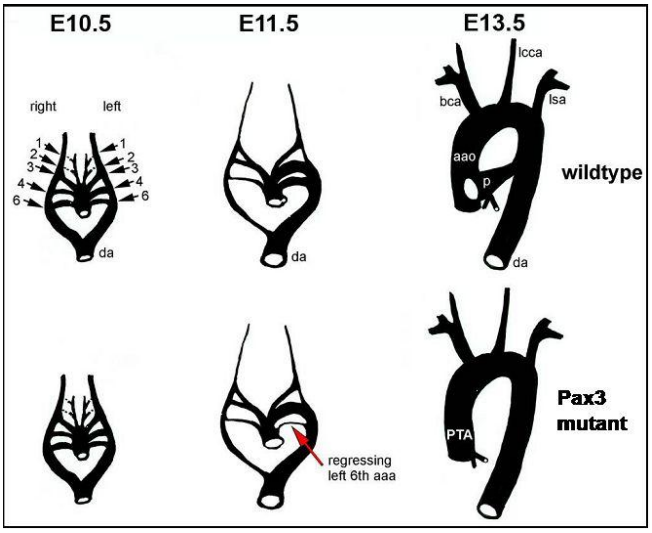

Figure 2: Schematic representation of the sequential changes that occur during remodeling of aortic arch arteries. Adapted from [2, 15].

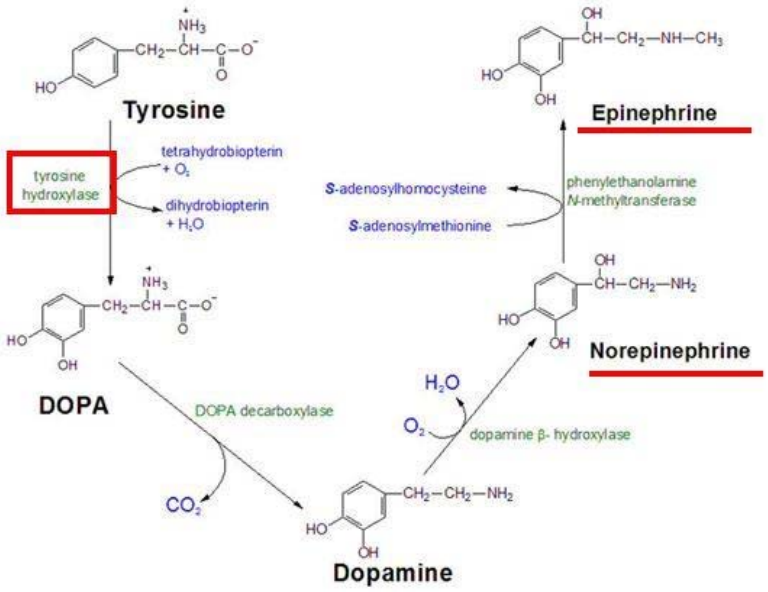

Figure 3: Catecholamine synthesis. Adapted from image obtained from http://themedicalbiochemistrypage.org/nerves.html.

Chapter II: Pax3 is required during very early neural crest formation and specification for normal cardiogenesis

1. Abstract

Pax3 is a transcription factor that is important in regulating several developmental processes during embryogenesis. Its restricted expression to the dorsal NT, premigratory NC and somitic mesoderm has allowed for several loss-of-function studies to be performed. However, to address the NC-specific requirement of Pax3, a floxed Pax3 allele was generated. This allowed for both systemic and conditional knockout studies to be carried out via selective Cre-mediated recombination. NC lineage mapping studies revealed that systemic Pax3 mutants phenocopy the previously published *Splotch* (Sp^{2H}) homozygous phenotypes, including AAA remodeling defects, PTA/VSD, and mid-gestation lethality by embryonic day 14. This abnormal remodeling is due to insufficient CNC colonizing the AAA's and OFT region of the developing heart. However, NC-specific deletion of Pax3 using both *Wnt1Cre* and *Ap2aCre* failed to fully recapitulate these defects, and these embryos survived to birth. In order to assess the tissue-specific contribution of CNC to heart development, genetic ablation of NC using a *Wnt1Cre*-activated *ROSA26*-diphtheria toxin fragment-A (*Wnt1Cre/DTA*) cell-killing system was performed. Ablation of *Wnt1Cre*-expressing NC generated fully penetrant PTA/VSD defects similar to the Pax3 systemic mutants. However, astonishingly, ablated mutants survive to birth (well

past the E14.0 lethality observed in systemic Pax3 mutants) similar to the conditional Pax3 mutants. Taken together, these data suggest that Pax3 is important in early neural crest specification and formation prior to the expression of both *Wnt1Cre* and *Ap2aCre*.

2. Introduction

The NC is a multipotent, undifferentiated population of cells, which are derived from the region of the neuroepithelium that borders the surface ectoderm of the NT [1]. They contribute to the development of several different tissue and organ types in the mammalian embryo including the PNS (neurons, sensory ganglia, sympathetic/parasympathetic ganglia/plexus and Schwann cells); endocrine derivatives (adrenal medulla, calcitonin-secreting and carotid body cells); melanocytes, facial cartilage/bone/teeth papillae and elements of the great arteries/OFT. They do so in four steps, which include proper formation and specification, delamination from the neural folds via epithelial-to-mesenchymal transformation, migration to their target tissue and, finally, differentiation and colonization [4, 6]. Defects in one or more of these steps have been implicated in several CHDs [5, 35]. This is because a subpopulation of NC, known as the CNC has been shown to be important in contributing to heart morphogenesis and remodeling.

Based on lineage mapping studies done in mouse, it has now been conclusively shown that the CNC is derived from the region corresponding between rhombomeres 5 - 8 [2, 4, 25, 26]. In addition to providing all of the parasympathetic innervation of the developing mammalian heart [14], migratory CNC also contribute to the smooth muscle cells that surround the aortic arches and the mesenchymal cells that colonize the OFT. They migrate through the

pharyngeal arches 3, 4 and 6 [17], on their way to colonizing the OFT where they coalesce into ridges of connective tissue [6]. Importantly, the CNC are not required for the initial formation of the AAA's, but are required for their final patterning [18]. The CNC cells migrate into each arch as it successively forms where they surround the endothelial cells that form the emerging AAA's. Thus, improper specification or migration of CNC can lead to abnormal regression/persistence of AAA's [5], which results in OFT defects such as PTA/VSD.

Pax3 is a transcription factor that is involved in numerous developmental processes including cardiac development. In mice, *Pax3* expression begins ~ E8 [82]. It is expressed in the dorsal NT (including but not restricted to NC progenitors) and somites (musculature) of the developing embryo. It is involved in early NC migration and formation/migration of myogenic precursors [83], PNS, and involved in melanocyte differentiation [84]. Previously published Pax3 homozygote *Splotch* mutant embryos display NT (spina bifida, exencephaly) and NC-related defects. They also display absent limb and hypaxial muscles. In the heart, these mice exhibit 100% PTA/VSD and AAA remodeling defects [58, 85] and die by E14.0. Previous transgenic rescue studies using a 1.6kb *Pax3*-promoter ($Pax3^{1.6kb}$) showed re-expression of *Pax3* in the NT/NC alone in a *Pax3* null background was sufficient to rescue the heart phenotype [86]. Not only was PTA rescued, but these mice also survived to birth. However, they still had musculature defects and eventually died due to respiratory failure. Thus, it is

clear that *Pax3* expression in NT/NC is important in maintaining normal heart function in the developing mouse embryo. However, since *Pax3* is not expressed in the heart, its role in heart development is most likely linked to its role in NC development.

To address this possibility, a novel *Pax3* allele was utilized [87], which allowed for the generation of both homozygote systemic Pax3 delta-exon5 (*Pax3*$^{d5/d5}$) knockout and conditional Pax3 (*Pax3*$^{f/d5}$*/Wnt1Cre* and *Pax3*$^{f/d5}$*/Ap2aCre*) knockout mice. These mouse lines were then compared to the *Wnt1Cre/DTA* mouse, which allowed for permanent, genetic ablation of the *Wnt1Cre*-expressing NC lineage in the developing embryo. The results of this project provide more insight into understanding the role that Pax3 plays intrinsically within the CNC in both AAA and OFT remodeling. Specifically, these results suggest that Pax3 plays an early role in NC formation and specification, but is not required for the secondary stages of NC development involving its migration and colonization.

3. Materials and Methods

3.1. Mouse colonies, breeding, genotyping and PCR

The *Pax3* floxed conditional allele was generated as previously described [87, 88]. Exon 5 of the *Pax3* gene, which encodes the Pax3 homeodomain, was flanked by 5' and 3' *loxP* sites. This allowed for Cre-mediated removal of the floxed *Pax3* homeodomain. To selectively remove the floxed allele in the germline, adult male heterozygous floxed Pax3 ($Pax3^{f/+}$) mice were crossed to female C57Bl6/129 *Tie2Cre*-positive females to generate heterozygous delta exon 5 Pax3 ($Pax3^{d5/+}$) adult mice. The resultant $Pax3^{d5/+}$ males were crossed to wildtype C57Bl6/129 females to remove the *Tie2Cre* transgene. $Pax3^{d5/+}$ (*Tie2Cre*-negative) mice were then intercrossed to generate $Pax3^{d5/d5}$ mutant embryos. Furthermore, adult $Pax3^{d5/+}$ (*Tie2Cre*-negative) were crossed to adult homozygous $Pax3^{f/f}$ mice to generate adult heterozygous $Pax3^{f/d5}$. PCR screening strategy was used as previously described [88]. The $Pax3^{f/d5}$ and $Pax3^{d5/+}$ mice were then crossed into both the *Wnt1Cre* mouse [4] and *Ap2aCre* mouse (generous gift from Anne Moon, University of Utah) to carry out conditional knockout and lineage mapping studies (Scheme 1). The *R26R-lacZ* reporter mice were obtained from Jackson Laboratories (JaxLab stock #003474) and the *ROSA26-eGFP-DTA (R26R-DTA)* mice were generously gifted by A. Copp (University College London, England). The *R26R-DTA* was made by introducing an *eGFP-DTA* (enhanced green fluorescent protein-diphtheria toxin fragment A) cassette into the ubiquitous *ROSA26* reporter locus [89]. As a

result, *R26R-DTA* mice express eGFP ubiquitously, but diphtheria toxin A-chain (DTA) is switched on only when Cre is present to remove the floxed stop codon sequence in front of DTA-encoding sequence (Scheme 2). To generate the *Wnt1Cre/DTA* ablated mutant embryos, *Wnt1Cre* mice were crossed into the *R26R-DTA* mouse line to produce progeny that were both *Wnt1Cre*-positive and *R26R-DTA* positive. All mouse colonies for this study were maintained on a mixed C57Bl6/129 genetic background. Mice were housed and handled in accordance with Indiana University Institutional Animal Care and Use Committee guidelines. For timed pregnancies, the day of observed vaginal plug was designated embryonic day 0.5 (E0.5).

3.2. Histological, *in situ* hybridization and immunohistochemistry analyses

Embryos were fixed in 4% PFA overnight at 4°C and processed for paraffin histology as previously described [90]. Immunohistochemistry was carried out using ABC kit (Vectastain) with DAB and hydrogen peroxide as chromogens. The endogenous peroxidase was quenched via incubation in 0.3% hydrogen peroxide in methanol for 30min. For detection of Pax3, sections were boiled in antigen retrieval buffer (Dako) for 2min and then cooled to room temperature prior to blocking. Melanin intensification was performed by addition of exogenous DOPA (1mg/ml in PBS) for 10mins. Dilutions of primary antibody were 1:200 for goat anti-Pax3 antibody (Santa Cruz sc-7748) and 1:1000 for secondary anti-goat antibody. Incubation in primary antibody was carried out at 4°C overnight, and incubation in secondary antibody at room temperature for 30 minutes.

Radioactive *in situ* hybridization for *Wnt1, Pax3,* and *Sox10* expression was performed as previously described [91]. Both sense and antisense ^{35}S-UTP-labeled probes were used as negative controls and experimental samples respectively. Analyses were performed on serial sections within at least three independent embryos of each genotype. To quantify expression differences, silver grains were counted per square area on serial sections.

3.3. Wholemount X-gal (*lacZ*) staining

Whole embryos were fixed in 4% PFA immediately after dissection for 2h. They were then washed 10min in PBS and subsequently washed 2x in β-gal buffer (0.058 M Na_2HPO_4, 0.042 M NaH_2PO_4, 0.001M $MgCl_2$, 0.01% NP40), 5mins each. An additional wash was done overnight at 4°C, then embryos were changed into X-gal substrate (0.1% X-gal, 0.005M $K_3Fe(CN)_6$, 0.005M $K_4Fe(CN)_6$, 0.001M EGTA), and incubated at 37°C in the dark. Embryos were then fixed in 4% PFA after successful X-gal staining was completed.

3.4. Immunoblot and reagents

Immunoblots were performed using mouse monoclonal anti-Pax3 and anti-Pax7 antibodies (both obtained from Hybridoma Bank, University of Iowa); mouse monoclonal anti-β-tubulin antibody (Roche); and HRP-conjugated goat anti-mouse IgG (Jackson Laboratories). Both the anti-Pax3 (1:1000) and anti-Pax7 (1:1000) antibodies were incubated overnight at 4°C. Anti-β-actin (1:10000) and goat anti-mouse (1:5000) antibodies were incubated for 1h at room temperature.

Antibodies were detected using the enhanced chemiluminescence (ECL) plus detection system (Amersham). To maintain equal loading between blots, membranes were stripped after each blot using stripping buffer (Thermo Scientific) at 55°C for 30min, and then subsequently oscillated for additional 30min, before being blocked in 5% milk dissolved in 0.1% PBS-Tween20 and reprobed. Densitometry of immunoreactive bands was performed using Image J 1.37v (NIH).

3.5. Cardiac ink injection analysis

For gross examination of the cardiovascular system, embryos were injected with Pelican India ink (diluted 50% in PBS) into the left ventricle of the heart, accessed through the pericardium or into the umbilical vessels. Glass capillary tubes (1-2mm internal diameter) were drawn over a Bunsen flame and then broken diagonally to give long, fine, sharp glass needles. Needles were loaded with ink and injected using a standard mouth pipette. Prior to injection, maternal-embryonic connections were maintained and the embryos kept at 37°C to maintain continuous heartbeat. Immediately following injection, embryos were fixed in 4% PFA at 4°C overnight, processed through a series of methanol/PBS dilutions (10%, 20%, 30%, 50%) to 100% methanol, and cleared for several hours in 2:1 volume of benzyl benzoate and benzyl alcohol respectively. Genotypes of all embryos were confirmed by DNA extraction from the yolk sac, and successive PCR analysis.

4. Results

4.1. *Pax3*$^{d5/d5}$ systemic knockout recapitulates *Sp*^{2H} mutant embryos

Mice homozygous for *Pax3* conditional allele (*Pax3*$^{f/f}$) were generated, with exon5 flanked by *loxP*-sites. Crossing male *Pax3*$^{f/+}$ with *Tie2Cre* transgenic females generated germline (via oocyte-expressing Cre activity) heterozygous deletion of exon5 (*Pax3*$^{d5/+}$). Although *Tie2Cre* is normally expressed in the endothelium, it is also transiently expressed in adult ovary oocytes [92]. Thus, by crossing a *Tie2Cre*-positive female with a *Pax3*$^{f/+}$ male, generation of heterozygous *Pax3*$^{d5/+}$ systemic knockouts was possible. Intercrossing of *Pax3*$^{d5/+}$ heterozygotes generated *Pax3*$^{d5/d5}$ mutants. Deletion of exon5 creates a premature stop codon and loss of Pax3 homeodomain and its downstream sequence. Western analysis using antibody that recognizes the C-terminus of *Pax3* (missing in d5 mutant protein) confirmed that wildtype *Pax3* protein is absent in the homozygous mutant, but levels of the closely related Pax7 are unaffected. All protein samples were normalized relative to Actin protein (Figure 4A). *Pax3*^{d5} allele recapitulates all aspects of *Splotch* (*Pax3*^{Sp2H}) allele (4B-I) including pigmentation defects in heterozygotes (*Pax3*$^{d5/+}$), 100% penetrant PTA/VSD, NT closure defects and mid-gestational lethality by embryonic day 14 (E14.0) in homozygote mutants (*Pax3*$^{d5/d5}$). Furthermore, analysis of *Pax3*$^{d5/+}$ and *Pax3*$^{Sp2H/+}$ compound mutants (i.e. *Pax3*$^{d5/Sp2H}$) demonstrated that the *Pax3*^{d5} allele is genetically identical to the *Pax3*^{Sp2H} allele (data not shown).

4.2. *Pax3*$^{d5/d5}$ systemic knockout displays specific regression of left 6th AAA

The pathogenesis of the OFT remodeling defect in *Pax3* mutants is due to the failure of the left 6th AAA to persist, which normally gives rise to the pulmonary trunk. Thus, in its absence, there is formation of a single OFT from the left 4th AAA (normally gives rise to aorta), leading to PTA/VSD. At E10.5, there are no observable differences in AAA remodeling between Pax3 mutants and control littermates (Figure 5A-C). However, by E11.5 the left 6th AAA undergoes regression in mutant embryos when compared to controls (5D, E). Interestingly, there are no observable differences in left 3rd, 4th AAA remodeling between the two genotypes. Also, other AAA's undergo normal regression/persistence, suggesting a Pax3-specific role in left 6th AAA remodeling. Due to the regression of the left 6th AAA, OFT septation is abnormal by E13.5 in Pax3 mutants. Control embryo hearts at E13.5 undergo proper septation of the OFT into the pulmonary artery and aorta (5F). However, *Pax3* mutant embryo hearts develop a range of PTA defects including Types I and III (5G, H), which respectively involve two incompletely separated vessels and a single vessel exiting the heart.

4.3. Migratory NC in *Pax3*$^{d5/d5}$ mutants is appreciably reduced

NC lineage mapping studies with *Wnt1Cre* to permanently label NC-derived cells via *R26R-lacZ* reporter were performed. This allowed for fate-mapping studies to be done in NC cells from ~E8.5 onwards, when *Wnt1Cre* expression begins in the CNC region. Differences in *lacZ* patterns as early as E9.0 (Figure 6A, B) in mutants were observed. In *Pax3*$^{d5/d5}$ mutants, *lacZ*-positive cells appeared to

accumulate along the axis of the NT, which led to an overall delay in lateral emigration of NC. As a result, in addition to differences in overall number, a slight temporal delay in delamination of the NCC from the NT was observed in mutants at the E9 stage. This led to a delay in formation of NC-derived structures at this stage, including 1st and 2nd branchial arches, which were appreciably regressed in mutants (6B). By E9.5, NC cells appear to be migrating properly in both mutants and controls. However, there is a significant reduction in the number of NC cells that begin to colonize the 3rd/4th/6th pharyngeal aortic arches. The reduction in migratory CNC was determined to be Pax3-dose dependent, as slightly fewer *lacZ*-positive cells were observed in *Pax3*$^{d5/+}$ heterozygote embryos when compared to wildtype littermates. However, there was an even more drastic reduction in migratory CNC observed in *Pax3*$^{d5/d5}$ mutants even compared to heterozygote *Pax3*$^{d5/+}$ embryos (6C). Histological examination of older *lacZ*-stained embryos also revealed that the number of NC colonizing AAA's that eventually invade the OFT region is reduced in mutants (6D, E). The aorticopulmonary and OFT cushions in *Pax3*$^{d5/+}$ embryos are slightly less populated with NC cells when compared to wildtype. However, this slight reduction is not sufficient to affect normal OFT remodeling as Pax3 heterozygote (*Pax3*$^{d5/+}$) embryo hearts undergo normal septation (data not shown). By E13.5, NC cells have completely colonized the distal region of the OFT as can be seen by the observed invasion of two streams of *lacZ*-positive cells. However, despite their ability to colonize the mutant OFT, they do so in fewer numbers (6F, H).

The *Wnt1Cre* lineage mapping studies was complemented with an additional NC reporter – *AP2aCre* – which was used to determine the effect of Pax3 deletion in a slightly earlier population of NC (as AP2aCre is expressed earlier by ~E8 in CNC region). Based on NC lineage mapping studies with *Ap2aCre,* both derivatives of the NC (known region of Pax3 expression) and ectoderm (known region of no Pax3 expression) were able to be permanently labeled and fate-mapped in both Pax3 wildtype and mutant backgrounds. Results from this fate-map study correlate with that of *Wnt1Cre*, and demonstrate that there is a marked reduction in overall numbers of migratory NC (Figure 7A, B). Furthermore, migratory CNC that colonize the 4th AAA is appreciably reduced (asterisks in 7E, F) and virtually no *lacZ*-positive cells within the 6th AAA of Pax3 mutants were observed when compared to their littermate controls (asterisk in 7G). In addition, a progressive loss of migratory CNC was observed in Pax3 mutants from the 3rd to the 4th and finally the 6th AAA.

4.4. Genetic ablation of CNC gives rise to OFT and AAA remodeling defects

In order to assess the specific role of the *Wnt1Cre*-expressing population of NC in heart morphogenesis, the entire population of *Wnt1Cre*-expressing NC was ablated using the *R26R-DTA* system. Cre-mediated activation of DTA kills cells via apoptosis by interfering with the RNA translation machinery in each individual cell. This system is highly cell autonomous and only cells that express the DTA are ablated without any effects on neighboring non-Cre expressing cells. Ablation of *Wnt1Cre*-expressing NC lineage led to fully penetrant PTA/VSD (Figure 8A-G).

Surprisingly, these embryos are viable and go on to live to birth (n=24/24 mutants). *Wnt1Cre/DTA* ablated mutants also displayed craniofacial defects (8A) including severe microcephaly (white arrow) consistent with significant NC contribution to the cranial region. An absence of NC-derived structures such as thymus, dorsal root ganglia, and Schwann cells (not shown) was also observed.

In order to visualize the DTA expressing cells and to determine how quickly the apoptosis of these cells was occurring, the *Wnt1Cre/DTA* mouse was crossed into the *R26R-lacZ* reporter mouse system to lineage map any potentially remaining *Wnt1Cre*-expressing migratory NC. Based on this analysis, it was determined that as early as E8.5 (when *Wnt1Cre* is expressed), the NC cells were almost completely gone in the NT as shown by an absence of *lacZ*-positive cells (Figure 9A). Later stage analysis at E9.5 also confirmed successful ablation of *Wnt1Cre*-expressing NC (9B, C). Therefore, this data suggests that the DTA is working very quickly-within ~6 hours of Cre expression and successive recombination.

To determine the pathogenesis of the observed PTA/OFT defects, cardiac ink injections were performed in 3 separate *Wnt1Cre/DTA* mutant littermates at E11.5. All 3 embryos analyzed displayed severe defects in AAA remodeling. However, these defects were completely randomized and varied from each individual embryo. Embryo #1 had only 1 caudal AAA persisting on both the left and right side (9D, E). Embryo #2 displayed abnormal persistence of left 1st AAA but regression of left 6th AAA. In addition, it displayed abnormal regression of right

4th AAA (9F, G). Embryo #3 displayed abnormal persistent of left and right 1st and 2nd AAA's. In addition, it displayed abnormal regression of left 3rd AAA (9H, I).

4.5. *Wnt1Cre*-mediated ablation fails to capture earlier wave of NC cells

In order to determine if indeed the entire NC population was being ablated, marker analyses on ablated mutant embryos at E13.5 were performed by radioactive *in situ* hybridization. To do this, a series of well-established markers of premigratory NC (*Wnt1*), migratory NC (*Sox10*), and both premigratory and early migratory NC (*Pax3*) were used (Figure 10). It was determined that *Wnt1Cre*-mediated ablation was successful in ablating both *Wnt1*- and *Pax3*-expressing population of premigratory and early migratory NC cells (10: top and middle panel). However, a few late-stage migratory *Sox10*-expressing cells were detected in ablated embryos (10: lower panel). This suggests that *Wnt1Cre*-mediated ablation does not successfully kill the entire NC population, and suggests that there is an earlier wave of NC delaminating from the NT that does not express *Wnt1Cre*. However, this earlier wave of NC cells is still insufficient for proper AAA and OFT remodeling.

4.6. *Pax3$^{f/d5}$/Wnt1Cre* conditional mutants do not phenocopy *Pax3$^{d5/d5}$* OFT defects

To determine the CNC-intrinsic role of Pax3, conditional knockout studies were performed as described earlier to ablate *Pax3* in the *Wnt1Cre*-expressing NC cell lineage. Surprisingly, conditional mutants (*Pax3$^{f/d5}$/Wnt1Cre*) were found to not

display defects in OFT/AAA remodeling as seen in *Pax3*$^{d5/d5}$ systemic mutants and were viable till birth (based on analysis of >200 embryos, from E10.5 – E19.5). However, consistent with the rostrocaudal onset of *Wnt1Cre*-expression, 56% of these mutants displayed exencephaly (n=28/50) but not spina bifida (Figure 10C, F).

Wholemount embryo analysis of *lacZ*-positive cells did not reveal any defects in CNC migration or colonization of AAA or OFT regions (10A, D). However, some disorganization of dorsal root ganglia and NC-derived Schwann cells in mutant embryos was observed (10B, E). In addition, newborn conditional mutants displayed pigmentation defects due to anomalous differentiation of NC-derived melanocytes. This was determined based on the similar distribution of NC-derived melanocytes in the basal epidermis of both conditional mutants and control pups (10 day old), but a significant reduction in melanin synthesis in mutants (10I, J).

To confirm successful *Wnt1Cre*-mediated recombination of the *Pax3*$^{f/d5}$ allele, *in situ* hybridization was performed at E10 using both an exon5-specific *Pax3* probe, which detects only wildtype *Pax3* transcript. The exon5-specific probe did not detect signal in dorsal-most region of the NT corresponding to known *Wnt1Cre*-expression domain (10G, H). In addition, immunohistochemistry analysis was performed using anti-Pax3 antibody at E10 to determine presence/absence of Pax3 protein. The antibody failed to detect any Pax3

protein in the *Wnt1Cre*-expressing region of the NT of conditional mutants (arrow in 10J) when compared to control littermate (10I). Together, these results confirmed successful deletion of exon5 within the *Wnt1Cre*-expressing domain of the NT.

4.7. *Pax3$^{f/d5}$/AP2aCre* conditional mutants display less severe OFT/AAA defects than *Pax3$^{d5/d5}$* systemic mutants

Due to the absence of AAA/OFT remodeling defects in the *Pax3$^{f/d5}$/Wnt1Cre* conditional mutants, an alternative conditional approach was used in an attempt to recapitulate the *Pax3$^{d5/d5}$* phenotype. Alternative conditional knockout studies were performed as described earlier to delete *Pax3* in an earlier population of NC cells via *AP2aCre*-mediated recombination. *AP2aCre* expression can be seen as early as E8 (~0.5 day earlier than *Wnt1Cre*) within the neural folds and neuroepithelium (Figure 11A). Importantly, it marks CNC-derived cells that eventually colonize the OFT region (11B, C). As a result, this alternative conditional approach was done to determine if the lack of phenotype seen in *Pax3$^{f/d5}$/Wnt1Cre* mutants was due to an inability of *Wnt1Cre* to successfully delete Pax3 early enough within the NC before they had undergone proper formation and specification. As anticipated, *Pax3$^{f/d5}$/AP2aCre* mutants were observed to have some OFT/AAA defects, although not as severe as *Pax3$^{d5/d5}$* mutants. Similar to *Pax3$^{f/d5}$/Wnt1Cre* mutants, these conditional mutants were viable till birth and displayed exencephaly, but not spina bifida (Figure 11F).

Wholemount embryo analysis of *lacZ*-positive cells revealed decreased CNC migration and colonization of caudal AAA's ($3^{rd}/4^{th}/6^{th}$) and OFT region (11D-G). Histological analysis confirmed reduced distribution of CNC cells colonizing the AAA's and invading the OFT (11H, I). However, ectodermal derivatives were unaffected, as Pax3 is not expressed in this region (arrows in 11H, I). In addition, conditional mutants displayed AAA/OFT remodeling defects including DORV/VSD (11J-M). However, fully penetrant PTA as seen in Pax3d5/d5 mutants was not observed.

5. Discussion

This project focused on the CNC-intrinsic role of Pax3 during OFT/AAA remodeling. In order to do this, a number of mouse models were utilized to elucidate the effect of ablation of *Pax3* within the CNC and how that compared to a gross ablation of the CNC population itself.

First, we compared *Pax3*$^{d5/d5}$ systemic mutants to previously published *Pax3*^{sp2H} mutants. Based on the NC lineage mapping and histological analyses done on *Pax3*$^{d5/d5}$ mutants, it is clear that the *Pax3*^{d5} allele completely recapitulates the previously published *Pax3*^{sp2H} allele [58, 85]. By comparing *Pax3*$^{d5/d5}$ systemic mutants to *Wnt1Cre/DTA* ablated mutants, we were able to tease out the Pax3-specific role in CNC during AAA remodeling. The fact that *Pax3*$^{d5/d5}$ mutants only display specific regression in the left 6th AAA, despite the reduction in migratory CNC to caudal AAA (3rd/4th/6th) suggest a potential left 6th AAA-specific role encoded by *Pax3*. It may also be indicative of a 6th AAA over-sensitivity to loss of Pax3 when compared to the other caudal AAA's (i.e., 3rd/4th). Surely, the rostrocaudal progressive loss of migratory CNC observed in *Pax3*$^{d5/d5}$ mutant AAA's (based on both *Wnt1Cre* and *Ap2aCre* lineage mapping data), which is most severe in the 6th AAA compared to 3rd/4th, lends credence to this theory. Although migratory NC's are not important for the initial formation of AAA's, they are required for their remodeling. This has been successfully demonstrated by surgical ablation studies done in chick embryos, which result in a wide variation

of AAA anomalies [14, 18]. Given the absence of migratory NC's in *Wnt1Cre/DTA* mutants, we expected randomized AAA remodeling defects in the ablated model. However, the differences in severity of AAA remodeling between the ablated mutants and *Pax3* mutants may be important in determining consequences of incorrectly programmed mutant *Pax3* NC's vs. absent NC.

Further elucidation of these differences may be important in also explaining the pathogenesis leading to subsequent embryonic death typical in *Pax3* mutants [15] but not seen in the ablated mutants. *Pax3* mutants all die by E14 and exhibit NT defects similar to chick surgical ablations that die ~day 8 and encompass a larger NT ablation [6, 14, 18]. Both the *Pax3* and *Wnt1Cre/DTA* mutants were bred on the same mixed genetic background (C57Bl6/129). Thus, observed differences in embryonic lethality were not influenced by background. NC marker analysis in *Wnt1Cre/DTA* mutants revealed that, unlike surgically ablated chick embryos, there is presence of *Sox10*-positive NC derivatives at E13.5 that appear to have emigrated from the NT prior to *Wnt1Cre/DTA*-mediated ablation. *Sox10* is an established marker for NC-derived Schwann cells and is important in peripheral neuronal differentiation during development [93, 94]. Also, *Sox10* is believed to interact cooperatively with Pax3 [94], and we have already established that *Sox10* mRNA levels are diminished in *Pax3* mutants (unpublished data) most likely due to their severe lack of NC-derived Schwann cells and dorsal root ganglia. Thus, in order to understand the differences in temporal lethality between these two models, follow up studies comparing

differences in peripheral neuronal differentiation between *Pax3* and *Wnt1Cre/DTA* mutants, and the potential effect of this on *in utero* lethality due to poor cardiac output were performed (described in detail in Chapter III). In addition, follow up marker analysis at earlier stages of NC migration (prior to E13) in *Wnt1Cre/DTA* mutants may be informative in determining the temporal origin of these NC derivatives. Collectively, these data indicate that *Wnt1Cre*-expressing CNC lineage is indeed required for normal structural heart development, as ablation leads to PTA/VSD and recapitulates the *Pax3* mutant OFT defects.

Given the failure of *Wnt1Cre* to capture this earlier population of migratory NC, the fact that *Pax3*$^{f/d5}$*/Wnt1Cre* conditional mutants failed to recapitulate the OFT/AAA phenotypes of the *Pax3*$^{d5/d5}$ systemic mutants is less surprising. Given the important role of CNCs for OFT septation, the PTA defect observed in *Pax3*$^{d5/d5}$ embryos suggests *Pax3* is required for heart development via influencing CNC behavior. Also, the fact that these conditional mutants displayed defects in melanocyte differentiation, suggests a possible variation in spatiotemporal requirements for Pax3 in different lineages. However, the absence of fully penetrant OFT/AAA phenotypes even in *Pax3*$^{f/d5}$*/AP2aCre* conditional mutants is difficult to explain. *Ap2aCre* is expressed slightly earlier (~E8.0) than *Wnt1Cre* and should in theory have been able to successfully ablate Pax3 in all CNC-lineages. Although unexpected, the lack of fully penetrant OFT/AAA defects raises several intriguing questions concerning the role Pax3

plays in CNC morphogenesis and OFT septation. Recent studies involving the use of *Wnt1Cre* to restore *Pax3* enhancer function in the NC in an already Pax3-deficient environment [95], suggest that the *Wnt1Cre*-expressing population of NC cells is sufficient to regulate OFT remodeling when these cells are properly specified. Taken together, the results of this project demonstrate that Pax3 is required in a CNC-cell autonomous role during heart development.

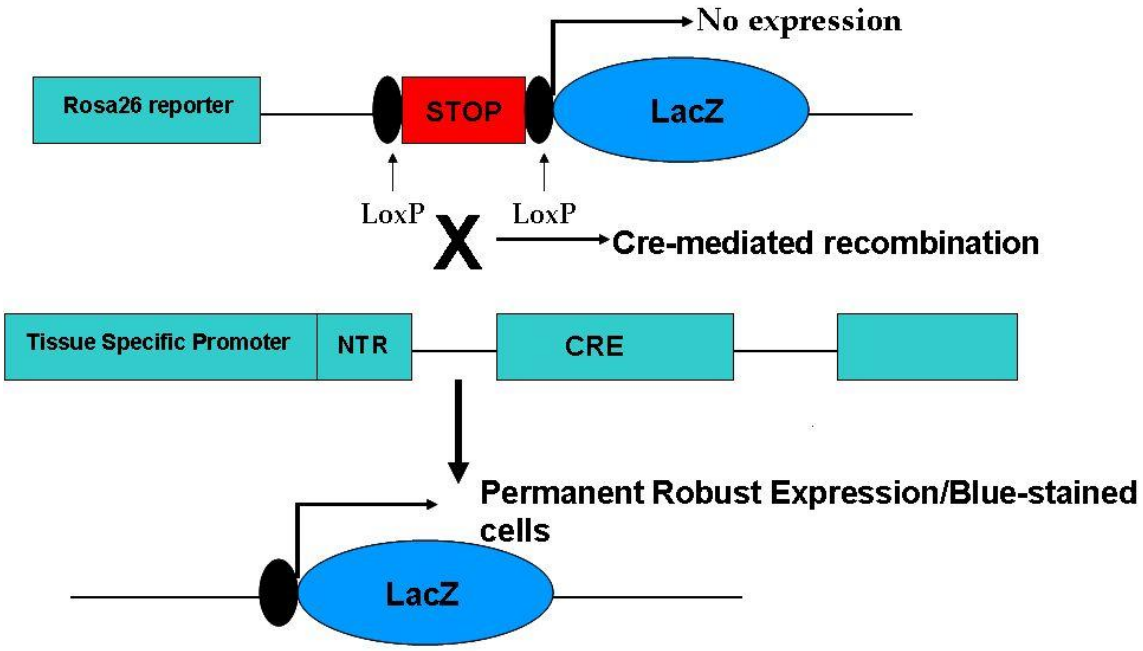

Scheme 1: Cre-inducible lineage mapping using *ROSA26R-LACZ* (*R26R-lacZ*) reporter/promoter mice. NTR = non-translated region of IRES (internal ribosome entry site) sequence.

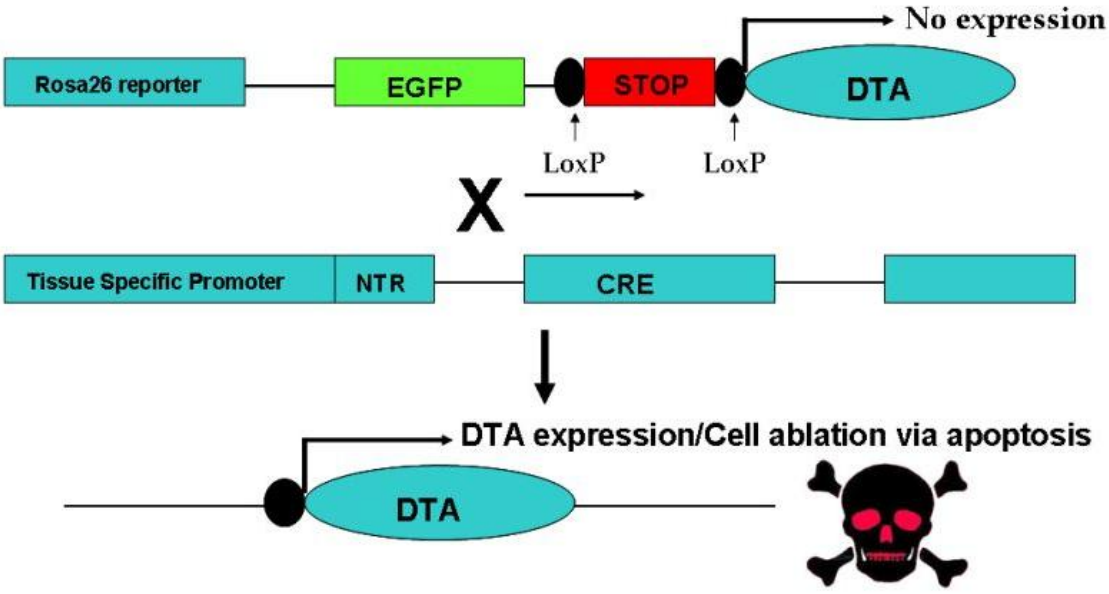

Scheme 2: Cre-inducible genetic ablation using *ROSA26R-EGFP-DTA* (*R26R-DTA*) reporter/promoter mice. NTR = non-translated region of IRES (internal ribosome entry site) sequence.

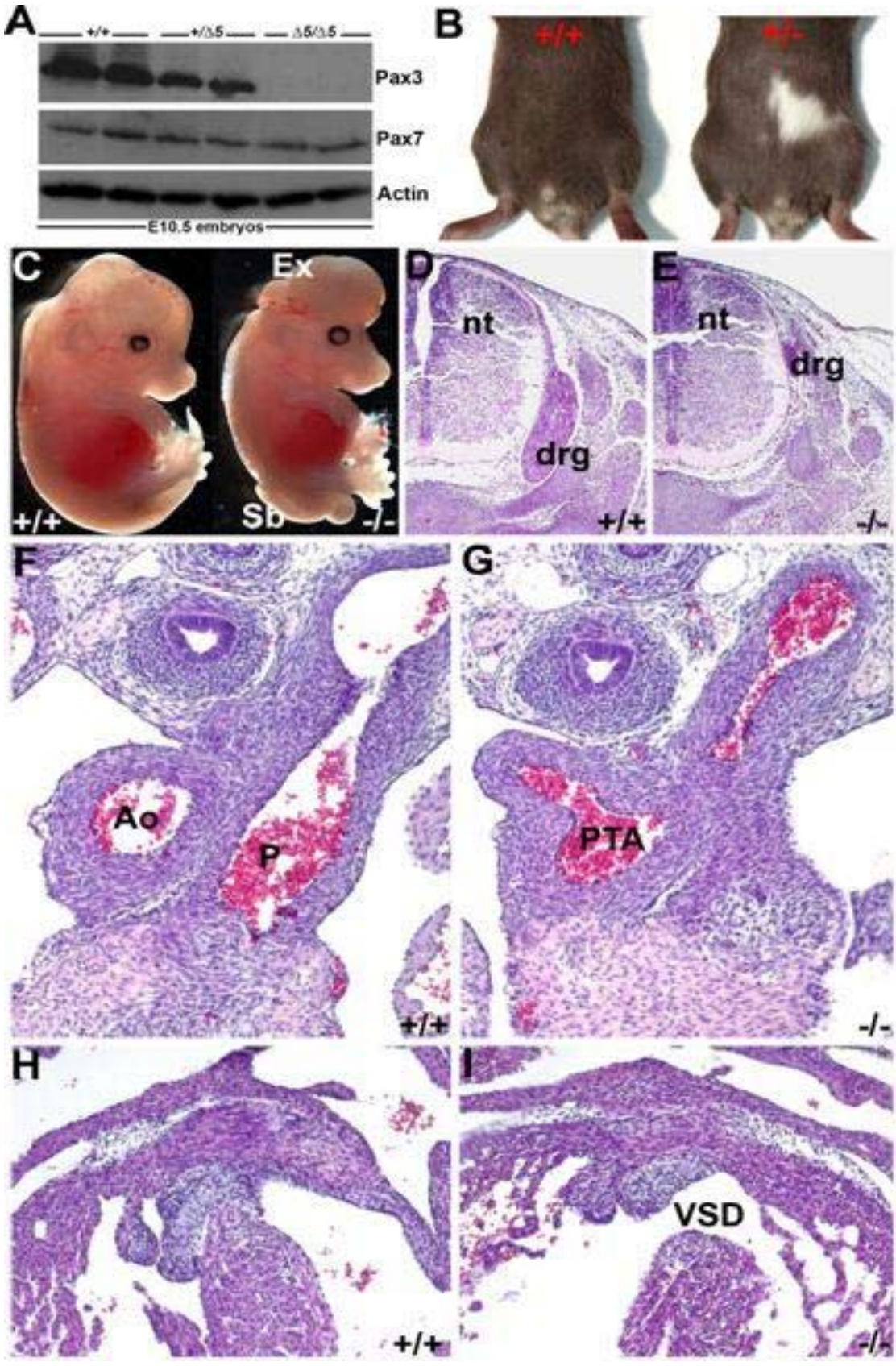
A
+/+
+/Δ5
Δ5/Δ5
Pax3
Pax7
Actin
E10.5 embryos
B
+/+
+/-
C
Ex
+/+
Sb
-/-
D
nt
drg
+/+
E
nt
drg
-/-
F
Ao
P
+/+
G
PTA
-/-
H
+/+
I
VSD
-/-

Figure 4: Characterization of *Pax3*^{d5} allele

(A) Western showing wildtype Pax3 protein is reduced in heterozygotes (d5/+) and absent in *Pax3*$^{d5/d5}$ mutant E10.5 embryos, but that closely related Pax7 protein and housekeeping actin expression is unaffected. (B) Heterozygote mutant mice exhibit white spots on their forehead and belly. (C) *d5/d5* homozygous embryos were present in normal Mendelian ratios at E13.5 but died thereafter. Nulls exhibited exencephaly (Ex) and spina bifida (Sb) NT defects. (D, E) NC-derived dorsal root ganglia are hypoplastic in *d5/d5* homozygote embryos (E), when compared to normal littermate controls (D). (F-I) H&E staining of E13.5 wildtype (F, H) and mutant (G, I) heart sections showing PTA and VSDs in *Pax3*$^{d5/d5}$ hearts. Ao = aorta, Ex = exencephaly, drg = dorsal root ganglia, nt = neural tube, p = pulmonary artery, PTA = persistent truncus arteriosus, VSD = ventricular septal defect. (Western performed by Dr. Hong-Ming Zhou, PhD).

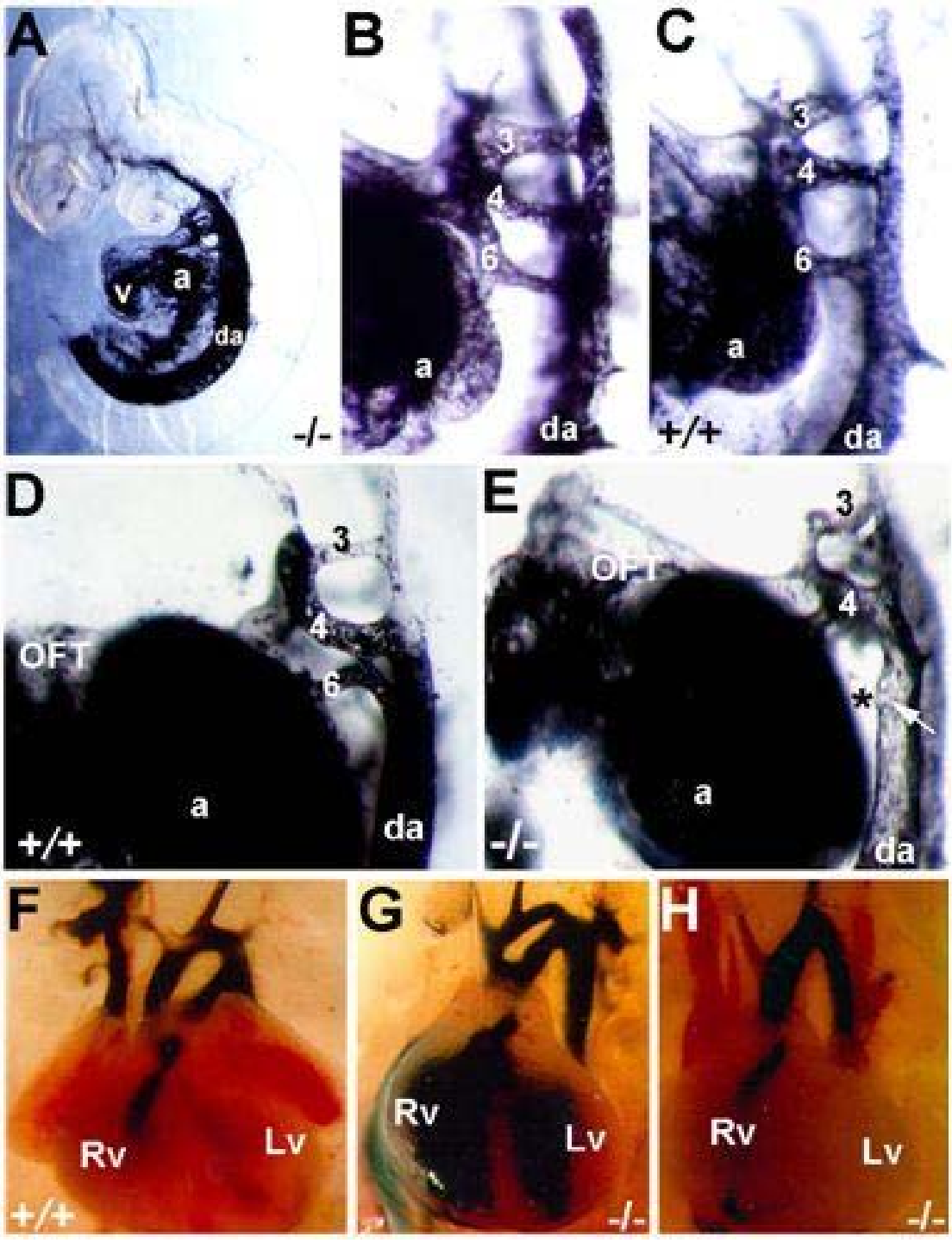
A
v
a
da
B
3
4
6
a
-/-
da
C
3
4
6
a
+/+
da
D
3
4
6
OFT
a
+/+
da
E
3
OFT
4
*
a
-/-
da
F
Rv
Lv
+/+
G
Rv
Lv
-/-
H
Rv
Lv
-/-

Figure 5: Ink injection analysis of aortic arch artery formation and remodeling during OFT morphogenesis

(A-C) E10.5 AAA system is revealed. Note normal AA formation in both -/- (A, B) and wildtype (C). (D, E) However, in E11.5 *Pax3* deficient embryos (E), the left 6^{th} AA has abnormally regressed. (F-H) E13.5 *Pax3* deficient embryos all have PTA (single vessel exiting the right ventricle with concomitant VSD), but exhibit a range of types (Type-I in G, Type-III in H), when compared to wildtype littermates that have separate aorta and pulmonary trunks exiting the respective right and left ventricles. dA = dorsal aorta, oft = outflow tract, LV = left ventricle, RV = right ventricle. (Ink injections performed by Dr. Simon J. Conway, PhD).

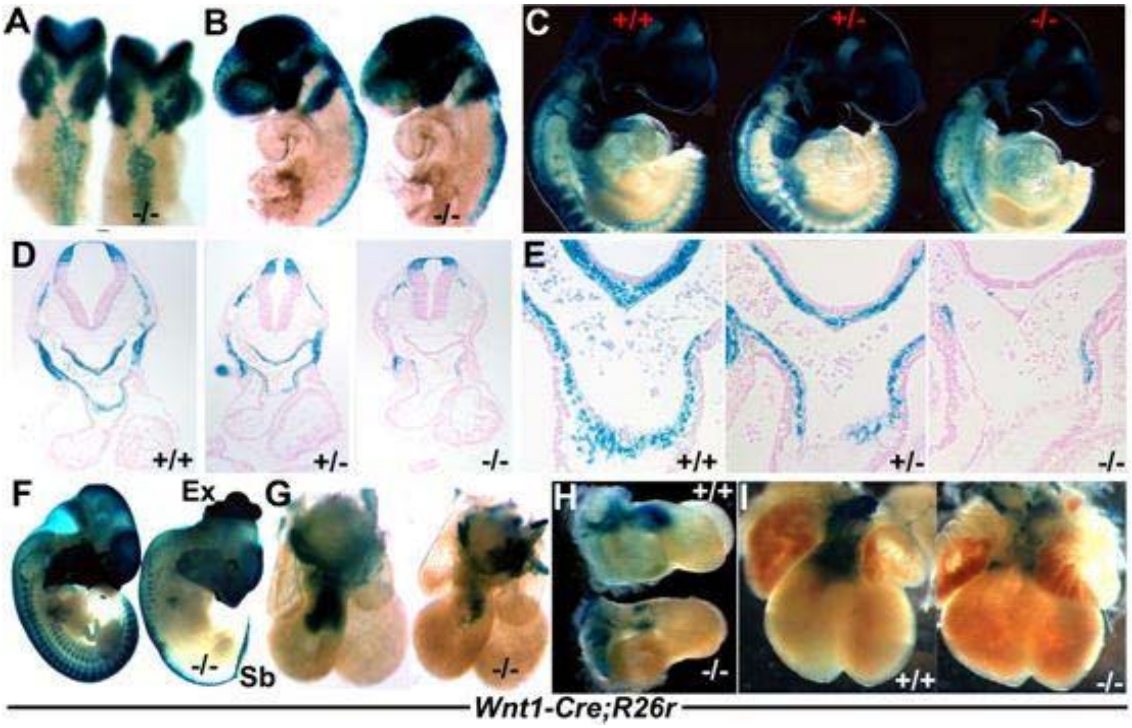
A
B
C
+/+
+/-
-/-
-/-
-/-
D
E
+/+
+/-
-/-
+/+
+/-
-/-
F
Ex
G
H
+/+
I
-/-
Sb
-/-
-/-
+/+
-/-
Wnt1-Cre;R26r

Figure 6: Lineage mapping of *lacZ* stained CNC and their derivatives (marked via *Wnt1Cre;R26R* reporter)

(A-H) *Wnt1Cre;R26R* lineage mapping. Dorsal (A) and left lateral (B) views of E9 embryos showing impaired *Pax3*$^{d5/d5}$ CNC migration when compared to wildtype littermates. (C) Right lateral views of E9.5 +/+, +/d5 and *d5/d5* littermates showing fewer CNC populate the 3rd/4th/6th pharyngeal *+/d5* arches, and still even less the *d5/d5* arches. (D, E) Sections going through OFT region of E9 embryos shown in (C) reveal lack of *Wnt1Cre*-marked CNC in aorticopulmonary septum and OFT cushions. (F) Lateral view of E12 wildtype and null embryos, illustrating wide-ranging NC reduction and spina bifida (Sb) and exencephaly (Ex) in nulls. (G, H) Note reduction in E12 null OFT colonization, viewed frontally (G) and from the right (H). (I) Reduced CNC colonization is most evident in E13.5 -/- hearts (J, K).

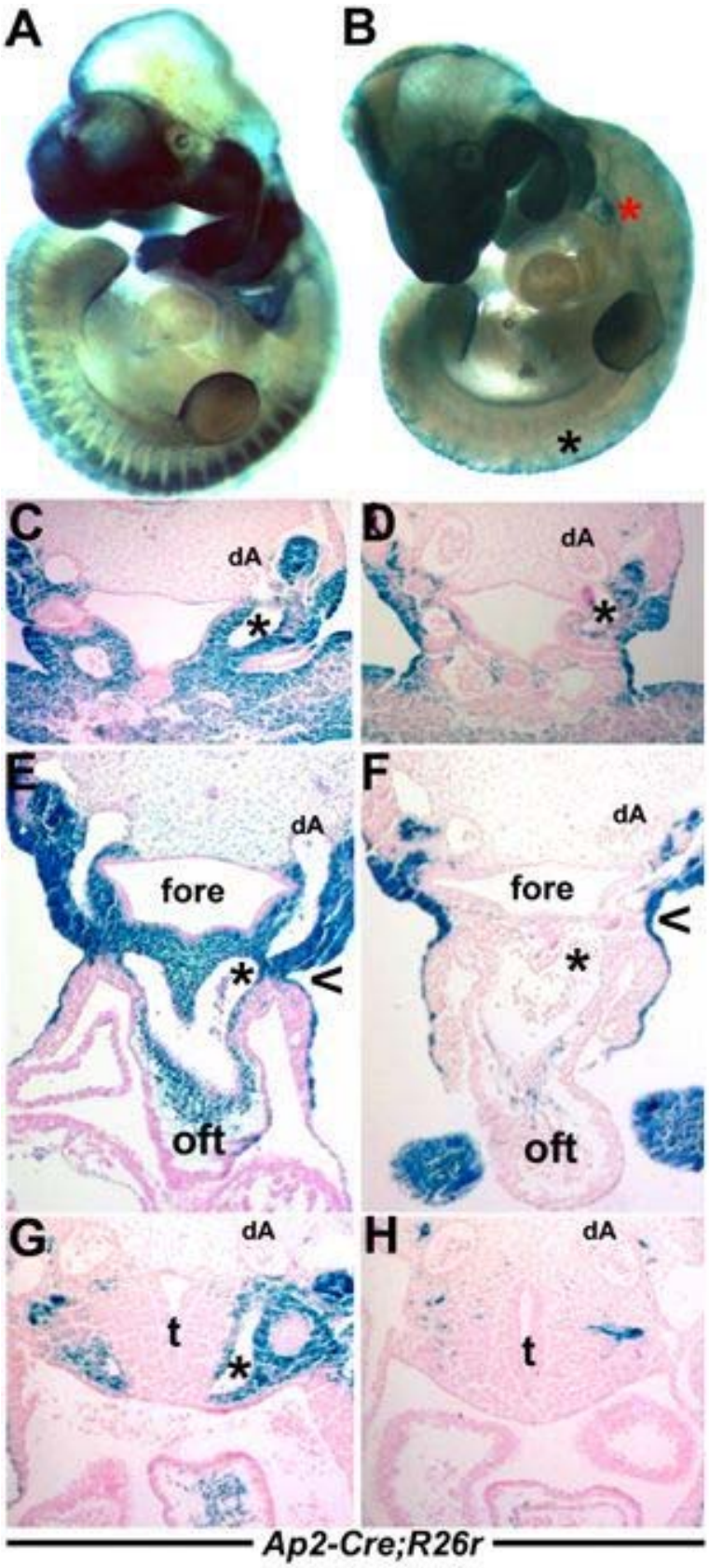
A
B
C
dA
D
dA
E
dA
fore
oft
F
dA
fore
oft
G
dA
t
H
dA
t
Ap2-Cre;R26r

Figure 7: Lineage mapping *lacZ* stained CNC and their derivatives (marked via *Ap2aCre;R26R* reporter)

(A-H) *Ap2aCre;R26R* lineage mapping. (A-B) Left lateral views of E10.5 embryos showing impaired *Pax3*$^{d5/d5}$ CNC migration when compared to wildtype littermates. Note lack of migratory CNC (red asterisk in B) and reduced drg (black asterisk in B). Histology reveals slightly reduced A*p2aCre*-marked cells in mutant 3rd arch (black asterisk in D), appreciably reduced in mutant 4th arch (asterisk in F) and completely absent in mutant 6th arch (H). Note reduced *lacZ*-positive cells in mutant OFT (F). dA = dorsal aorta, drg = dorsal root ganglia, fore = foregut, oft = outflow tract, t = truncus, *left 3rd/4th/6th arches respectively.

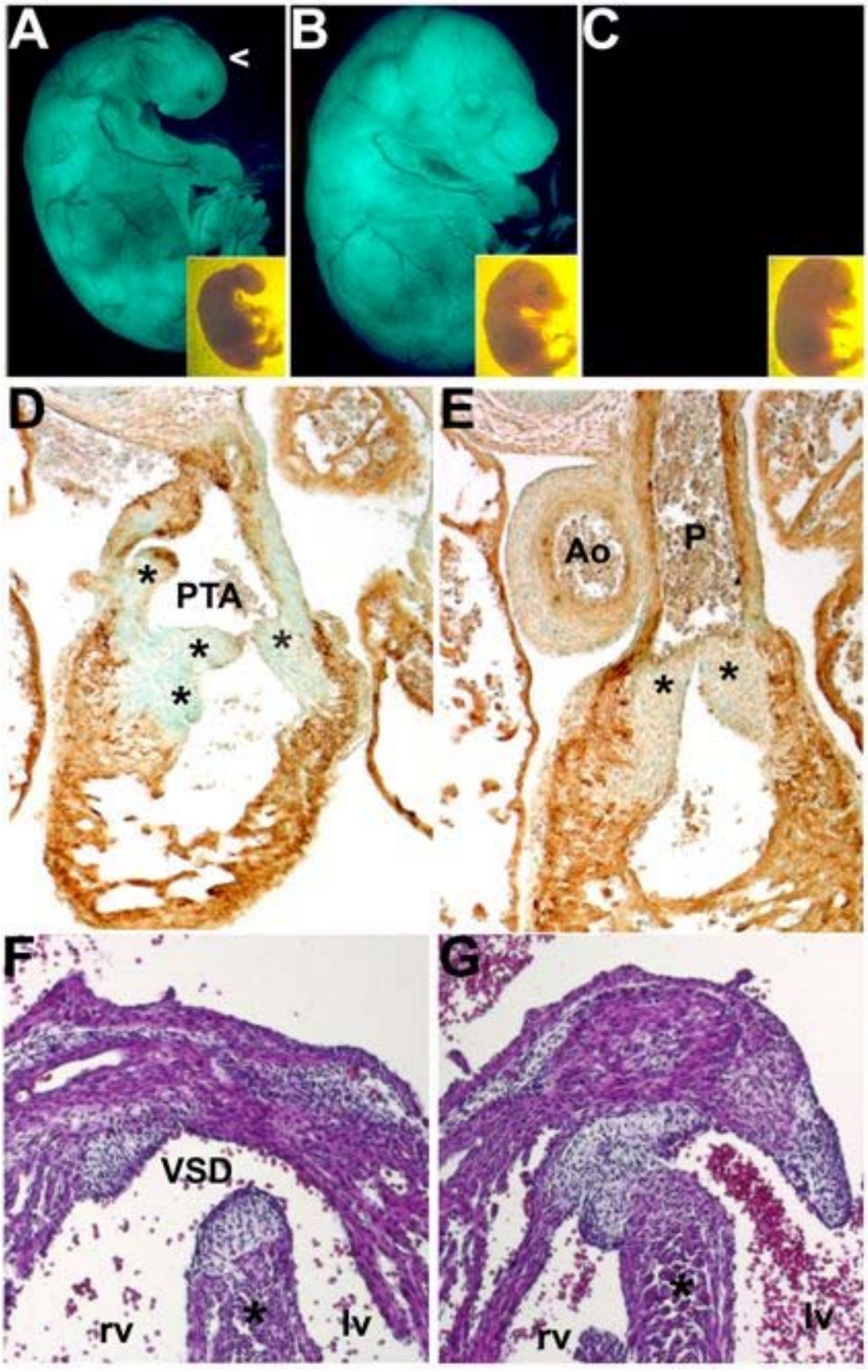
A
B
C
D
PTA
E
Ao
P
F
VSD
rv
lv
G
rv
lv

Figure 8: Genetic ablation of NC lineage in *Wnt1Cre/DTA* mutants

(A-C) *Wnt1Cre/DTA* mutant (A), *R26R-DTA* only littermate control (B) and *Wnt1Cre* only littermate control (C) whole fetuses at E15.5 under UV. Note lack of craniofacial structures, internalized eyes following genetic NC ablation (arrowhead in A). Insets show same embryos under bright light. (D-E) Control (E) and mutant (D) transverse sections stained with anti-smooth muscle actin and counterstained with methyl green. Note enlarged OFT valve leaflets in mutant (asterisks in D). (F-G) Control (G) and mutant (F) transverse H&E sections showing VSD in mutants. Ao = aorta, p = pulmonary artery, PTA = persistent truncus arteriosus, lv = left ventricle, rv = right ventricle, VSD = ventricular septal defect. (*Wnt1Cre/DTA* transgenic crosses were performed by Dr. Paige Snider, PhD; histology performed by Mica Gosnell).

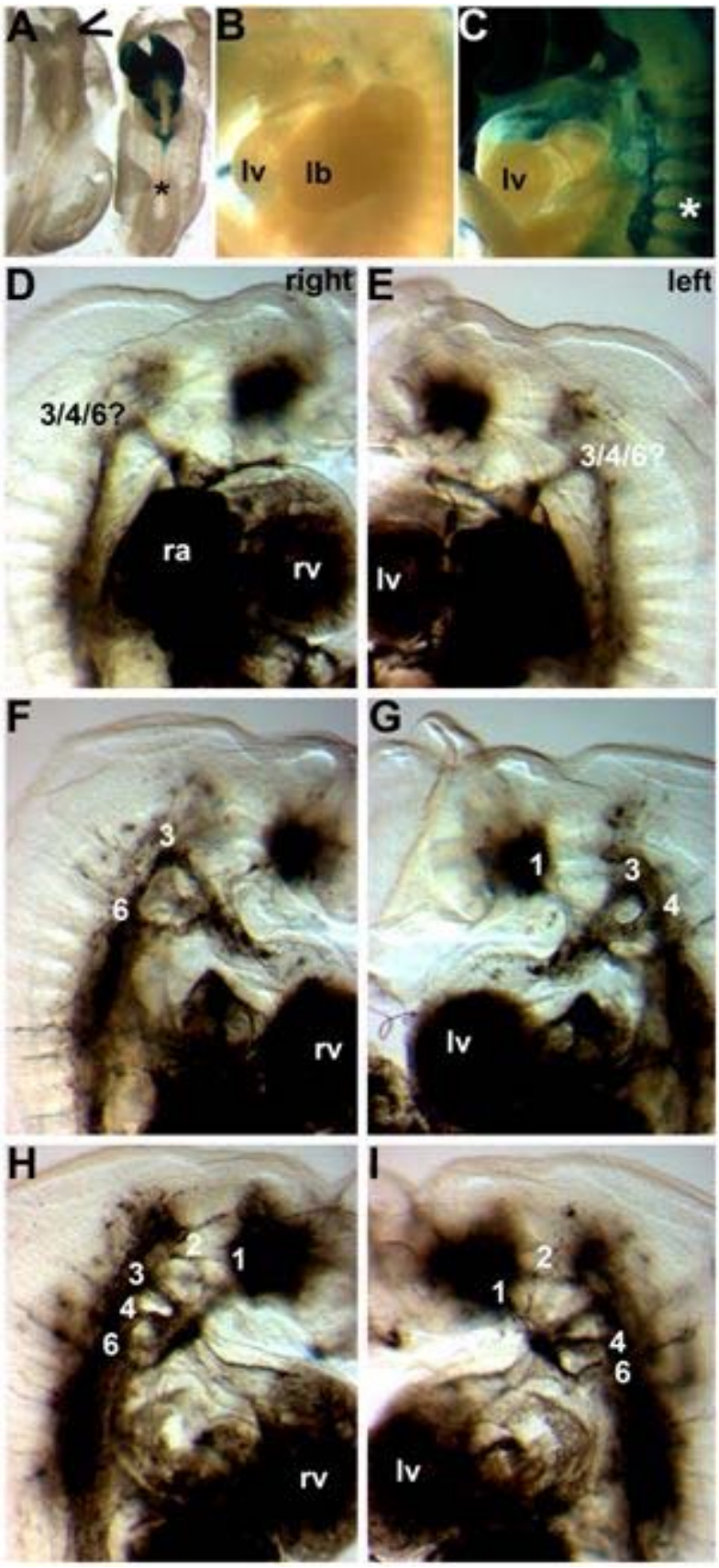
A
B
lv
lb
C
lv
*
D
right
3/4/6?
ra
rv
E
left
3/4/6?
lv
F
3
6
rv
G
1
3
4
lv
H
2
1
3
4
6
rv
I
2
1
4
6
lv

Figure 9: NC lineage mapping and AAA analyses in *Wnt1Cre/DTA* mutants

(A-C) Lineage mapping of *Wnt1Cre* positive cells in triple *Wnt1Cre/R26R-DTA/R26R-lacZ* reporter mice shows efficient ablation of cells. (A) At E8.5, the only few *Wnt1Cre* cells remaining are in the head (arrowhead in A). Note lack of *Wnt1Cre* expression in region corresponding to trunk NC site of formation (asterisk in A) in the E8.5 control embryo. (B) By E9.5, the *lacZ*-positive *Wnt1Cre*-expressing cells are almost completely gone within the ablated embryo compared to control (C). (D-I) Ink injections on 3 individual *Wnt1Cre/DTA* mutant embryos at E11 reveal randomized defects in left-right AAA remodeling. (D, E) Ink injection reveals just 1 arch artery on both sides in 1 mutant. (F, G) Ink injection reveals right $3^{rd}/6^{th}$ AAA's and left $1^{st}/3^{rd}/4^{th}$ AAA's in 1 mutant. (H, I) Ink injection reveals right $1^{st}/2^{nd}/3^{rd}/4^{th}/6^{th}$ AAA's and left $1^{st}/2^{nd}/3^{rd}/4^{th}/6^{th}$ AAA's in 1 mutant. lv = left ventricle, lb = limb bud, ra = right atria, rv = right ventricle (numbers indicate position of AAA's). (Ink injections performed by Dr. Simon J. Conway, PhD).

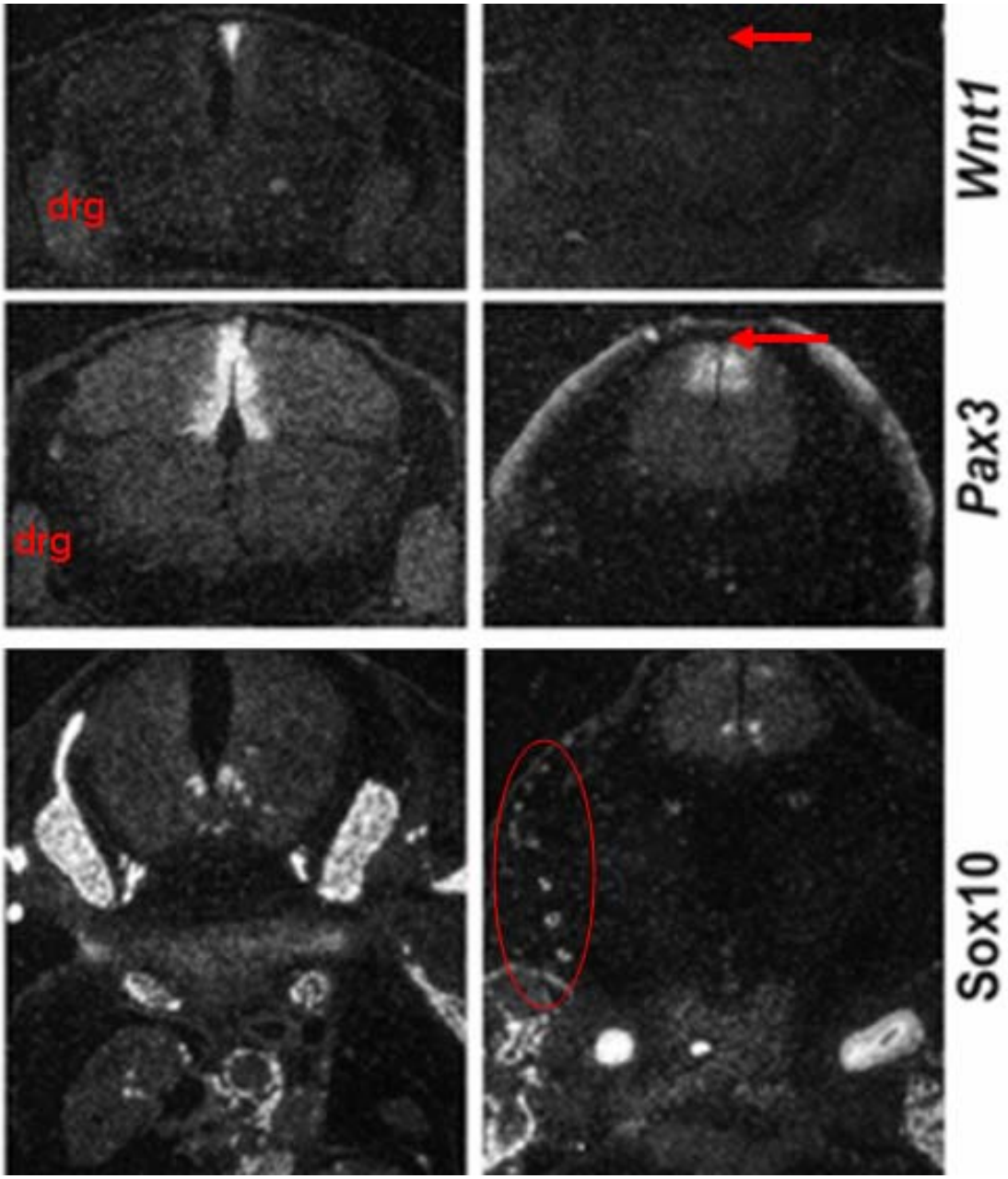
drg
drg
Wnt1
Pax3
Sox10

Figure 10: *In situ* hybridization analysis of NC markers in *Wnt1Cre/DTA* mutants.

Wildtype (left panels) and *Wnt1Cre/DTA* mutant (right panels) show differential expression of NC markers in E13.5 embryos. Transverse sections showing lack of expression of *Wnt1* and *Pax3* in mutant NT's compared to controls (red arrows in top and middle panels). Expression of *Sox10* is completely absent in mutant drg (lower panel), but still present in a few migratory NC that have presumably escaped *Wnt1Cre*-mediated ablation (red circle in lower panel). (drg: dorsal root ganglia). (*In situ* hybridization performed by Jian Wang).

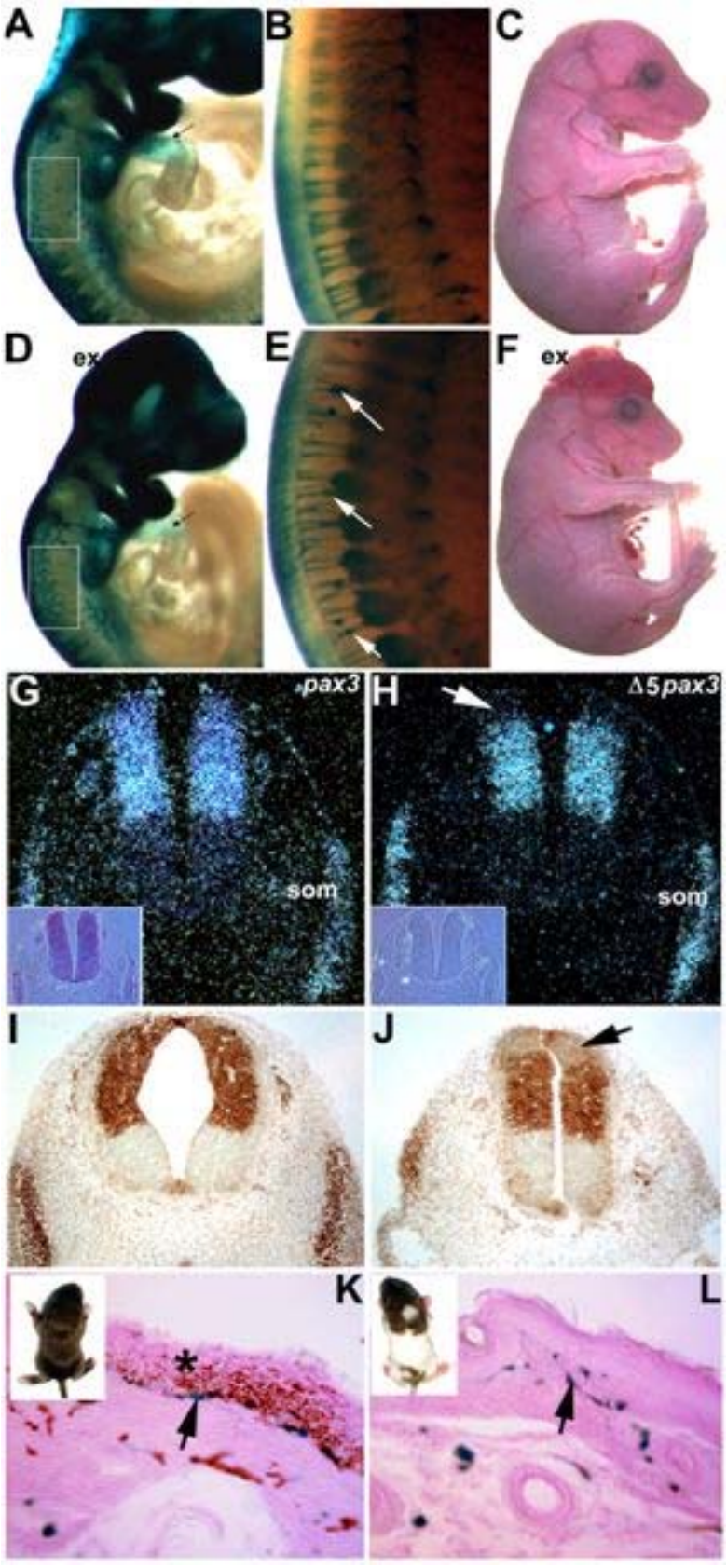
A
B
C
D
ex
E
F
ex
G
Δpax3
som
H
Δ5pax3
som
I
J
K
*
L

Figure 11: Analysis of *Pax3$^{f/d5}$/Wnt1Cre* conditional knockout. *Wnt1Cre/R26R-lacZ* lineage mapping of wildtype (A-C) and *Wnt1Cre* conditional mutant (D-F) NC. CNC colonization of E10.5 mutant 4th and 6th AAA's is equivalent to wildtype, but E11.5 mutants exhibit disorganized Schwann cell morphogenesis and clump on neurons (arrows in E). Conditional mutants also exhibit exencephaly (D&F), but are otherwise identical to wildtype littermates. (G&H) *In situ* hybridization at E10 using a *Pax3* exon5-specific probe on conditional mutant (H) and control (G). Note *d5* transcripts are missing in dorsal-most neural tube (arrow in G), but present in somites. Phase contrast images are inset to verify tissue integrity. (I&J) Immunohistochemistry at E10 using a Pax3 antibody on conditional mutant (J) and control (I). (K&L) P10 pups showing pigmentation defects in mutants (inset in L) compared to littermate control (inset in K). *LacZ*-staining revealed melanocytes (arrow in K) in control epidermal basal layer (*) that are positive for melanin (brown). Mutants exhibit *lacZ*-positive melanocytes at similar densities but are all negative for melanin synthesis (L). ex = exencephaly, som = somite. (*Pax3$^{f/d5}$/Wnt1Cre* data generated by Dr. Hong-Ming Zhou, PhD).

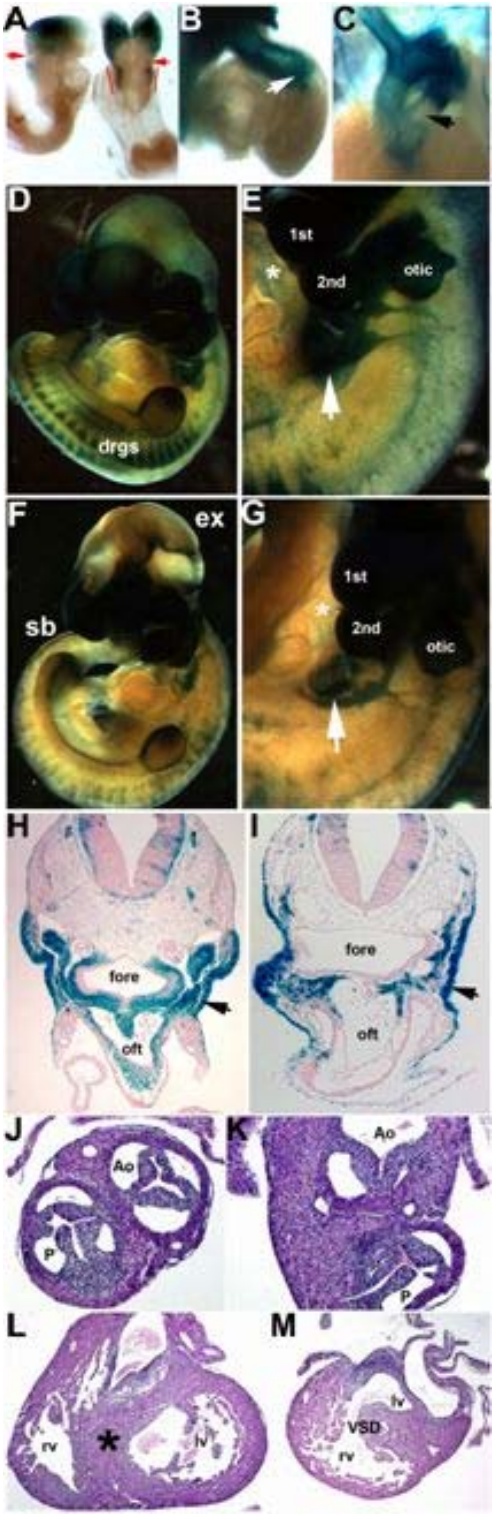
A
B
C
D
drgs
E
1st
2nd
otic
F
ex
sb
G
1st
2nd
otic
H
fore
oft
I
fore
oft
J
Ao
P
K
Ao
P
L
rv
lv
M
lv
VSD
rv

Figure 12: Analysis of *Pax3$^{f/d5}$/AP2aCre* conditional knockout. (A-C) *AP2aCre/R26R-lacZ* lineage mapping in wildtype embryos shows colonization of *lacZ*-positive cells in E8 neural folds (A) and E10.5 OFT (B&C). (D-G) *AP2aCre/R26R-lacZ* lineage mapping in wildtype (D&E) and conditional mutant (E&G) embryos at E10.5. Note reduced CNC colonization of E10.5 mutant 4th and 6th AAA's (arrow in G) compared to wildtype (arrow in E). Conditional mutants also exhibit exencephaly (D&F). (H-M) Histological analysis of transverse sections of embryos shown in (D-G). Reduced CNC colonization of OFT region in conditional mutant (I) compared to control (H). Conditional mutants display DORV/VSD (L&M) and enlarged OFT cushions (asterisk in L). Ao = aorta, ex = exencephaly, fore = foregut, lv = left ventricle, oft = outflow tract, otic = otic sulcus (presumptive ear), rv = right ventricle (numbers indicate position of AAA's). (*Pax3$^{f/d5}$/AP2aCre* data generated by Dr. Hong-Ming Zhou, PhD).

Chapter III: Beta-adrenergic signaling is essential for maintaining embryonic cardiac output and *in utero* viability

1. Abstract

The origins of heart failure in newborns are linked to malformations present before birth or acquired postnatally. Congenital malformations are due primarily to aberrant gene expression, which ultimately leads to poor cardiac output both *in utero* and after birth. However, there is still much to understand about the etiology of CHDs and their link to embryonic heart failure and eventual prenatal lethality. In this study, two mouse models of NC deficiency were used as tools to study the mechanisms underlying CHDs *in utero* with a particular focus on the novel role of NC on myocardial homeostasis during early embryonic development. The first mouse model is a *Pax3* systemic knockout (*Pax3*$^{d5/d5}$). Homozygous embryonic mutants display 100% embryonic lethality by embryonic day 14 (E14.0) accompanied by defects in OFT septation, PTA/VSD, EC-coupling, NT closure, PNS and adrenal development. The second mouse model is a genetic ablation model using a *Wnt1Cre*-activated *ROSA26*-diphtheria toxin fragment-A (*R26R/DTA*) cell-killing system. Ablation of *Wnt1Cre*-expressing NC generated fully penetrant PTA/VSD defects. However, ablated mutants (*Wnt1Cre/DTA*) survived to birth (well past the E14.0 lethality observed in systemic *Pax3* mutants). This difference in temporal lethality led to the examination of the underlying cause of poor cardiac function and eventual

embryonic death in *Pax3* mutants. Based on molecular comparison of these two models, the underlying cause was determined to be insufficient stimulation of the beta-adrenergic pathway due to significantly reduced levels of circulating catecholamines in affected *Pax3* mutant embryos. As a result, pharmacological rescue to birth of these embryos was made possible via administering isoproterenol (a synthetic catecholamine) or forskolin (a pro-adrenergic stimulant) to pregnant dams. This study is the first of its kind to conclusively delineate the role of Pax3-mediated NC deficiency in pathogenesis of embryonic heart failure and eventual *in utero* lethality.

2. Introduction

Congenital heart defects (CHDs) are the most common birth defect in humans, present in approximately 1% of all live births and up to 10% of stillbirths [96]. Although a profundity of literature exists on the pathogenesis of heart failure in the adult, less is known about the underlying causes in newborns [97]. Nevertheless, some progress in the field has been made on the etiology [98], diagnosis and repair [99] of CHDs in the newborn. Based on such reports, it is believed that heart failure in newborns is linked to malformations present before birth or acquired postnatally [100, 101]. These malformations are due primarily to aberrant gene expression [102], which can ultimately lead to poor cardiac output both *in utero* and after birth.

The role of NC cells in heart development and their impact on CHDs is well studied. The NC is a multipotent and transient migratory lineage originating from the neuroepithelium, which borders the surface ectoderm and gives rise to the embryonic neural tube [5]. They give rise to an array of different cell types, tissues, and organs [1, 2]. Different subpopulations of NC have been identified based on their rostrocaudal position of origin along the axis of the developing embryo, their specific properties, and the nature of their derivatives. The developing neural tube extends in a rostral to caudal direction beginning at the mid-diencephalon. As a result, NC cells have been broadly subdivided into cranial, cardiac, trunk and vagal crests [5]. The aim of this project was to focus

primarily on the roles of both cardiac and trunk NC cell populations on regulating myocardial structure and function respectively. A specific emphasis was placed on the importance of these two aspects of cardiogenesis in preventing embryonic lethality due to poor cardiac output.

Previous studies [64, 65, 67] have shown that *Gata3, Th*, and *Dbh* mutants die by E11 due to deficiencies in noradrenaline levels. Specifically, *Th* and *Dbh* mRNA was reduced, leading to overall reduction in catecholamine synthesis and subsequent noradrenaline levels. Furthermore, pharmacological recue of *in utero* lethality was possible by feeding pregnant dams with L-DOPA, which is a catecholamine intermediate. Similarly, dying catecholamine-deficient fetuses have been rescued to birth via isoproterenol (a beta-adrenergic receptor agonist) feeding, as beta-adrenergic receptors are expressed in embryonic hearts [103]. The authors of this study postulated that the observed lethality, which was directly due to a significant deficiency in catecholamine levels, was caused by an underlying failure of trunk NC cells to properly give rise to developing sympathetic neurons, adrenal chromaffin cells and enteric neurons. Also, more recent studies demonstrated that *Insm1* mutants have delayed differentiation of NC-derived sympatho-adrenal precursor cells, reduced levels of both *Th* and *Dbh (*markers of differentiation of sympathetic neurons) and are upstream of such noradrenaline compounds as norepinephrine [104]. Furthermore, restoration of normal noradrenaline levels was possible by feeding agonists to pregnant dams. This clearly demonstrated that reduced noradrenaline levels were responsible for

Insm1 mutant embryonic lethality. However, these studies never determined the direct molecular pathogenesis of the lack of norepinephrine at these early stages on poor embryonic cardiac output and function. Nor did they conclusively link the role of trunk NC cell differentiation in regulating sympathetic innervation of the heart during early stages of cardiogenesis, and how such innervation may be important in embryonic cardiac output.

To address these concerns, a novel *Pax3* allele was utilized ([87, 88]; described in Chapter II), which allowed for the generation of homozygote systemic Pax3 delta-exon5 (*Pax3*$^{d5/d5}$) knockout mice. This mouse line was then compared to the *Wnt1Cre/DTA* mouse line ([89]; described in Chapter II), which allowed for permanent, genetic ablation of the *Wnt1Cre*-expressing NC lineage in the developing embryo. The results of this project, for the first time, conclusively describe the indirect role that Pax3 plays in regulating embryonic cardiac output as well as the underlying cause of embryonic lethality in *Pax3* mutants. In so doing, it is the first of its kind to provide significant insight into understanding the role that CNC-extrinsic factors play in regulating myocardial function during development.

3. Materials and Methods

3.1. Mouse colonies, breeding, genotyping and PCR

The *Pax3* floxed conditional allele was generated as previously described [87, 88]. Exon 5 of the *Pax3* gene, which encodes the *Pax3* homeodomain, was flanked by 5' and 3' *loxP* sites. This allowed for Cre-mediated removal of the floxed *Pax3* homeodomain. To selectively remove the floxed allele in the germline, adult male heterozygous floxed Pax3 ($Pax3^{f/+}$) mice were crossed to female C57Bl6/129 *Tie2Cre*-positive females to generate heterozygous delta exon 5 Pax3 ($Pax3^{d5/+}$) adult mice. The resultant $Pax3^{d5/+}$ males were crossed to wildtype C57Bl6/129 females to remove the *Tie2Cre* transgene. $Pax3^{d5/+}$ (*Tie2Cre*-negative) mice were then intercrossed to generate $Pax3^{d5/d5}$ mutant embryos. PCR screening strategy was used as previously described [88]. The $Pax3^{d5/+}$ mice were then crossed into the *Wnt1Cre* mouse [4] to carry out lineage mapping studies (Scheme 1). The *R26R-lacZ* reporter mice were obtained from Jackson Laboratories (JaxLab stock #003474) and the *ROSA26-eGFP-DTA (R26R-DTA)* mice were generously gifted by A. Copp (University College London, England). The *R26R-DTA* was made by introducing an *eGFP-DTA* (enhanced green fluorescent protein-diphtheria toxin fragment A) cassette into the ubiquitously expressed *ROSA26* reporter locus [89]. As a result, *R26R-DTA* mice express eGFP ubiquitously, but diphtheria toxin A-chain (DTA) is switched on only when Cre is present to remove the floxed stop codon sequence in front of DTA-encoding sequence (Scheme 2). To generate the *Wnt1Cre/DTA* ablated

mutant embryos, *Wnt1Cre* mice were crossed into the *R26R-DTA* mouse line to produce progeny that were both *Wnt1Cre*-positive and *R26R-DTA* positive. All mouse colonies for this study were maintained on a mixed C57Bl6/129 genetic background. Mice were housed and handled in accordance with Indiana University Institutional Animal Care and Use Committee guidelines. For timed pregnancies, the day of observed vaginal plug was designated embryonic day 0.5 (E0.5).

3.2. Histological immunohistochemistry and *in situ* hybridization

Embryos were fixed in 4% PFA overnight at 4°C and processed for paraffin histology as previously described [90]. Immunohistochemistry was carried out using ABC kit (Vectastain) with DAB and hydrogen peroxide as chromogens. The endogenous peroxidase was quenched via incubation in 0.3% hydrogen peroxide in methanol for 30min. Dilutions of primary antibody were 1:10000 for mouse anti-αSMA (Sigma), 1:500 for rabbit anti-Th (Cell Signaling), 1:1000 for secondary anti-mouse and 1:1000 (Jackson Labs) for secondary anti-rabbit antibody (Jackson Labs). Incubation in primary antibody was carried out at 4°C overnight, and incubation in secondary antibody at room temperature for 30 minutes. Radioactive *in situ* hybridization for *ANF* expression was performed as previously described [91]. Both sense and antisense ^{35}S-UTP-labeled probes were used as negative controls and experimental samples respectively. Analyses were performed on serial sections within at least three independent embryos of

each genotype. To quantify expression differences, silver grains were counted per square area on serial sections and averaged.

3.3. Wholemount X-gal (*lacZ*), immunostaining and *in situ* hybridization

For X-gal staining, whole embryos were fixed in 4% PFA immediately after dissection for 2h. They were then washed 10min in PBS and subsequently washed 2x in β-gal buffer (0.058 M Na_2HPO_4, 0.042 M NaH_2PO_4, 0.001M $MgCl_2$, 0.01% NP40), 5mins each. An additional wash was done overnight at 4°C, then embryos were changed into X-gal substrate (0.1% X-gal, 0.005M $K_3Fe(CN)_6$, 0.005M $K_4Fe(CN)_6$, 0.001M EGTA), and incubated at 37°C in the dark. Embryos were then fixed in 4% PFA after successful X-gal staining was completed. Wholemount immunostaining for anti-neurofilament was performed by fixing embryos in methanol:DMSO (4:1) solution to allow for efficient permeabilization. Embryos were then processed into methanol for storage, or rehydrated for immediate staining. For staining, anti-neurofilament antibody (1:200, Sigma) was incubated at 4°C overnight. After color intensification with 0.03% H_2O_2, embryos were post-fixed in 4% PFA. For wholemount *in situ* hybridization, embryos were stored in 100% methanol, then rehydrated and digested in proteinase K. Embryos were processed following routine procedures as previously described [105, 106] into prehybridization buffer (Formamide, 20X SSC pH 4.5, yeast tRNA, 50 μg/mL Heparin with DEPC H_2O, 10% SDS) at 70°C for up to 15h. Both *Ncx1* and *α1c* antisense and sense probes were used as experimental and negative controls respectively.

3.4. Western and RT-PCR analyses

Westerns were performed using mouse monoclonal anti-serca2a (1:500, Sigma), rabbit polyclonal anti-Th (1:1000, Cell Signaling), rabbit polyclonal phospho- and total- anti-phospholamban, anti-troponin I, and anti-ERK 1/2 (1:1000, Cell Signaling). All antibodies were incubated 1h at room temperature, except for phospho-antibodies which were incubated at 4°C overnight. To confirm equal loading, mouse monoclonal anti-β-tubulin antibody (1:10000, Roche) was used. Secondary HRP-conjugated goat anti-mouse and goat anti-rabbit IgG (Jackson Laboratories) were used. Antibodies were detected using the enhanced chemiluminescence (ECL) plus detection system (Amersham). To maintain equal loading between blots, membranes were stripped after each blot using stripping buffer (Thermo Scientific) at 55°C for 30min, and then subsequently oscillated for additional 30min, before being blocked in 5% milk dissolved in 0.1% PBS-Tween20 and reprobed. Densitometry of immunoreactive bands was performed using Image J 1.37v (NIH). RT-PCR analyses was performed on cDNA synthesized from RNA extracted from isolated E13 embryo hearts of control, mutant and mutant treated with isoproterenol (n = 3). This was done using a Superscript-II kit (Invitrogen) with 5μg RNA samples and random primers (Invitrogen). cDNA samples were mixed with SYBR green PCR master mix reagent (Roche) and amplified in 96-well plates, using a Lightcycler machine (Roche). To ensure specific amplification, specific primers for b1ar (forward primer 5' - CGA GCT CTG GAC TTC GGT AG - 3' and reverse primer 5' - GGC ACG TAG AAG GAG ACG AC - 3'), b2ar (forward primer 5' - AAG AAT AAG

GCC CGA GTG GT - 3' and reverse primer 5' - GTC TTG AGG GCT TTG TGC TC - 3'), ac5 (forward primer 5' - ACA ACA TTC TGC CCA AGG AC - 3' and reverse primer 5' - CAT TTG GTC CAT CAG CTT CA - 3'), ncx1 (forward primer 5' - CAA TTG CTT GTC TTG GGT CA - 3' and reverse primer 5' - TCA CTC ATC TCC ACC AGA CG - 3') and ryr2 (forward primer 5' - CAC ATG GAC GAT GGT TTG AA - 3' and reverse primer 5' - TGT TCT GCT TGT CCT CAT GC - 3') were used. Amplification signals for all primer products were normalized with levels of GAPDH.

3.5. HPLC and PKA activity assays

HPLC analyses were performed as previously described [107]. Embryos were harvested and immediately placed into liquid nitrogen. Frozen embryos were homogenized in cold buffer (2M Tris, pH 8.6; 5mg activated alumina). Samples were vortexed, centrifuged and supernatant discarded. Alumina was transferred to a 0.22-µm Ultrafree MC filter (Millipore) and washed in distilled H_2O. Catecholamines were eluted using cold 0.2 N perchloric acid and then re-centrifuged through a fresh 0.22-µm Ultrafree filter at 5,000 rpm for 10 min at 4°C. Catecholamines were separated by HPLC on a 3 × 150-mm (3 µm) C-18 column (ESA) at a flow rate of 0.5 ml/min at room temperature with MD-TM mobile phase (ESA) and quantified by electrochemical detection (EC) using an ESA model 5020 guard cell set to +350 mV, followed by an ESA model 5014B analytical cell (electrode 1 at −150 mV and electrode 2 at +220 mV). The data are expressed as average (+/- standard error) norepinephrine and dopamine

concentration (pmol/embryo) normalized to DHBA (3,4-Dihydroxybenzylamine). PKA activity assays were performed using SignaTECT PKA Assay system kit (Promega) following manufacturer's instructions. Briefly, embryos were homogenized in 5ml cold extraction buffer (25mM Tris-HCl, pH 7.4; 0.5mM EDTA; 0.5mM EGTA; 10mM β-mercaptoethanol; 1ug/ml leupeptin; 1ug/ml aprotinin), centrifuged (5min, 4°C, 14000 x *g*) and supernatant was kept. Supernatant enzyme preparations were radioactively labeled using γ-^{32}P-ATP (3000Ci/mmol) 10uCi/ul and serially diluted in 0.1mg/ml BSA, before incubating for 5min at 30°C with reaction mix (provided by manufacturer) +/- 5ul/reaction of 0.025mM exogenous cAMP. To ensure specificity, biotinylated Kemptide (LRRASLG), which is a known specific target of PKA, was used as substrate in the reaction. Incubated samples were then spotted onto SAM® (Streptavidin-biotinylated biotin capture Membrane) paper. Spotted SAM blots were washed 3x in 2M NaCl, and then in 2M NaCl in 1% H_3PO_4. SAM blots were dried at room temperature for 30min or under a heat lamp for 5min, then total radioactive counts were determined. Counts were done by placing blots into scintillation vials containing 1ml scintillation fluid (ScintiVerse cocktail, Fisher) and measured using a scintillation counter machine (Beckman Coulter LS 6500). PKA enzyme activity was measured in pmol/min/ug of protein relative to specific activity of γ-^{32}P-ATP.

3.6. Proliferation analyses

Cell proliferation analyses were performed using Ki67 and BrdU incorporation.

For Ki67 staining, monoclonal rat anti-Ki67 antibody (1:25, DakoCytomation) was used. For detection, sections were boiled in 1x antigen retrieval buffer (Dako) for 20min and then cooled to room temperature prior to blocking. BrdU analysis was performed by injecting pregnant dams with reagent (Invitrogen) at a concentration of 1ml/100g mouse body weight for 1h prior to harvesting embryos. Embryos were processed for routine paraffin sectioning. Incorporated BrdU was detected using mouse anti-BrdU antibody (2 drops/section, Zymed) following manufacturer's instruction. Detection of antibody localization was performed using ABC kit (Vectastain) with DAB and hydrogen peroxide as chromogens. For comparison of both Ki67 and BrdU staining, sections from age-matched littermate embryos for each genotype (n = 3) were used. For quantification of both assays, positive cells were counted per square area on serial sections and averaged.

3.7. Echocardiography functional analysis

For echocardiography analysis, pregnant dams were anesthetized using 3% isoflurane / 97% oxygen for initial induction and maintained on 1-2% isoflurane / 98% oxygen. Regular monitoring of effectiveness of anesthesia was done by checking for pinch or stretch reflexes. For measurements, Visualsonics Vevo 770 machine was used operated by Visualsonics Vevo software version 3.0. For detection of embryonic signals, imaging was performed using Probe # RMV-704

at 40MHz. To avoid background, mouse chest hair was removed using a spatula after application of Nair shaving cream. For this study, 9 litters were analyzed (E13.5 – 16.5), and data obtained from all experimental embryos were compared only to their littermate controls.

3.8. Mouse surgical implantation of osmotic mini-pumps

Pregnant dams were anesthetized using 5% isoflurane / 95% oxygen for initial induction and maintained on 3% isoflurane / 97% oxygen. Regular monitoring of effectiveness of anesthesia was done by checking for pinch or stretch reflexes. Beta-dyne was used to sterilize the surgical incision site. Osmotic 7-day mini-pumps (Alzet 2001, flow rate ~1ul/h) filled with saline or isoproterenol (28mg/ml in saline) or forskolin (3.4mg/ml in 70:30 DMSO:Saline) were implanted subcutaneously into pregnant dams at the 8.5 day-stage or 10.5 day-stage of gestation. For survival studies, embryos were harvested E14.5 onwards. For molecular analytical studies, embryos were harvested at the time-point required for study (E10.5, E12.5, E13 and E16.5). For duration studies, mini-pumps were removed at E10.5 (2 days post-implantation) and embryos were harvested at E14.5 onwards; alternatively, mini-pumps were implanted at E10.5 and embryos harvested E14.5 onwards.

4. Results

4.1. *Pax3*$^{d5/d5}$ mutant embryos display early signs of embryonic heart failure

As mentioned earlier (Chapter II), *Pax3* mutant embryos display defects in OFT remodeling (PTA) and NT closure (exencephaly, rachischisis / spina bifida) (Figure 13A-D). In order to assess the effects, if any, of *Pax3* deletion on heart functional development, *in situ* hybridization for *ANF* (a marker for heart failure) was performed on E13 mutant and control hearts. Results indicate a significant increase in *ANF* mRNA expression in both the atrial and ventricular myocardium of *Pax3* mutant hearts compared to littermate controls (13E, F). In order to determine the temporal origin of the pathogenesis of heart failure, marker analyses were performed on earlier stage embryos (E9). Based on wholemount *in situ* hybridization using *α1c* and *Ncx1*, it was determined that as early as E9, *Pax3* mutant hearts display defects in EC-coupling as expression of these markers were both appreciably increased in mutant hearts compared to littermate controls (13G, H). In order to determine the effect of misexpression of these markers on myocardial structure, histological and proliferation analyses was performed on E12.5 mutant and control hearts. However, based on results from both Ki67 and BrdU staining, no observable differences were found in proliferation levels (13I, J). Furthermore, the myocardium appeared intact and normal in mutants analyzed at this stage compared to their littermate controls.

4.2. *Pax3*$^{d5/d5}$ mutant embryos lack PNS derivatives

As described previously (Chapter II), based on NC lineage mapping data performed using *Wnt1Cre/R26R-lacZ*, *Pax3* mutants have reduced numbers of migratory NC and NC-derived structures. To follow up on these previous observations, this project focused primarily on the lack of NC-derived PNS structures and the potential effect this may have on cardiac output. Based on NC lineage mapping data, it was determined that *Pax3* mutants have deficiencies in derivatives of the TNC, including the PNS, adrenal medulla and dorsal root ganglia (Figure 14A-E; 14G, H). NC lineage mapping results performed at E11 revealed a severe lack of migratory NC contributing to the dorsal root ganglia, sympathetic ganglia and enteric neurons (14A-E). To confirm the effects of reduced numbers of NC, histological transverse sections of the dorsal root ganglia were analyzed at E10.5. X-gal staining confirmed fewer *lacZ*-positive cells colonizing the dorsal root ganglia in *Pax3* mutants compared to controls (14G, H). As a result, the size of the dorsal root ganglia in *Pax3* mutants was appreciably reduced. To determine the global effect of *Pax3* deletion on PNS structure and function, wholemount anti-neurofilament (a neuronal marker of differentiation for the PNS neuronal network) staining was performed at E11. This revealed not just defects in structural organization of the PNS neuronal network in *Pax3* mutants, but also in their ability to differentiate properly as levels of neurofilament expression were appreciably reduced (14F). In contrast to *Pax3* mutants that develop poor cardiac output, *Wnt1Cre/DTA* mutants appear to have no observable embryonic heart functional defects, as these embryos survive to

birth (Chapter II). In order to determine if *Wnt1Cre* expression could successfully ablate the population of TNC cells that fail to give rise to the defective structures in *Pax3* mutants, NC lineage mapping analysis was performed (described in more detail previously in Chapter II). As mentioned previously, *Wnt1Cre* expression was determined to not be expressed in the region of NT that gives rise to TNC at early E8.5 stages. Thus, *Wnt1Cre*-mediated ablation only affected later waves (E9.5 onwards) of TNC cells originating from this region. This was due to a normal spatiotemporal delay in its rostrocaudal expression along the axis of the developing tube (14l).

4.3. *Pax3*$^{d5/d5}$ mutants display severe deficiencies in tyrosine hydroxylase and catecholamine levels

To determine the role of this early (*Wnt1Cre*-negative) population of TNC on PNS development, sympathoadrenal differentiation and catecholamine levels were assessed. Based on immunostaining analyses using anti-Th antibody, it was determined that there is a lack of Th expression in *Pax3* mutant adrenals when compared to *Wnt1Cre/DTA* adrenals (Figure 15A-C). This apparent deficiency appears to be due to a lack of formation or maintenance of the adrenal medulla in the *Pax3* mutants. This indicates that the early subpopulation of TNC observed in *Wnt1Cre/DTA* mutants is capable of colonizing the adrenals and supporting normal adrenal development. As reported previously (Chapter II), even though there is a lack of NC migration in *Pax3* mutants, there is still successful colonization (albeit in reduced numbers) of NC cells at the dorsal root ganglia

and neurons of the PNS network. In order to determine why these few NC cells were incapable of supporting sympathoadrenal development, analysis of Th expression in this subpopulation of cells was performed. Based on anti-Th immunostaining done on lineage mapped NC cells, it was determined that in addition to fewer TNC cells colonizing the dorsal aortae (the site of induction of TNC cells fated to develop along the sympathoadrenal lineage), these cells also failed to express proper levels of Th (15D-G). This indicates a Pax3-specific role in TNC specification and differentiation along the sympathoadrenal lineage. To determine the global effect of lack of differentiation of these cells on Th levels, whole embryo protein lysates were analyzed. Western analyses confirmed a 70% reduction in Th levels in *Pax3* mutants as early as E10.5, and a progressive loss of Th expression up till E13 (15H, I). Th levels were also assessed by Western in whole embryo lysates extracted from E13 *Wnt1Cre/DTA* mutants. However, no significant differences were observed between mutants and littermate controls (data not shown). Since Th is a noradrenaline precursor, HPLC measurements were performed to determine the effect on global catecholamine levels in E13.5 *Pax3* mutants. HPLC data confirmed a 93% reduction in norepinephrine levels in *Pax3* mutants compared to littermate controls. This reduction was determined to be Pax3-dose dependent as $Pax3^{d5/+}$ heterozygote embryos displayed a 21% reduction in norepinephrine levels (Table 1). However, this slight reduction does not appear to be significant enough to cause lethality as *Pax3* heterozygote mice are viable. Dopamine levels were also measured and determined to be slightly lower in *Pax3* mutants. However, at these early stages, levels of dopamine were

too low to determine any significant difference between *Pax3* mutants and controls.

4.4. *Pax3*$^{d5/d5}$ mutants are rescued to birth via isoproterenol or forskolin treatment

To compensate for low fetal catecholamine levels, isoproterenol (a synthetic catecholamine) was administered to pregnant dams via mini-pump implantation. Since isoproterenol is permeable pass the maternal placenta, treatment of pregnant dams was capable of supplementing the observed reductions in catecholamine levels. More importantly, by doing so, *Pax3* mutants were viable until birth. In order to achieve rescue, pregnant dams were treated as early as E8.5, and litters were analyzed from E14.5 (normal time-point of lethality) onwards. Analyses of treated litters (n = 40) revealed presence of *Pax3* mutants in normal Mendelian ratios (~28%) from E14.5 until birth (Table 2). In order to determine the temporal window required for successful rescue, pregnant dams were treated as late as E10.5, and this was determined to be sufficient for rescue. Interestingly, only ~50% rescue of *Pax3* mutants occurred when pregnant dams were treated at E8.5 and taken off the treatment at E10.5, indicating that from E10.5 onwards cardiac development has a critical requirement for normal catecholamine levels. Since catecholamines are important in beta-adrenergic stimulation, to determine the functional importance of the adrenergic pathway on early embryonic cardiac output, an alternative pharmacological approach was performed. To do this, isoproterenol treatment

was replaced with forskolin, which is a specific activator of adenylate cyclase, an important intermediary in the beta-adrenergic pathway. Surprisingly, forskolin treatment of pregnant dams was also capable of rescuing *Pax3* mutants to birth. Analysis of litters (n=9) treated with forskolin revealed that *Pax3* mutants were present in normal Mendelian ratios (~22%) from E14.5 onwards (Table 1).

4.5. Structural defects persist in isoproterenol-treated *Pax3*$^{d5/d5}$ mutants

Despite pharmacological rescue by either isoproterenol or forskolin, treated *Pax3* mutants still displayed all of the classical structural defects associated with Pax3-deficiency. Analysis of E18.5 isoproterenol-treated *Pax3* mutants revealed a presence of NT defects (exencephaly, spina bifida) and hypoplastic limbs (Figure 16A). In addition, based on NC lineage mapping analysis, there is still a deficiency in numbers of migratory NC at E10.5 (16B) and in formation of smooth muscle cells derived from *Pax3*-expressing somite-derived muscle progenitor cells (16C). Furthermore, due to lack of migratory NC cells, OFT remodeling defects are still present including PTA and accompanied VSD (16D-G). There was also a gross reduction in dorsal root ganglia size of treated mutants compared to littermate controls (16H, I). In summary, despite being viable until birth, treated *Pax3* mutants are still structurally similar to untreated.

4.6. Echocardiography analyses reveal appreciably improved cardiac function in isoproterenol-treated *Pax3*$^{d5/d5}$ mutants

To determine the effect of isoproterenol treatment on cardiac output and function, echocardiography analyses was performed. Echo data confirmed poor cardiac function in Pax3 mutants at E13.5 (1 day prior to dying). Both cardiac contractility and heart rate were diminished in Pax3 mutants compared to littermate controls (Figure 17A, top and middle panels). However, isoproterenol treatment was capable of restoring normal cardiac output based on analyses performed at E16.5 on *Pax3* mutants, which were functionally indistinguishable from their littermate controls (17A, lower panel). For this analysis, it was possible to correctly distinguish mutants from their littermate controls *in utero*. This was done by correctly identifying NT defects (exencephaly) in *Pax3* mutants as early as E13.5 *in utero* (17B).

4.7. Insufficient stimulation of the beta-adrenergic pathway is the underlying cause of poor cardiac output and subsequent lethality in *Pax3*$^{d5/d5}$ mutants

In order to determine the effect of reduced catecholamine synthesis and subsequent isoproterenol treatment on the embryonic beta-adrenergic pathway, extensive analysis of key molecular factors in the pathway was carried out. In the absence of dependable antibodies at these early stages, mRNA levels of molecular factors involved in the upstream beta-adrenergic pathway were analyzed. Based on RT-PCR analysis done on mRNA extracted from E13

isolated hearts, it was determined that mRNA levels of b1ar, b2ar and ac5 were significantly reduced in *Pax3* mutant hearts compared to controls. However, these levels were normalized upon treatment with isoproterenol (Figure 18A). Since an increase in expression of both *α1c* and *Ncx1* mRNA levels in E9 *Pax3* mutant embryos had been observed, analysis of downstream key elements in the beta-adrenergic pathway that are important in regulating calcium handling was also carried out. RT-PCR analysis using mRNA extracted from E13 isolated hearts revealed a similar increase in mRNA levels of *Ncx1* and *Ryr2* in *Pax3* mutant hearts. Similarly, these levels were normalized upon treatment with isoproterenol (18B). Since Echo studies had revealed improved cardiac function, markers important in regulating embryonic cardiac contraction / relaxation were examined. Specifically, phosphorylated levels of phospholamban (a regulator of Serca activity and cardiac relaxation) and phosphorylated levels of troponin I (a regulator of cardiac contraction) were identified as being important players in regulating embryonic contraction / relaxation. Based on Western analyses on protein samples extracted from E13 isolated hearts, it was determined that expression of these molecular targets was decreased in *Pax3* mutant hearts. However, reduced levels of expression were normalized post-isoproterenol treatment (18C). Interestingly, no observable differences were observed in Serca protein levels between *Pax3* mutant and control hearts. However, based on phospholamban results, it is unclear whether protein level is an adequate reflection of Serca activity. Although there was no observable difference in phosphorylated levels of ERK 1/2 between *Pax3* mutant and control hearts,

isoproterenol treatment always led to a significant increase. As a result, as an internal technical control for all protein samples extracted from treated hearts, phosphorylated levels of ERK 1/2 were used to determine effective delivery and activity of the drug.

4.8. Role of cAMP/PKA in regulating embryonic cardiac output and embryonic survival

PKA activity assays were performed on whole embryo lysates at E12.5 to determine effect of PKA activity. It was determined that PKA activity was diminished by ~50% in *Pax3* mutants compared to wildtype controls. These diminished levels were significantly increased by isoproterenol treatment (Figure 18D). Furthermore, when embryo extracts were treated with 5ul exogenous cAMP (0.025mM), PKA activity increased in all groups. However, the PKA response to exogenous cAMP was still less in *Pax3* mutants compared to wildtype controls. More interestingly, the response to cAMP in *Pax3* mutants was greater than in *Pax3* mutants treated with isoproterenol. This suggests that there is a rate-limiting response to both cAMP and isoproterenol treatment in *Pax3* mutants.

5. Discussion

The results of this project have conclusively shown that low levels of norepinephrine lead to poor stimulation of the beta-adrenergic pathway, which causes poor cardiac output and eventual prenatal lethality. The importance of the beta-adrenergic pathway in survival was demonstrated by using two independent pharmacological approaches, which specifically targeted the embryonic pathway at two different cascade levels – the receptor levels (i.e., beta-receptors) and receptor targets (i.e., adenylate cyclase V). Via administering isoproterenol to pregnant dams, we were able to supplement maternal levels of catecholamine, which is necessary to have effective compensation of low levels in mutant embryos. In so doing, we demonstrated that we can effectively bypass the catecholamine synthesis pathway during development. Furthermore, by treating pregnant dams with forskolin, which specifically targets adenylate cyclase, we successfully demonstrated that the underlying cause of lethality was not directly due to low catecholamine levels. Rather it is due to the secondary effect of having low levels, which is a lack of sufficient adrenergic stimulation on the developing heart. To our knowledge, this is the first study to mechanistically demonstrate the important of adrenergic stimulation on embryonic cardiac output.

This project, for the first time, definitively determined the underlying cause of heart failure in *Pax3* mutants and subsequent lethality. Based on analyses done on early embryos, we determined that the onset of heart failure in these embryos

occurs prior to colonization of CNC, which conclusively rules out a CNC-intrinsic effect. The effect of *Pax3*-deficiency appears to not just be restricted to reduction in NC formation and migration; it also affects the ability of the few migratory NC cells to differentiate properly along the sympathoadrenal lineage, leading to an overall insufficiency in catecholamine synthesis. This suggests a Pax3-specific role in early NC specification and differentiation even at later stages of development when Pax3 expression is turned off.

Beyond the effects of Pax3, our data is significant in delineating the dose-dependent importance of catecholamine levels in embryonic heart function and survival. Through the use of two mouse models, we have elegantly demonstrated the presence of a required threshold level below which, embryonic heart function can not be supported. Building on previous studies that showed *Th*-happloinsufficiency and subsequent noradrenaline deficiency lead to *in utero* lethality [64-67], we can now demonstrate a dose-dependent requirement of *Th* in maintaining embryonic cardiac output and survival. Since *Th* is important in catalyzing the initial rate-limiting step in catecholamine synthesis [69], it is no surprise that as *Th* levels are diminished in our different mouse models, we observed a corresponding drop in norepinephrine levels. This is further supported by the fact that *Wnt1Cre/DTA* mutants can survive to birth despite having an apparent fewer number of migratory NC cells compared to *Pax3* mutants. It appears that mere number of NC cells is not important when it comes to maintaining embryonic cardiac function. Instead, the origin and functional

ability of those crest cells to differentiate along the sympathoadrenal lineage is the key to embryonic survival. It is important to not confuse structural and functional development of the embryonic heart. As, while the numbers of migratory CNC is clearly important in supporting structural remodeling [2, 5, 18], the specification of TNC is more important in maintaining functional development of the heart. As a result, we can now state definitively that both the CNC and TNC are important during cardiogenesis. The CNC provides structural support to the heart, via its contribution to the ectomesenchymal cells of the aorticopulmonary septum [6] and the smooth muscle cells that surround the aortic arches [18, 19]. However, the TNC is also important in cardiac development, via its contribution to the adrenal medulla and sympathetic ganglia which innervate the dorsal aortae, and are both important in providing beta-adrenergic stimulation to the heart.

Additionally, we have identified the temporal window of catecholamine requirement during development. Despite early signs of EC-coupling defects by E9, *Pax3* mutants could be treated as late as E10.5 and still survive to birth. However, only ~50% of mutants survived when treatment was initiated at E8.5 (before onset of cardiac functional anomalies) and terminated at E10.5. This suggests that post-E10.5 gestational stage, catecholamine is critically required for embryonic cardiac output. This result is consistent with existing models of noradrenaline deficiency in which the onset of embryonic lethality occurs from E11 onwards [64-67, 69]. Future studies will focus on narrowing this time-window

even further, as determining the minimum dosage and duration of treatment to get the most optimal result may have significant clinical implications.

Furthermore, we have identified downstream molecular targets such as phospholamban and troponin I as being important players in regulating embryonic cardiac contraction/relaxation. These molecular targets are misexpressed in *Pax3* mutants, but normalized post-isoproterenol treatment. Also of interest are results from activity assays we have performed, indicating that cAMP/PKA activity is perturbed in *Pax3* mutants but normalized post-isoproterenol treatment. Ongoing studies are addressing the specific role of PKA by using a host of phospho-antibodies to determine which PKA isoforms are important and potentially identify which phosphorylation sites may play a role in regulation of embryonic cardiac output. Taken together, the results of this project demonstrate that proper TNC cell specification is required to support beta-adrenergic stimulation of the developing heart, loss of which leads to poor embryonic cardiac output and eventual fetal lethality. This is the first study of its kind to link CNC-extrinsic factors to early embryonic cardiac function and survival.

Catecholamine	Wild type	Pax3 Heterozygote (% of Wt)	Pax3 Null (% of Wt)
Dopamine	2.7 ± 0.4 (100%)		2.4± 0.4 (89%)
Norepinephrine	137 ± 12.4 (100%)	108 ± 5.8 (79%)	9.8* ± 2.5 (7.1%)

Table 1: Measurement via HPLC of catecholamine levels. Performed on E13.5 whole embryo lysates. Note dose-dependent decrease in norepinephrine levels corresponding to Pax3 levels. Each data set represents average value (pmoles/embryo), n = 5; * = $p<0.05$. (HPLC measurement performed in collaboration with Dr. Jay R. Simon, PhD).

	# litters	# total embryos	# live -/-
isoproterenol	**40**	**204**	**58 (28%)**

	# litters	# total embryos	# live -/-
forskolin	**9**	**59**	**13 (22%)**

Table 2: Summary of number of pharmacologically (via isoproterenol or forskolin treatment) rescued *Pax3*$^{d5/d5}$ embryos (E14.5 – E18.5). Note rescued mutants are viable in Mendelian ratios. (Surgical implantations of osmotic mini-pumps performed in collaboration with Mark Soonpaa).

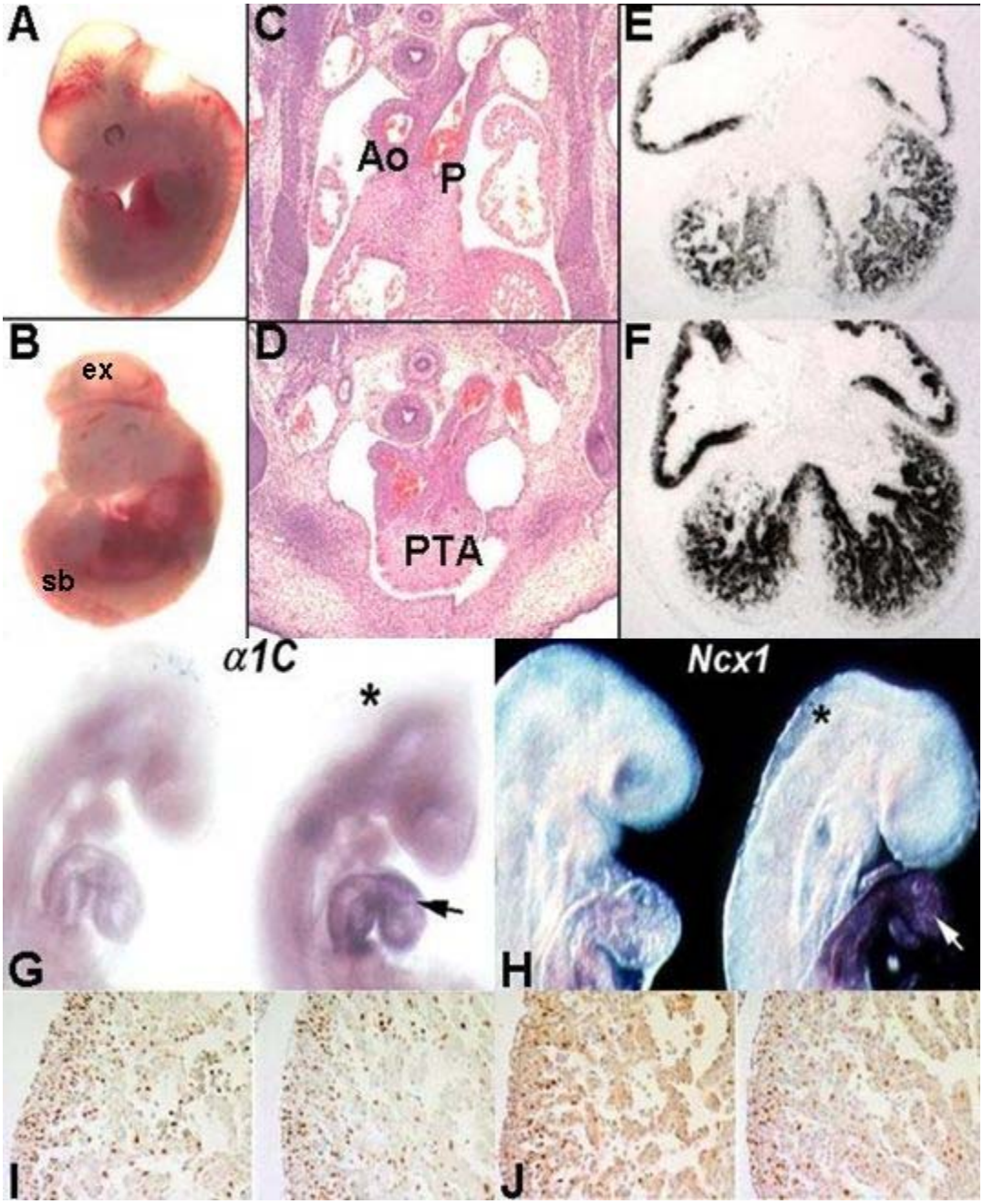
A
C
E
Ao
P
B
ex
D
F
sb
PTA
α1C
*
Ncx1
*
G
H
I
J

Figure 13: Structural and molecular analyses of *Pax3*$^{d5/d5}$ mutants

(A-D) Structural analyses of *Pax3* mutant embryos show defects in NT and OFT formation. (A, B) Gross structural analysis at E12.5 shows NT defects including exencephaly (ex) and spina bifida (sb) in *Pax3* mutants (B) compared to littermate control (A). (C, D) H&E histological analysis on transverse sections of embryos shown in (A, B) shows PTA in *Pax3* mutants (D) compared to properly septated OFT into aorta (Ao) and pulmonary artery (P) in control (D). (E-H) Molecular analyses of embryonic heart function shows early abnormalities in *Pax3* mutant embryo hearts. (E, F) ANF *in situ* hybridization on E13 transverse heart sections comparing wildtype (E) with mutant (F). Note significant upregulation in myocardium of mutant hearts. (G, H) Wholemount *in situ* staining of *α1c* (G) and *Ncx1* (H) at E9 showing increased mRNA expression levels in mutants (right) compared to littermate controls (left). Note: arrows indicate misexpression of markers in mutant myocardium; asterisk indicates exencephaly NT defect in *Pax3* mutants. (I, J) Proliferation analyses on E12.5 transverse heart sections. (I) Anti-Ki67 staining shows no observable difference in *Pax3* mutant (right) and littermate control (left) myocardium. (J) BrdU staining shows no observable differences in *Pax3* mutant (right) and littermate control (left) myocardium. Ao = aorta, ex = exencephaly, P = pulmonary artery, PTA = persistent truncus arteriosus, sb = spina bifida. (Radioactive *in situ* hybridization performed by Jian Wang).

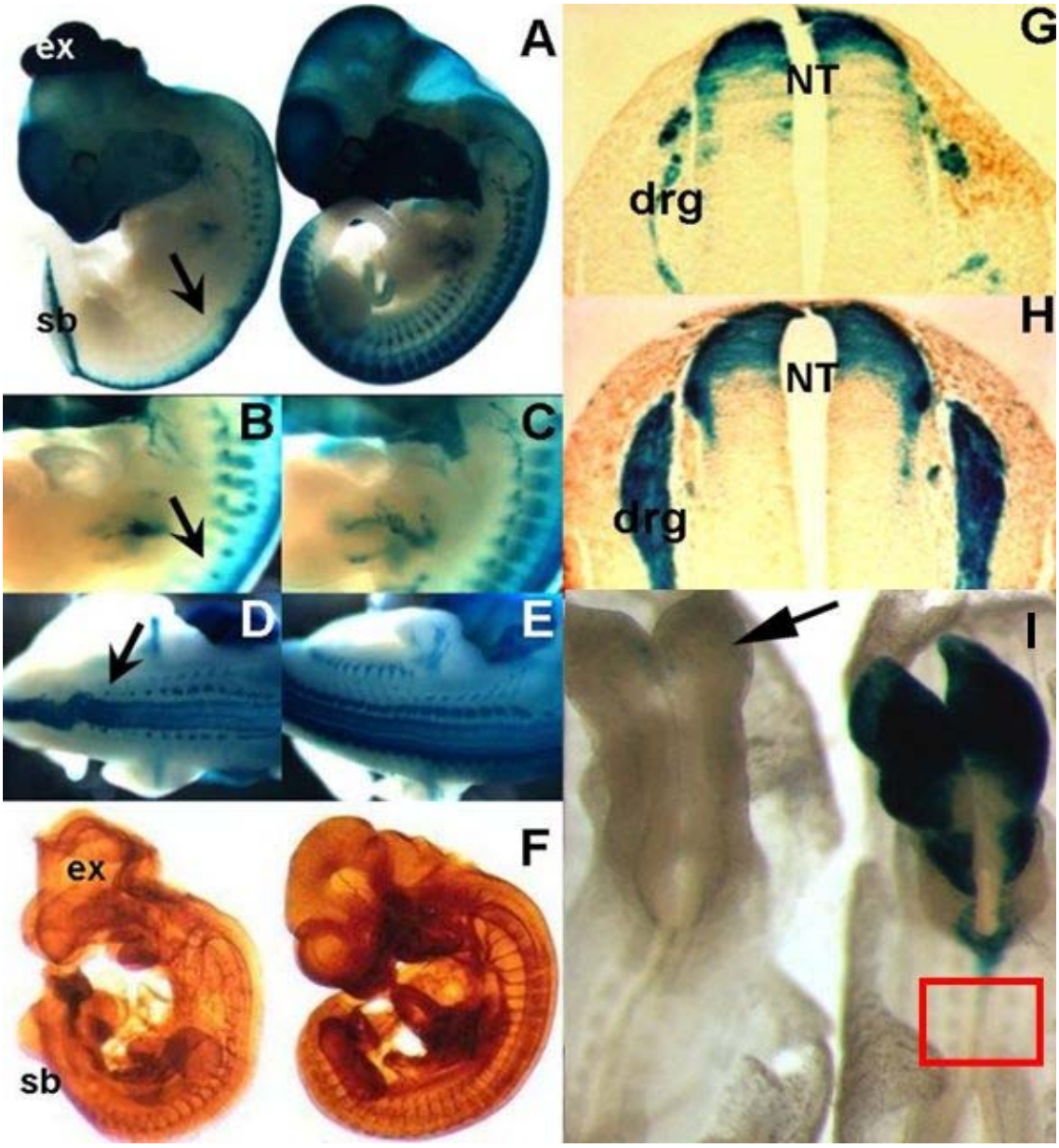
A
ex
sb
B
C
D
E
F
ex
sb
G
NT
drg
H
NT
drg
I

Figure 14: *Pax3*$^{d5/d5}$ mutants display insufficient NC-derived PNS structures

(A-E) NC lineage mapping analyses via *Wnt1Cre/R26R-lacZ* show lack of NC-derived PNS structures in *Pax3* mutants. (A) Gross analyses at E11 shows lack of PNS and enteric neurons in Pax3 mutant (left) compared to littermate control (right). Note: arrow indicates severe deficiency in migratory TNC-derived dorsal root ganglia structures. Note exencephaly (ex) and spina bifida (sb) in *Pax3* mutant embryo. (B, C) Higher magnification of lateral views of embryos shown in (A) shows disorganization of the reduced TNC-derived dorsal root ganglia (arrow in B) in *Pax3* mutant (B) compared to littermate control (C). (D, E) Higher magnification of dorsal views of embryos shown in (A) shows disorganization of the reduced TNC-derived dorsal root ganglia (arrow in D) in *Pax3* mutant (D) compared to littermate control (E). (F) Anti-neurofilament whole embryo staining at E11 on *Pax3* mutant (left) and littermate control (right) showing gross deficiency and disorganization of NC-derived PNS structures. Note exencephaly (ex) and spina bifida (sb) in *Pax3* mutant embryo. (G, H). NC lineage mapping analysis via *Wnt1Cre/R26R-lacZ* on E10.5 transverse sections counterstained with anti-αSMA. Note fewer migratory *lacZ*-positive cells in mutant (G) compared to littermate control (H) contributing to smaller dorsal root ganglia (drg) structures in mutant. Also note reduced NC-derived smooth muscle cells (brown anti-αSMA staining) in mutants. (I) NC lineage mapping via *Wnt1Cre/R26R-lacZ* on E8.5 *Wnt1Cre/DTA* mutant embryo (left) and littermate control (right). Note lack of *Wnt1Cre* expression in region corresponding to trunk NC site of formation at this

stage (red square). drg = dorsal root ganglia, ex = exencephaly, NT = neural tube, sb = spina bifida.

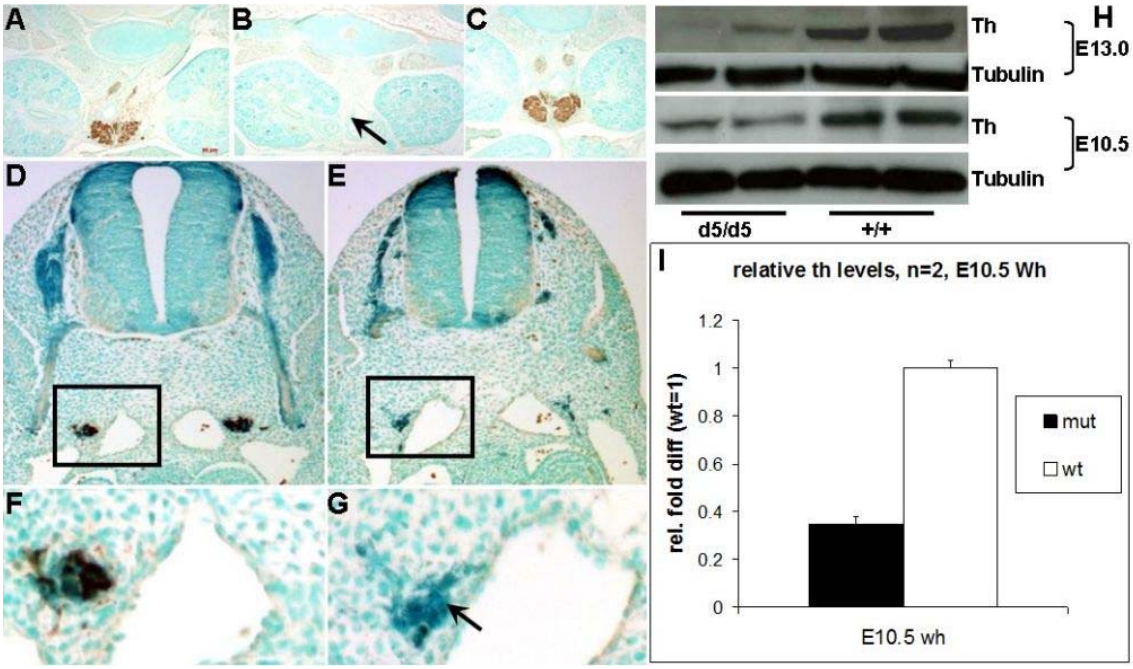
A
B
C
D
E
F
G
H
Th
Tubulin
E13.0
Th
Tubulin
E10.5
d5/d5
+/+
I
relative th levels, n=2, E10.5 Wh
rel. fold diff (wt=1)
1.2
1
0.8
0.6
0.4
0.2
0
mut
wt
E10.5 wh

Figure 15: Tyrosine hydroxylase is significantly reduced in *Pax3*$^{d5/d5}$ mutants but unaffected in *Wnt1Cre/DTA* mutant embryos

(A-C) Immunohistochemistry analysis using anti-Th antibody on E13.5 transverse sections counterstained with methyl green going through the adrenals of control (A) *Pax3* mutant (B) and *Wnt1Cre/DTA* mutant (C). Note severe lack of Th expression in *Pax3* mutant adrenals (arrow B). (D, E) NC lineage mapping via *Wnt1Cre/R26R-lacZ* using anti-Th antibody on E11 transverse sections counterstained with methyl green. Note reduced number of migratory *lacZ*-positive (dark blue) cells in *Pax3* mutant (E) compared to littermate control (D). (F, G) Higher magnification of sections shown in (D, E) showing Th-positive (brown staining) NC-derived cells (dark blue) as they colonize the dorsal aorta in control (F). However, there is a slightly reduced number of NC-derived cells (dark blue) colonizing the dorsal aorta in *Pax3* mutant (arrow in G). Note lack of Th expression (appreciably reduced brown staining) in the mutant NC cells that successfully colonize the *Pax3* mutant dorsal aorta (arrow in G). (H) Western analysis on whole embryo lysates shows reduced Th protein levels in *Pax3* mutants compared to littermate controls at E13 and E10.5. Each lane represents single whole embryo homogenized protein lysates. Equal loading between samples was confirmed with tubulin. (I) Stastical analysis on E10.5 westerns shown in (H) shows Th levels is reduced by 70% in *Pax3* mutants (black bar) compared to littermate control (white bar). Each bar represents average value (+/- standard error) relative to control (normalized to 1), n = 2. mut = mutant, wt = wildtype. (Histology performed by Mica Gosnell).

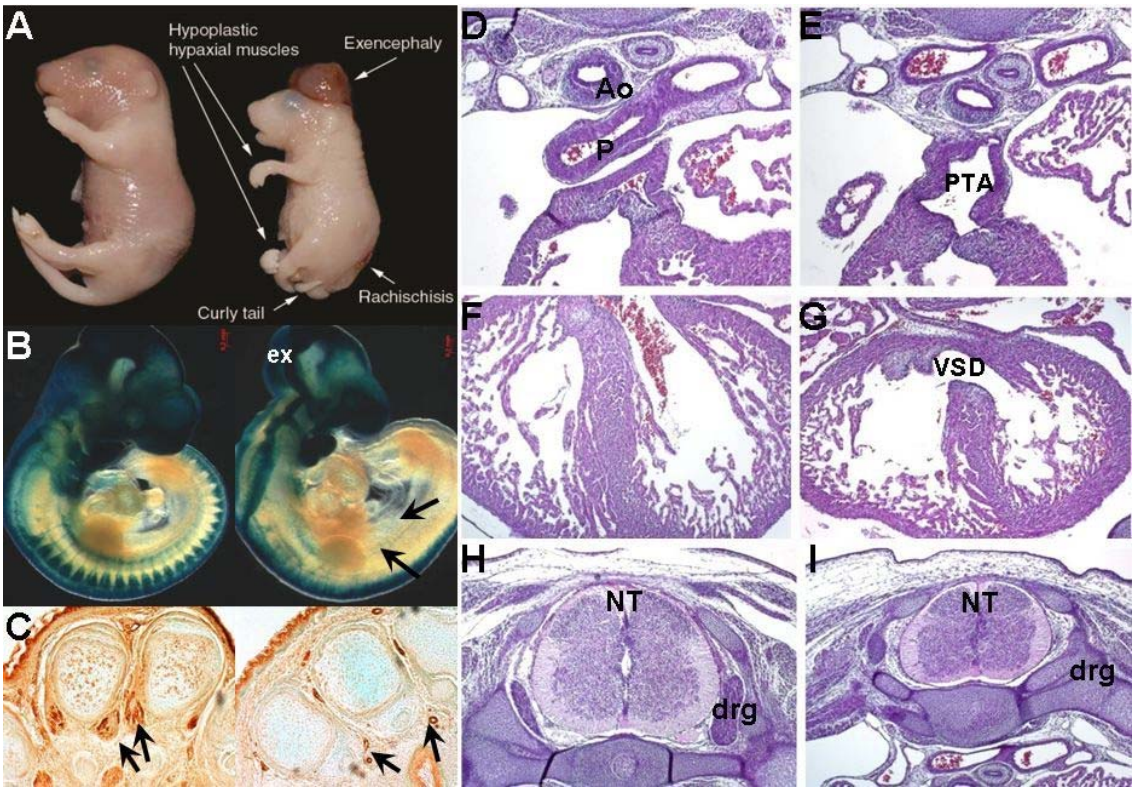
A
Hypoplastic
hypaxial muscles
Exencephaly
Curly tail
Rachischisis
B
ex
C
D
Ao
P
E
PTA
F
G
VSD
H
NT
drg
I
NT
drg

Figure 16: Histological analyses show structural defects in *Pax3*$^{d5/d5}$ mutants remain after isoproterenol treatment but they survive to birth

(A-I) Structural analyses on *Pax3* mutants treated after isoproterenol treatment. (A) E18.5 littermates treated with isoproterenol showing NT defects (exencephaly, rachischisis / spina bifida) and hypoplastic hypaxial muscles in limbs of *Pax3* mutant (right) compared to control (left). (B) NC lineage mapping analysis via *Wnt1Cre/R26R-lacZ* on E10.5 littermate embryos treated with isoproterenol shows fewer migratory NC cells in mutant (right) compared to control (left). Note exencephaly (ex) and lack of migratory NC cells (black arrows) in mutant. (C) anti-αSMA staining on transverse sections on E18.5 limbs of embryos shown in (A). Note lack of smooth muscle cells (absent brown staining indicated by arrows on right) in mutant (right) compared to normal smooth muscle cells (present brown staining indicated by arrows on left) in control (left). (D-I) H&E histological analysis on transverse sections of E15.5 littermate embryos treated with isoproterenol. (D-G) Histological analysis on control (D, F) and mutant (E, G) hearts shows PTA (E) and accompanied VSD (G) in mutant hearts compared to normal septation in control hearts. (H, I) Histological analysis on control (H) and mutant (I) transverse sections going through the NT region shows misshapen NT and reduced dorsal root ganglia (drg) in mutant (I) compared to control (H). Ao = aorta, drg = dorsal root ganglia, P = pulmonary artery, PTA = persistent truncus arteriosus, VSD = ventricular septal defect.

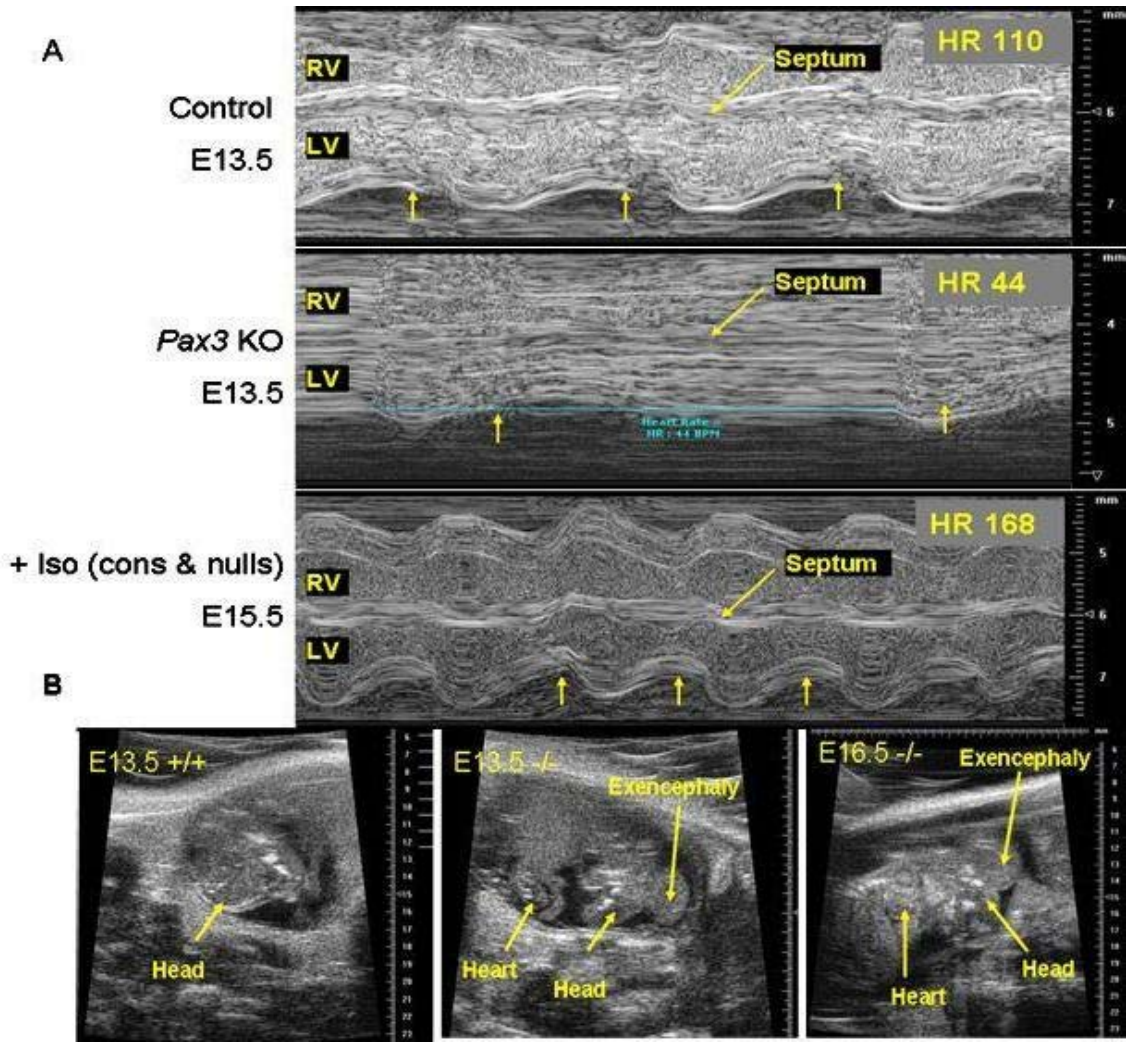
A
Control
E13.5
RV
LV
Septum
HR 110
Pax3 KO
E13.5
RV
LV
Septum
HR 44
+ Iso (cons & nulls)
E15.5
RV
LV
Septum
HR 168
B
E13.5 +/+
Head
E13.5 -/-
Exencephaly
Heart
Head
E16.5 -/-
Exencephaly
Heart
Head

Figure 17: Echocardiography analyses show poor cardiac function in *Pax3*$^{d5/d5}$ mutants are rescued by isoproterenol treatment

(A) Fetal M-mode echocardiogram analyses on E13.5 littermates of control (top panel) and *Pax3* mutant littermates (center panel). E15.5 *Pax3*$^{d5/d5}$ mutant treated with isoproterenol (bottom panel). Note that bottom panel in (A) is also representative of control littermates treated with isoproterenol, which are indistinguishable from *Pax3* mutants treated with isoproterenol. (B) Echocardiogram images of E13.5 control and *Pax3* mutant littermates (left and center panel). Right panel shows E16.5 *Pax3* mutant treated with isoproterenol. Note that visualization of NT defects (exencephaly) and, thus, identification of *Pax3* mutants is possible even at these early stages. (Echocardiography performed in collaboration with Dr. R. Mark Payne, MD).

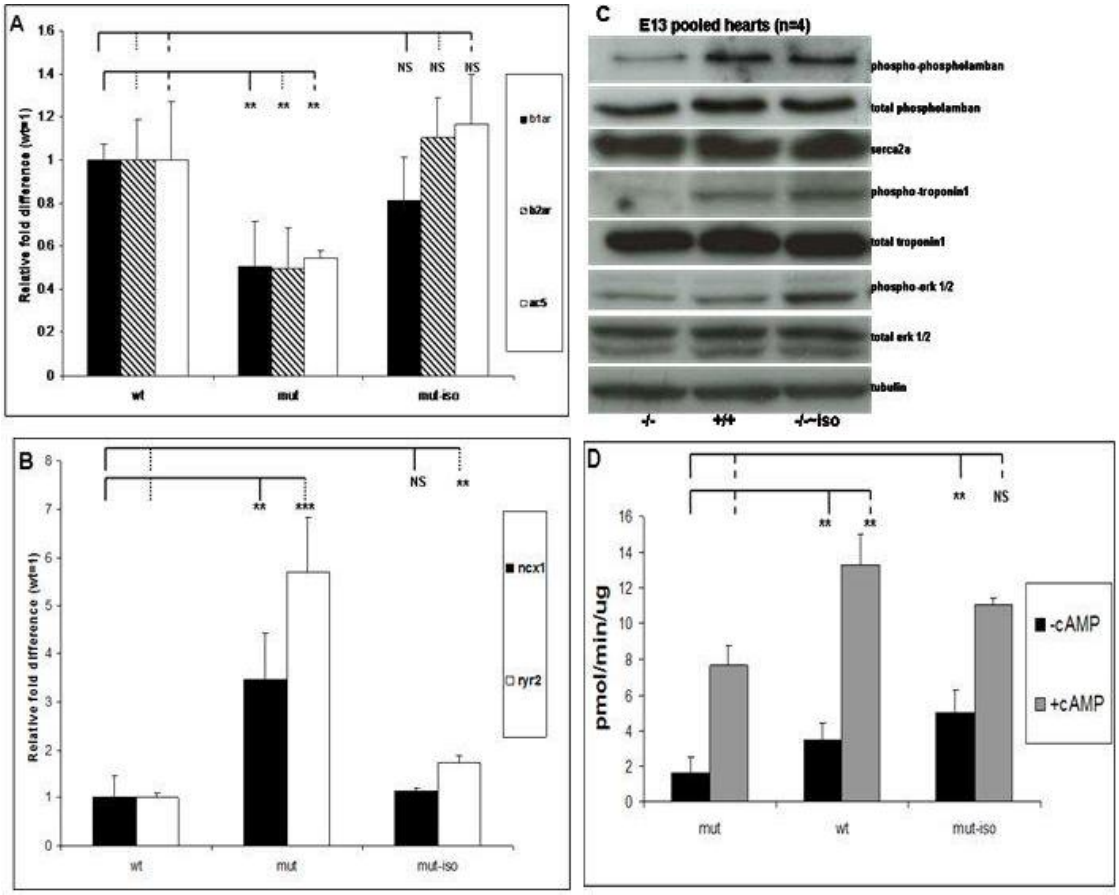
A
Relative fold difference (wt=1)
1.6
1.4
1.2
1
0.8
0.6
0.4
0.2
0
NS NS NS
** ** **
b1ar
b2ar
ac5
wt
mut
mut-iso
C
E13 pooled hearts (n=4)
phospho-phospholamban
total phospholamban
serca2a
phospho-troponin1
total troponin1
phospho-erk 1/2
total erk 1/2
tubulin
-/-
+/+
-/-iso
B
Relative fold difference (wt=1)
8
7
6
5
4
3
2
1
0
NS **
** ***
ncx1
ryr2
wt
mut
mut-iso
D
pmol/min/ug
16
14
12
10
8
6
4
2
0
** NS
** **
-cAMP
+cAMP
mut
wt
mut-iso

Figure 18: Molecular analyses show molecular defects in *Pax3*$^{d5/d5}$ mutants are rescued by isoproterenol treatment

(A-B) Real-time PCR on E13.0 isolated heart mRNA from wildtype (wt), *Pax3* mutants (mut) and *Pax3* mutants treated with isoproterenol (mut-iso), shows post-treatment normalization of initial misexpression in *Pax3* mutants of upstream elements in the beta-adrenergic pathway (A) and downstream elements (B). (b1ar = beta-adrenergic receptor I, b2ar = beta-adrenergic receptor II, ac5 = adenylate cyclase V, ncx1 = sodium-calcium exchanger channel I, ryr2 = ryanodine receptor II). Each bar represents triplicates each of 3 pooled hearts, NS = not significant, ** = significant difference, $p<0.05$, *** = significant difference, $p<0.01$). (C) Western analyses of molecular targets important for cardiac contractility (Each band represents protein lysates from E13.0 isolated pooled hearts, n=4). (D) PKA activity assay on E12.5 whole embryo lysates from wildtype (wt), *Pax3* mutants (mut) and *Pax3* mutants treated with isoproterenol (mut-iso), shows post-treatment normalization of initial decreased PKA activity (measured in pmol/min/ug of protein). N=3, NS = not significant, ** = $p<0.05$. Note differences in response +/- addition of exogenous cAMP (5ul/reaction 0.025mM).

Chapter IV: Discourse

1. Review

The overall aim of my project was twofold. First, I wanted to determine the specific role of Pax3 in early NC specification and its effect on AAA and OFT remodeling. Second, I wanted to determine the potential secondary effect that migratory *Pax3* mutant NC cells have on myocardial dysfunction and *in utero* lethality. To address this question, I used two mouse models with PTA/VSD but different lethality time points. My original hypothesis was that having *Pax3* mutant CNC, albeit in fewer numbers (as is the case in *Pax3* mutants), is more detrimental than complete absence of wildtype CNC (as is the case in the NC-ablated model).

My data suggests that, indeed, improperly specified NC cells in *Pax3* mutants are unable to undergo proper differentiation at their sites of colonization. This lack of differentiation led to incorrect specification of NC cells fated along the sympathoadrenal lineage. As a result, NC-derived tissues responsible for Th expression and catecholamine synthesis were affected. On the other hand, my hypothesis assumed that there was a complete absence of migratory NC cells in *Wnt1Cre/DTA* mutants. However, based on analysis of the *Wnt1Cre/DTA* mutants, it is clear that there is an early subpopulation of TNC cells that escape *Wnt1Cre*-mediated ablation. So while *Pax3* mutant NC cells were proven to be

detrimental, they are not more so than a complete absence, as originally postulated. More importantly, the underlying cause of lethality in *Pax3* mutants was not due to a CNC-intrinsic factor as originally believed. Instead, it was secondary to lack of TNC-intrinsic factors.

My data also suggests that catecholamines are not critically required for embryonic cardiac output prior to E10.5 (Figure 19). Ongoing studies are focusing on narrowing this time-window even further, as determining the minimum dosage and duration of treatment to get the most optimal result may have significant clinical implications.

One easy to do follow up experiment will be to test whether pharmacological suppression of beta-adrenergic stimulation yields lethality around mid-gestation in control embryos. This could be achieved via bupranolol treatment, which is an effective antagonist of the beta-adrenergic receptor pathway [103]. However, I will have to be wary of initial results, as beta-blockers are also known to cause uterine contractions during late stage pregnancy and could affect embryonic survival independent of noradrenaline levels.

2. Other studies of relevance

Previous research has shown that *Msx2* is a direct downstream target of *Pax3* in the neural tube [80]. Furthermore, *Pax3* is required to repress *Msx2,* failure of which leads to a range of NC related defects. Specifically, *Pax3* binds to an 8bp consensus sequence (GTCACACA) region located in a 660bp fragment of the *Msx2* promoter [80]. More recently, another group working with Pax7 (a closely-related protein to Pax3) identified a 5bp Pax7 core consensus motif (GTCAC). This was based on bioinformatic prediction of *Pax7*-ChIP consensus sites [108]. However, they did not specifically identify *Msx2* as a downstream target of *Pax7*. Due to the identical nature of both consensus motifs and the close relation of *Pax3* and *Pax7*, I sought to find out if *Pax7* could play a similar repressive role on *Msx2* in the NT. I did this through the use of luciferase constructs expressing the *Msx2* promoter region, which were then transfected into NIH-3T3 cells.

2.1. Summary of Materials and Methods

Briefly, a pgl2 luciferase vector containing the *Msx2* promoter sequence (pMsx2wt-luc) was used (gift from R. Maxson, USC). Site-specific mutagenesis was performed using the QuikChange Site Directed Mutagenesis Kit (Stratagene) according to the manufacturer's instructions to generate the pgl2 luciferase vector containing the mutated *Msx2* promoter sequence (pMsx2mut-luc). To generate the mutated sequence (underlined) the following pair of primers were used: forward primer 5’ - GAG AGG TGC CAT CTT TTG CCC GAA

GGATATCG GCG AAT GTC CAC GGA TTG GAG GGC – 3’ and reverse primer 5’ - GCC CTC CAA TCC GTG GAC ATT CGC CGATATCC TTC GGG CAA AAG ATG GCA CCT CTC - 3’. Mutagenesis was confirmed by sequencing.

NIH-3T3 cells were grown and maintained in DMEM, supplemented with sodium pyruvate, glutamate, antibiotic mix (penicillin and streptomycin), and 10% fetal calf serum. Cells were transfected in triplicate using Transfectin Reagent (Biorad) according to the manufacturer's instructions in 6-well plates. Each well was transfected with a total of 4ug DNA (2ug effector vector + 2ug luciferase vector). As an internal control, each well was also transfected with 50ng of the Renilla luciferase vector (pRLCMV) in order to normalize for variation in transfection efficiency. After 48h, cells were washed briefly in PBS then lysed using 1x Passive Lysis Buffer (Promega) following manufacturer’s instructions. Cell samples were assayed for luciferase activity using the Dual Luciferase Reporter Assay system (Promega) on a Luminoskan Ascent microplate luminometer (ThermoScientific).

Immunoblots were performed using mouse monoclonal anti-Pax3 and anti-Pax7 antibodies (both obtained from Hybridoma Bank, University of Iowa); mouse monoclonal anti-β-tubulin antibody (Roche); and HRP-conjugated goat anti-mouse IgG (Jackson Laboratories). Both the anti-Pax3 (1:1000) and anti-Pax7 (1:1000) antibodies were incubated overnight at 4C. Anti-β-tubulin (1:10000) and goat anti-mouse (1:5000) antibodies were incubated for 1h at room temperature.

Antibodies were detected using the enhanced chemiluminescence (ECL) plus detection system (Amersham). Densitometry of immunoreactive bands was performed using Image J 1.37v (NIH).

2.2. Summary of Results and Discussion

My luciferase results suggest that Pax7 is capable of repressing *Msx2*, albeit not as well as Pax3 (Figure 20). It also appears to do so cooperatively with *Pax3* based on results from co-transfections of both *Pax3* and *Pax7*. However, the mechanism by which this occurs is still not clear. One possible mechanism could be that that both Pax3 and Pax7 compete with each other to bind to the *Msx2* promoter at the consensus site with Pax3 being a stronger competitor. Alternatively, they may both have similar binding affinity with Pax3 being the stronger repressor. The fact that Pax7, in the absence of Pax3, fails to repress *Msx2* promoter activity as efficiently as Pax3 suggests that the latter may be the case. If so, it will be interesting to determine whether or not both Pax3/7 can repress *Msx2* as part of a single complex or if they bind *Msx2* exclusively independent of each other. Previous research has already shown that both Pax3 and Pax7 can cooperatively heterodimerize with each other on palindromic homeodomain binding sequences [109]. However, since the consensus motifs through which both transcription factors bind *Msx2* (GTCACaca) is not palindromic, I believe this suggests a cooperative but independent role of both Pax3 and Pax7 in repressing *Msx2*.

3. Future studies

Based on preliminary results from luciferases experiments mentioned above, elucidating the role of Pax7 (if any) on *in utero* lethality and cardiac function may be useful. There is already some suggestion that both Pax3 and Pax7 may share similar roles and that Pax3 may function cooperatively with Pax7 [110, 111]. Thus, Pax7 may be capable of regulating myocardial homeostasis via *Msx2* regulation or some other common downstream target. To address this, we already have both *Pax3* and *Pax7* null mice. Since *Pax7* null mice are viable to birth (Mansouri, 1996), it is clear that Pax7 independently is not important *in utero* lethality. However, this does not rule out the possibility that Pax7 in conjunction with Pax3 may play a role in embryonic survival. To test this, we plan to cross the previously described (Chapter II) *Pax3$^{f/d5}$/Wnt1Cre* conditional knockout mice (which are viable) unto a Pax7 haploinsufficient background (i.e., Pax7+/- and Pax7-/-). We will then determine if *in utero* lethality is observed in the normally viable *Pax3$^{f/d5}$/Wnt1Cre* conditional mutants, when Pax7 levels are reduced. If we observe lethality, we will perform similar analyses to determine effects on norepinephrine levels and the possibility of pharmacological rescue.

Another direction worth pursuing is based on recent hyperoxia studies in mice, which show that high maternal oxygen can rescue catecholamine-deficient embryos [107]. This occurs due to an increase in blood oxygen levels that is delivered to the developing embryo. This results in increased embryonic heart

rate and overall improved cardiac output. Based on these studies, we propose to test whether an increase in maternal oxygen levels can similarly rescue our *Pax3* mutants by directly stimulating heart function. We believe this may be an important follow up study to identify alternative approaches, which can be used to rescue impaired embryonic cardiac function.

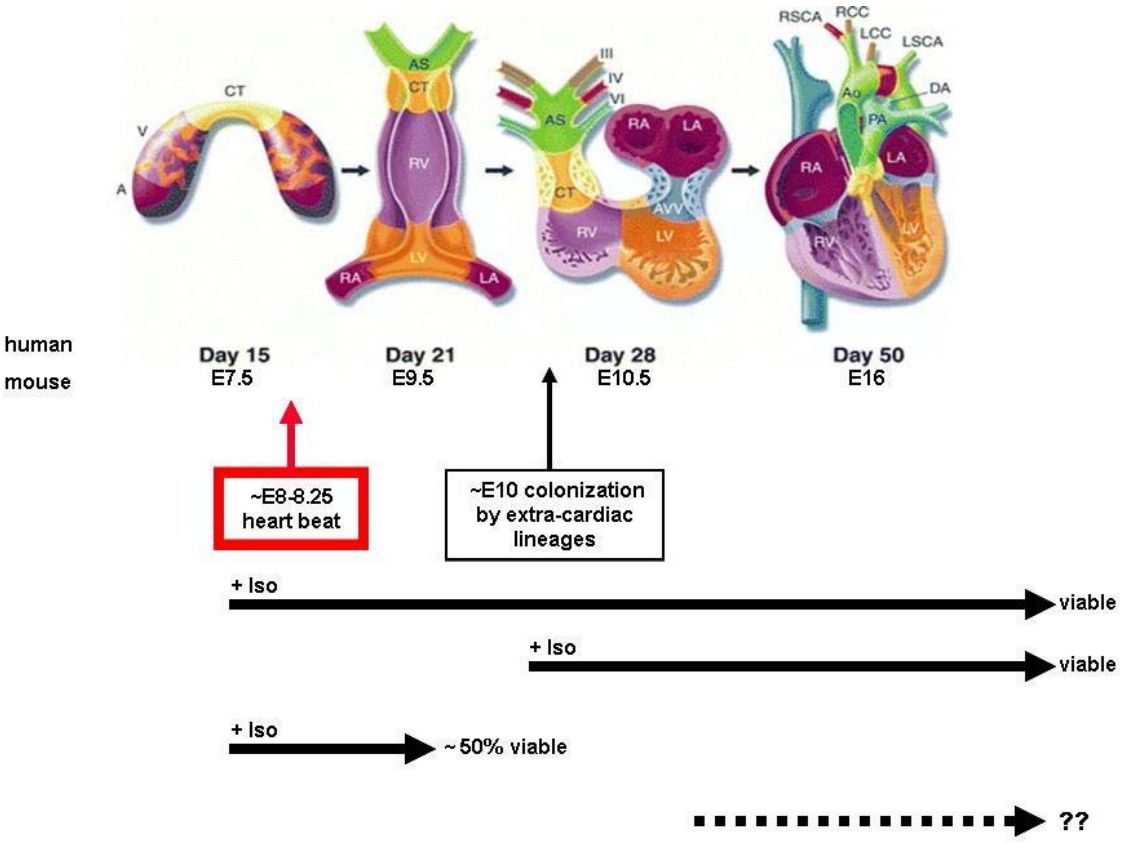

Figure 19: Critical temporal requirement of catecholamines during embryonic development. Adapted from [112].

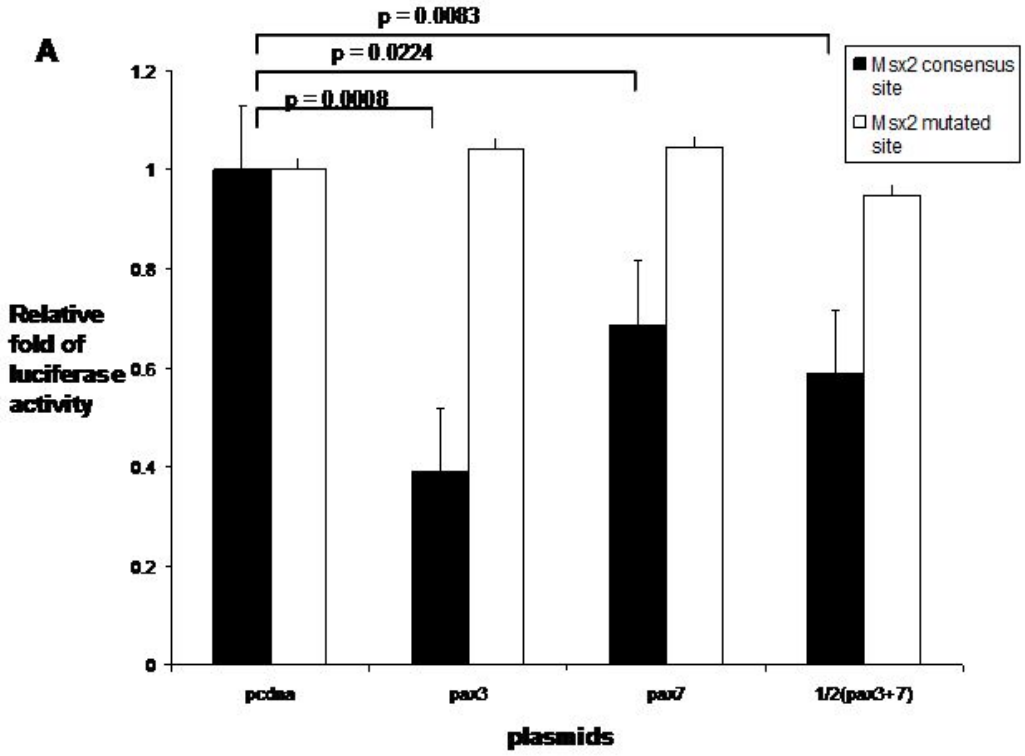
A
p = 0.0083
p = 0.0224
p = 0.0008
Msx2 consensus site
Msx2 mutated site
Relative fold of luciferase activity
1.2
1
0.8
0.6
0.4
0.2
0
pcdna
pax3
pax7
1/2(pax3+7)
plasmids

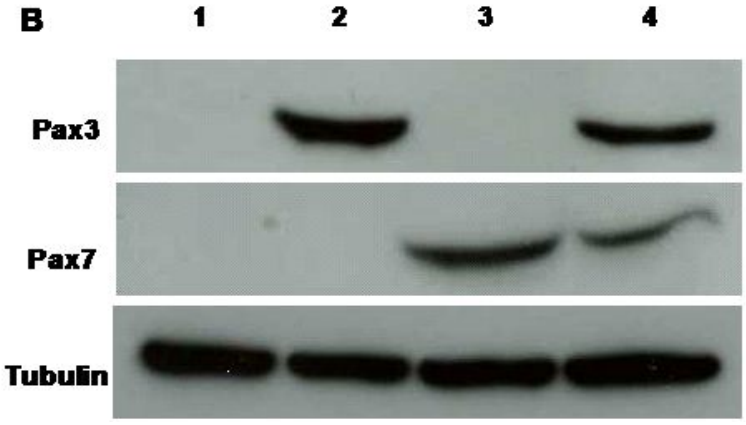
B
1
2
3
4
Pax3
Pax7
Tubulin

Figure 20: *Pax7* can substitute role of *Pax3* in suppression of *Msx2*

(A) Relative fold repression of luciferase activity with empty Pcdna vector control nominally set to 1. Both Pax3 and Pax7 independently and cooperatively repress the 660bp Msx2 promoter containing consensus site (shaded bars, $p<0.05$). However, they fail to repress the 660bp Msx2 promoter containing the 8bp mutated sequence (dashed bars; $p>0.05$). Each bar represents 2ug total transfected DNA of empty *Pcdna* control, *Pax3*, *Pax7* respectively. Also included are combined transfections of 1ug each of Pax3 and Pax7 indicated by ½(pax3+7). Data are expressed as relative fold of luciferase activity to empty *Pcdna* vector control. Data represents the average of n = 6 ± standard error of the mean for each set. (B) Western blots of cell lysates from respective wells transfected with 2ug empty Pcdna control (lane 1), 2ug Pax3 (lane 2), 2ug Pax7 (lane 3), 1ug Pax3 + 1ug Pax7 (lane 4); β-tubulin was used as a loading control.

References

1. Teillet, M.A., C. Ziller, and N.M. Le Douarin, *Quail-chick chimeras.* Methods Mol Biol, 1999. **97**: p. 305-18.
2. Snider, P., et al., *Cardiovascular development and the colonizing cardiac neural crest lineage.* ScientificWorldJournal, 2007. **7**: p. 1090-113.
3. Chai, Y., et al., *Fate of the mammalian cranial neural crest during tooth and mandibular morphogenesis.* Development, 2000. **127**(8): p. 1671-9.
4. Jiang, X., et al., *Fate of the mammalian cardiac neural crest.* Development, 2000. **127**(8): p. 1607-16.
5. Hutson, M.R. and M.L. Kirby, *Model systems for the study of heart development and disease. Cardiac neural crest and conotruncal malformations.* Semin Cell Dev Biol, 2007. **18**(1): p. 101-10.
6. Creazzo, T.L., et al., *Role of cardiac neural crest cells in cardiovascular development.* Annu Rev Physiol, 1998. **60**: p. 267-86.
7. Selleck, M.A. and M. Bronner-Fraser, *Origins of the avian neural crest: the role of neural plate-epidermal interactions.* Development, 1995. **121**(2): p. 525-38.
8. Barembaum, M. and M. Bronner-Fraser, *Early steps in neural crest specification.* Semin Cell Dev Biol, 2005. **16**(6): p. 642-6.
9. Liem, K.F., Jr., et al., *Dorsal differentiation of neural plate cells induced by BMP-mediated signals from epidermal ectoderm.* Cell, 1995. **82**(6): p. 969-79.
10. Monsoro-Burq, A.H., R.B. Fletcher, and R.M. Harland, *Neural crest induction by paraxial mesoderm in Xenopus embryos requires FGF signals.* Development, 2003. **130**(14): p. 3111-24.
11. Mayor, R., N. Guerrero, and C. Martinez, *Role of FGF and noggin in neural crest induction.* Dev Biol, 1997. **189**(1): p. 1-12.
12. Garcia-Castro, M.I., C. Marcelle, and M. Bronner-Fraser, *Ectodermal Wnt function as a neural crest inducer.* Science, 2002. **297**(5582): p. 848-51.
13. Burstyn-Cohen, T. and C. Kalcheim, *Association between the cell cycle and neural crest delamination through specific regulation of G1/S transition.* Dev Cell, 2002. **3**(3): p. 383-95.
14. Kirby, M.L., T.F. Gale, and D.E. Stewart, *Neural crest cells contribute to normal aorticopulmonary septation.* Science, 1983. **220**(4601): p. 1059-61.
15. Conway, S.J., et al., *What cardiovascular defect does my prenatal mouse mutant have, and why?* Genesis, 2003. **35**(1): p. 1-21.
16. Kuratani, S.C. and M.L. Kirby, *Migration and distribution of circumpharyngeal crest cells in the chick embryo. Formation of the circumpharyngeal ridge and E/C8+ crest cells in the vertebrate head region.* Anat Rec, 1992. **234**(2): p. 263-80.
17. Miyagawa-Tomita, S., et al., *Temporospatial study of the migration and distribution of cardiac neural crest in quail-chick chimeras.* Am J Anat, 1991. **192**(1): p. 79-88.

18. Waldo, K.L., D. Kumiski, and M.L. Kirby, *Cardiac neural crest is essential for the persistence rather than the formation of an arch artery.* Dev Dyn, 1996. **205**(3): p. 281-92.
19. Bradshaw, L., et al., *Dual role for neural crest cells during outflow tract septation in the neural crest-deficient mutant Splotch(2H).* J Anat, 2009. **214**(2): p. 245-57.
20. Ruhin, B., et al., *Patterning of the hyoid cartilage depends upon signals arising from the ventral foregut endoderm.* Dev Dyn, 2003. **228**(2): p. 239-46.
21. Yanagisawa, H., et al., *Role of Endothelin-1/Endothelin-A receptor-mediated signaling pathway in the aortic arch patterning in mice.* J Clin Invest, 1998. **102**(1): p. 22-33.
22. Yashiro, K., H. Shiratori, and H. Hamada, *Haemodynamics determined by a genetic programme govern asymmetric development of the aortic arch.* Nature, 2007. **450**(7167): p. 285-8.
23. Tallquist, M.D. and P. Soriano, *Cell autonomous requirement for PDGFRalpha in populations of cranial and cardiac neural crest cells.* Development, 2003. **130**(3): p. 507-18.
24. Liu, C., et al., *Regulation of left-right asymmetry by thresholds of Pitx2c activity.* Development, 2001. **128**(11): p. 2039-48.
25. Brown, C.B., et al., *PlexinA2 and semaphorin signaling during cardiac neural crest development.* Development, 2001. **128**(16): p. 3071-80.
26. Lee, M., et al., *P0 is constitutively expressed in the rat neural crest and embryonic nerves and is negatively and positively regulated by axons to generate non-myelin-forming and myelin-forming Schwann cells, respectively.* Mol Cell Neurosci, 1997. **8**(5): p. 336-50.
27. van den Hoff, M.J., et al., *Myocardialization of the cardiac outflow tract.* Dev Biol, 1999. **212**(2): p. 477-90.
28. van den Hoff, M.J. and A.F. Moorman, *Wnt, a driver of myocardialization?* Circ Res, 2005. **96**(3): p. 274-6.
29. Phillips, H.M., et al., *Vangl2 acts via RhoA signaling to regulate polarized cell movements during development of the proximal outflow tract.* Circ Res, 2005. **96**(3): p. 292-9.
30. Somi, S., et al., *Dynamic patterns of expression of BMP isoforms 2, 4, 5, 6, and 7 during chicken heart development.* Anat Rec A Discov Mol Cell Evol Biol, 2004. **279**(1): p. 636-51.
31. Poelmann, R.E. and A.C. Gittenberger-de Groot, *A subpopulation of apoptosis-prone cardiac neural crest cells targets to the venous pole: multiple functions in heart development?* Dev Biol, 1999. **207**(2): p. 271-86.
32. van Gijn, M.E., et al., *Frizzled 2 is transiently expressed in neural crest-containing areas during development of the heart and great arteries in the mouse.* Anat Embryol (Berl), 2001. **203**(3): p. 185-92.
33. Yamauchi, Y., et al., *A novel transgenic technique that allows specific marking of the neural crest cell lineage in mice.* Dev Biol, 1999. **212**(1): p. 191-203.

34. Black, B.L., *Transcriptional pathways in second heart field development.* Semin Cell Dev Biol, 2007. **18**(1): p. 67-76.
35. Kirby, M.L., et al., *Abnormal patterning of the aortic arch arteries does not evoke cardiac malformations.* Dev Dyn, 1997. **208**(1): p. 34-47.
36. Loring, J.F. and C.A. Erickson, *Neural crest cell migratory pathways in the trunk of the chick embryo.* Dev Biol, 1987. **121**(1): p. 220-36.
37. Gammill, L.S. and J. Roffers-Agarwal, *Division of labor during trunk neural crest development.* Dev Biol, 2010. **344**(2): p. 555-65.
38. Huber, A.B., et al., *Distinct roles for secreted semaphorin signaling in spinal motor axon guidance.* Neuron, 2005. **48**(6): p. 949-64.
39. Schwarz, Q., et al., *Neuropilin-mediated neural crest cell guidance is essential to organise sensory neurons into segmented dorsal root ganglia.* Development, 2009. **136**(11): p. 1785-9.
40. Schwarz, Q., et al., *Neuropilin 1 signaling guides neural crest cells to coordinate pathway choice with cell specification.* Proc Natl Acad Sci U S A, 2009. **106**(15): p. 6164-9.
41. Gammill, L.S., et al., *Guidance of trunk neural crest migration requires neuropilin 2/semaphorin 3F signaling.* Development, 2006. **133**(1): p. 99-106.
42. Roffers-Agarwal, J. and L.S. Gammill, *Neuropilin receptors guide distinct phases of sensory and motor neuronal segmentation.* Development, 2009. **136**(11): p. 1879-88.
43. Huber, K., *The sympathoadrenal cell lineage: specification, diversification, and new perspectives.* Dev Biol, 2006. **298**(2): p. 335-43.
44. Reiprich, S., et al., *SoxE proteins are differentially required in mouse adrenal gland development.* Mol Biol Cell, 2008. **19**(4): p. 1575-86.
45. Huber, K., et al., *The role of Phox2B in chromaffin cell development.* Dev Biol, 2005. **279**(2): p. 501-8.
46. Groves, A.K., et al., *Differential regulation of transcription factor gene expression and phenotypic markers in developing sympathetic neurons.* Development, 1995. **121**(3): p. 887-901.
47. Howard, M.J. and M. Bronner-Fraser, *The influence of neural tube-derived factors on differentiation of neural crest cells in vitro. I. Histochemical study on the appearance of adrenergic cells.* J Neurosci, 1985. **5**(12): p. 3302-9.
48. Teillet, M.A. and N.M. Le Douarin, *Consequences of neural tube and notochord excision on the development of the peripheral nervous system in the chick embryo.* Dev Biol, 1983. **98**(1): p. 192-211.
49. Ehrhart-Bornstein, M. and U. Hilbers, *Neuroendocrine properties of adrenocortical cells.* Horm Metab Res, 1998. **30**(6-7): p. 436-9.
50. Cheung, M., et al., *The transcriptional control of trunk neural crest induction, survival, and delamination.* Dev Cell, 2005. **8**(2): p. 179-92.
51. O'Donnell, M., et al., *Functional analysis of Sox8 during neural crest development in Xenopus.* Development, 2006. **133**(19): p. 3817-26.

52. Deal, K.K., et al., *Distant regulatory elements in a Sox10-beta GEO BAC transgene are required for expression of Sox10 in the enteric nervous system and other neural crest-derived tissues.* Dev Dyn, 2006. **235**(5): p. 1413-32.
53. Sock, E., et al., *Idiopathic weight reduction in mice deficient in the high-mobility-group transcription factor Sox8.* Mol Cell Biol, 2001. **21**(20): p. 6951-9.
54. Kapur, R.P., *Early death of neural crest cells is responsible for total enteric aganglionosis in Sox10(Dom)/Sox10(Dom) mouse embryos.* Pediatr Dev Pathol, 1999. **2**(6): p. 559-69.
55. Kim, J., et al., *SOX10 maintains multipotency and inhibits neuronal differentiation of neural crest stem cells.* Neuron, 2003. **38**(1): p. 17-31.
56. Lo, L., M.C. Tiveron, and D.J. Anderson, *MASH1 activates expression of the paired homeodomain transcription factor Phox2a, and couples pan-neuronal and subtype-specific components of autonomic neuronal identity.* Development, 1998. **125**(4): p. 609-20.
57. Leatherbury, L., et al., *Microcinephotography of the developing heart in neural crest-ablated chick embryos.* Circulation, 1990. **81**(3): p. 1047-57.
58. Conway, S.J., et al., *Decreased neural crest stem cell expansion is responsible for the conotruncal heart defects within the splotch (Sp(2H))/Pax3 mouse mutant.* Cardiovasc Res, 2000. **47**(2): p. 314-28.
59. Conway, S.J., et al., *Neural crest is involved in development of abnormal myocardial function.* J Mol Cell Cardiol, 1997. **29**(10): p. 2675-85.
60. Conway, S.J., D.J. Henderson, and A.J. Copp, *Pax3 is required for cardiac neural crest migration in the mouse: evidence from the splotch (Sp2H) mutant.* Development, 1997. **124**(2): p. 505-14.
61. Farrell, M.J., et al., *FGF-8 in the ventral pharynx alters development of myocardial calcium transients after neural crest ablation.* J Clin Invest, 2001. **107**(12): p. 1509-17.
62. Abu-Issa, R., et al., *Fgf8 is required for pharyngeal arch and cardiovascular development in the mouse.* Development, 2002. **129**(19): p. 4613-25.
63. Brown, C.B., et al., *Cre-mediated excision of Fgf8 in the Tbx1 expression domain reveals a critical role for Fgf8 in cardiovascular development in the mouse.* Dev Biol, 2004. **267**(1): p. 190-202.
64. Zhou, Q.Y., C.J. Quaife, and R.D. Palmiter, *Targeted disruption of the tyrosine hydroxylase gene reveals that catecholamines are required for mouse fetal development.* Nature, 1995. **374**(6523): p. 640-3.
65. Zhou, Q.Y. and R.D. Palmiter, *Dopamine-deficient mice are severely hypoactive, adipsic, and aphagic.* Cell, 1995. **83**(7): p. 1197-209.
66. Thomas, S.A., A.M. Matsumoto, and R.D. Palmiter, *Noradrenaline is essential for mouse fetal development.* Nature, 1995. **374**(6523): p. 643-6.
67. Lim, K.C., et al., *Gata3 loss leads to embryonic lethality due to noradrenaline deficiency of the sympathetic nervous system.* Nat Genet, 2000. **25**(2): p. 209-12.

68. Hong, S.J., et al., *GATA-3 regulates the transcriptional activity of tyrosine hydroxylase by interacting with CREB.* J Neurochem, 2006. **98**(3): p. 773-81.
69. Morikawa, Y., et al., *Hand2 determines the noradrenergic phenotype in the mouse sympathetic nervous system.* Dev Biol, 2007. **307**(1): p. 114-26.
70. Pattyn, A., et al., *The homeobox gene Phox2b is essential for the development of autonomic neural crest derivatives.* Nature, 1999. **399**(6734): p. 366-70.
71. Sommer, L., et al., *The cellular function of MASH1 in autonomic neurogenesis.* Neuron, 1995. **15**(6): p. 1245-58.
72. Tsarovina, K., et al., *Essential role of Gata transcription factors in sympathetic neuron development.* Development, 2004. **131**(19): p. 4775-86.
73. Asher, J.H., Jr., et al., *Effects of Pax3 modifier genes on craniofacial morphology, pigmentation, and viability: a murine model of Waardenburg syndrome variation.* Genomics, 1996. **34**(3): p. 285-98.
74. Asher, J.H., Jr., et al., *Missense mutation in the paired domain of PAX3 causes craniofacial-deafness-hand syndrome.* Hum Mutat, 1996. **7**(1): p. 30-5.
75. Tassabehji, M., V.E. Newton, and A.P. Read, *Waardenburg syndrome type 2 caused by mutations in the human microphthalmia (MITF) gene.* Nat Genet, 1994. **8**(3): p. 251-5.
76. Tsukamoto, K., et al., *Cloning and characterization of the inversion breakpoint at chromosome 2q35 in a patient with Waardenburg syndrome type I.* Hum Mol Genet, 1992. **1**(5): p. 315-7.
77. Goldmuntz, E., et al., *Frequency of 22q11 deletions in patients with conotruncal defects.* J Am Coll Cardiol, 1998. **32**(2): p. 492-8.
78. Taneyhill, L.A. and M. Bronner-Fraser, *Dynamic alterations in gene expression after Wnt-mediated induction of avian neural crest.* Mol Biol Cell, 2005. **16**(11): p. 5283-93.
79. Stottmann, R.W., et al., *BMP receptor IA is required in mammalian neural crest cells for development of the cardiac outflow tract and ventricular myocardium.* Development, 2004. **131**(9): p. 2205-18.
80. Kwang, S.J., et al., *Msx2 is an immediate downstream effector of Pax3 in the development of the murine cardiac neural crest.* Development, 2002. **129**(2): p. 527-38.
81. Satokata, I., et al., *Msx2 deficiency in mice causes pleiotropic defects in bone growth and ectodermal organ formation.* Nat Genet, 2000. **24**(4): p. 391-5.
82. Goulding, M.D., et al., *Pax-3, a novel murine DNA binding protein expressed during early neurogenesis.* EMBO J, 1991. **10**(5): p. 1135-47.
83. Epstein, J.A., et al., *Pax3 modulates expression of the c-Met receptor during limb muscle development.* Proc Natl Acad Sci U S A, 1996. **93**(9): p. 4213-8.

84. Galibert, M.D., et al., *Pax3 and regulation of the melanocyte-specific tyrosinase-related protein-1 promoter.* J Biol Chem, 1999. **274**(38): p. 26894-900.
85. Epstein, J.A., et al., *Migration of cardiac neural crest cells in Splotch embryos.* Development, 2000. **127**(9): p. 1869-78.
86. Li, J., et al., *Transgenic rescue of congenital heart disease and spina bifida in Splotch mice.* Development, 1999. **126**(11): p. 2495-503.
87. Koushik, S.V., et al., *Generation of a conditional loxP allele of the Pax3 transcription factor that enables selective deletion of the homeodomain.* Genesis, 2002. **32**(2): p. 114-7.
88. Zhou, H.M., et al., *Lineage-specific responses to reduced embryonic Pax3 expression levels.* Dev Biol, 2008. **315**(2): p. 369-82.
89. Ivanova, A., et al., *In vivo genetic ablation by Cre-mediated expression of diphtheria toxin fragment A.* Genesis, 2005. **43**(3): p. 129-35.
90. Snider, P., et al., *Generation and characterization of Csrp1 enhancer-driven tissue-restricted Cre-recombinase mice.* Genesis, 2008. **46**(3): p. 167-76.
91. Snider, P., et al., *Origin of cardiac fibroblasts and the role of periostin.* Circ Res, 2009. **105**(10): p. 934-47.
92. Koni, P.A., et al., *Conditional vascular cell adhesion molecule 1 deletion in mice: impaired lymphocyte migration to bone marrow.* J Exp Med, 2001. **193**(6): p. 741-54.
93. Lindsley, A., et al., *Identification and characterization of a novel Schwann and outflow tract endocardial cushion lineage-restricted periostin enhancer.* Dev Biol, 2007. **307**(2): p. 340-55.
94. Britsch, S., et al., *The transcription factor Sox10 is a key regulator of peripheral glial development.* Genes Dev, 2001. **15**(1): p. 66-78.
95. Degenhardt, K.R., et al., *Distinct enhancers at the Pax3 locus can function redundantly to regulate neural tube and neural crest expressions.* Dev Biol, 2010. **339**(2): p. 519-27.
96. Boneva, R.S., et al., *Mortality associated with congenital heart defects in the United States: trends and racial disparities, 1979-1997.* Circulation, 2001. **103**(19): p. 2376-81.
97. Olaopa, M., R.L. Caldwell, and R.M. Barnes, *Riley Heart Center Symposium on cardiac development 2009: transcriptional unification of heart morphogenesis.* Pediatr Cardiol, 2010. **31**(3): p. 315-7.
98. van den Hoff, M.J. and A.F. Moorman, *Cardiac neural crest: the holy grail of cardiac abnormalities?* Cardiovasc Res, 2000. **47**(2): p. 212-6.
99. Bossuyt, P.M., et al., *The STARD statement for reporting studies of diagnostic accuracy: explanation and elaboration.* Clin Chem, 2003. **49**(1): p. 7-18.
100. Abu-Issa, R., K. Waldo, and M.L. Kirby, *Heart fields: one, two or more?* Dev Biol, 2004. **272**(2): p. 281-5.
101. Seidman, J.G. and C. Seidman, *The genetic basis for cardiomyopathy: from mutation identification to mechanistic paradigms.* Cell, 2001. **104**(4): p. 557-67.

102. Olson, E.N., *Gene regulatory networks in the evolution and development of the heart.* Science, 2006. **313**(5795): p. 1922-7.
103. Portbury, A.L., et al., *Catecholamines act via a beta-adrenergic receptor to maintain fetal heart rate and survival.* Am J Physiol Heart Circ Physiol, 2003. **284**(6): p. H2069-77.
104. Wildner, H., et al., *Insm1 (IA-1) is a crucial component of the transcriptional network that controls differentiation of the sympatho-adrenal lineage.* Development, 2008. **135**(3): p. 473-81.
105. Barnes, R.M., et al., *Analysis of the Hand1 cell lineage reveals novel contributions to cardiovascular, neural crest, extra-embryonic, and lateral mesoderm derivatives.* Dev Dyn, 2010.
106. Firulli, B.A., et al., *Analysis of a Hand1 hypomorphic allele reveals a critical threshold for embryonic viability.* Dev Dyn, 2010.
107. Ream, M.A., et al., *High oxygen prevents fetal lethality due to lack of catecholamines.* Am J Physiol Regul Integr Comp Physiol, 2008. **295**(3): p. R942-53.
108. White, R.B. and M.R. Ziman, *Genome-wide discovery of Pax7 target genes during development.* Physiol Genomics, 2008. **33**(1): p. 41-9.
109. Schafer, B.W., et al., *Molecular cloning and characterization of a human PAX-7 cDNA expressed in normal and neoplastic myocytes.* Nucleic Acids Res, 1994. **22**(22): p. 4574-82.
110. Borycki, A.G., et al., *Pax3 functions in cell survival and in pax7 regulation.* Development, 1999. **126**(8): p. 1665-74.
111. Relaix, F., et al., *Divergent functions of murine Pax3 and Pax7 in limb muscle development.* Genes Dev, 2004. **18**(9): p. 1088-105.
112. Srivastava, D. and E.N. Olson, *A genetic blueprint for cardiac development.* Nature, 2000. **407**(6801): p. 221-6.

Curriculum Vitae

Michael A. Olaopa

Education

Indiana University – Purdue University at Indianapolis (IUPUI), Indianapolis, IN — 2005 - 2011
Doctor of Philosophy (PhD): Medical & Molecular Genetics
Minor: Life Sciences

Summary: Described molecular mechanism of two (2) therapeutic compounds, which have the potential to be developed into robust patient therapies for congenital heart failure; collaborated extensively with multi-disciplinary teams to achieve project milestones; published four (4) peer-reviewed publications and submitted one (1) manuscript for review; trained five (5) students and interns to advance project goals.

Indiana University (IU) – Kelley School of Business, Bloomington, IN — 2008 - 2009
Associate Certificate: Business of Life Sciences

Summary: Collaborated extensively with multi-disciplinary teams to successfully build a development and marketing model for a novel compound; resulted in two (2) distinct awards for best team projects.

Berea College (BC), Berea, KY — 2001 - 2005
Bachelor of Arts (BA): Biology

Awards and Honors

- Selected Platform presentation, Midwest Developmental Biology Meeting, Cincinnati — 2010
- Travel Award, Midwest Society for Developmental Biology — 2010
- Principal Investigator, Pre-doctoral Fellowship, American Heart Association — 2009 - 2010
- First Place, Graduate Student Poster presentation, IUPUI Research Day, Indianapolis, IN — 2009
- First Place (2x), Team Project and presentation, Center for the Business of Life Sciences, Kelley School of Business, Indiana University, Bloomington, IN — 2008, 2009
- Selected Platform presentation, Weinstein Cardiovascular International Conference, Houston, TX — 2008

Professional Associations

Member, Midwest Society for Developmental Biology — 2010 - present
Member, American Association of Anatomists — 2008 - 2009

Research Experience

Graduate Research Experience:

Researcher, Laboratory of Dr. Simon J. Conway (PhD), IUPUI 2006 - 2011

Project Title #1: Role of beta-adrenergic signaling in congenital heart failure and *in utero* lethality

Summary: Described molecular mechanism of two (2) compounds targeted at congenital heart failure.

Accomplishment: Potential for the development of new intervention therapies for newborns with congenital heart defects; one (1) pre-doctoral fellowship award to fund ongoing research; two (2) ongoing manuscripts; two (2) invitations to internationally-renowned conferences to present my findings.

Project Title #2: Neural Crest lineage mapping in Pax3-deficient mouse models

Summary: Characterized migration of neural crest cells into the embryonic heart in a novel genetic model.

Accomplishment: One (1) publication in peer-reviewed journal; one (1) submitted manuscript.

Project Title #3: Ectopic interaction of Pax3 and Pax7 in breast cancer cells

Summary: Identified a novel target of Pax7 via luciferase assays in “168” and “67NR” breast cancer cell lines.

Accomplishment: Resulted in identification of a cooperative role of ectopic Pax3 and Pax7 in cancer cells.

Graduate Research Rotations:

Researcher, Laboratory of Dr. Elliot D. Rosen (PhD), IUPUI 2005 - 2006

Project Title: Role of factor VII in blood clot formation

Summary: Analysis of a laser-induced vessel injury model, via tail vein injections of Rose Bengal, in factor VII-deficient mice.

Accomplishment: Assisted in developing an injury model to be used for future clot formation studies in affected blood vessels.

Researcher, Laboratory of Dr. Simon J. Conway (PhD), IUPUI 2005 - 2006

Project Title: RNA isolation from mouse embryonic cardiac tissue via laser capture microdissection

Summary: Modified and improved technique for isolating RNA from embryonic heart tissue.

Accomplishment: Resulted in design of one (1) RNA molecular probe; one (1) publication in peer-reviewed journal.

Undergraduate Research Internships:

Research Intern, Laboratory of Dr. Aruni Bhatnagar (PhD), 2003
Cardiovascular Research Center, University of Louisville, KY

Project title: Nitric Oxide-mediated glutathiolation in Cos-7 cells

Summary: Identified the role of nitric oxide and its effectiveness on glutathiolation in mammalian cells.

Accomplishment: Described novel mechanism by which nitric oxide can reduce oxidative stress in humans.

Undergraduate Research Internships (continued):
Research Intern, Laboratory of Dr. Lee Roecker (PhD), BC, KY 2002
Project title: Coordination of varying length hydrocarbons to Co (III) complexes by substitution of amine ligands
Summary: Developed a novel method of synthesizing organic compounds for studying membrane interaction.
Accomplishment: Generated preliminary data used in follow-up membrane interaction studies; Resulted in award-winning presentation at University of Kentucky undergraduate poster competition (2002).

Research Grant Support

AHA-Midwest 0910019G Grant Period: 01/01/09 - 12/31/10
Effects of Pax3 mutation and neural crest genetic ablation on heart development
This pre-doctoral fellowship grant seeks to dissect the contribution of cardiac neural crest and myocardial defects to *in utero* lethality observed in *Pax3* mutants. Role on grant: Principal Investigator. [$52,000 total costs]

Peer Reviewed Publications

- **Olaopa M**, Zhou HM, Snider P, Wang J, Moon A, Conway SJ. "Pax3 is required for cardiac neural crest specification but is redundant during migration and outflow tract septation". *Dev. Biol.* (2010) (*Submitted*).
- **Olaopa M** and Conway SJ. "Dual but converging roles: a tale of two crests". The Neural Crest - Breakthroughs and Applications. (Edited by Sieber-Blum, M.), World Scientific Publishing/Imperial College Press. Review (2010) (*In press*).
- **Olaopa M**, Caldwell RL and Barnes R. Riley Heart Center Symposium on cardiac development 2009: transcriptional unification of heart morphogenesis. *Pediatr. Cardiol.* (2010) 3:315-317.
- Snider P, **Olaopa M**, Firulli AB, Conway SJ. "Cardiovascular development and the colonizing cardiac neural crest lineage". *Scientific World Journal* (2007) 2:88-111.
- Lindsley A, Snider P, Zhou H, Rogers R, Wang J, **Olaopa M**, Kruzynska-Frejtag A, Koushik SV, Lilly B, Burch JB, Firulli AB, Conway SJ. "Identification and characterization of a novel Schwann and outflow tract endocardial cushion lineage-restricted *periostin* enhancer". *Dev. Biol.* (2007) 307**:**340-355.

In preparation:

- **Olaopa M**, Chikaraishi DM, Zhou HM, Snider P, Wang J, Payne RM, Conway SJ. "The role of the beta-adrenergic pathway in a novel neural crest deficiency model of congenital heart failure". (2011) (*In preparation*).

Notable Presentations

- "Delineating the role of the beta-adrenergic pathway in maintaining embryonic cardiac output and *in utero* survival". Dissertation Seminar (IUPUI, Indianapolis, IN, November 2010).

Notable Presentations (continued)

- "Rescuing a broken heart: A tale of survival". Medical & Molecular Genetics departmental seminar series (IUPUI, Indianapolis, IN, June 2010).
- "Effects of Pax3 mutation and neural crest genetic ablation on congenital heart function and embryonic lethality". *Genetics Society of America Conferences: Model Organisms to Human Biology* (Boston, MA, June 2010).
- "Effects of Pax3 mutation and neural crest genetic ablation on congenital heart function and embryonic lethality". *Midwest Society for Developmental Biology Conference* (Cincinnati, OH, May 2010).
- "Effects of Pax3 mutation and neural crest genetic ablation upon heart morphogenesis". *Weinstein International Cardiovascular Conference* (San Francisco, CA, May 2009).
- "Effects of Pax3 mutation and neural crest genetic ablation upon heart morphogenesis". *Research Day* (IUPUI, Indianapolis, IN, March 2009).
- "Temporal requirement of Pax3 in the neural crest cell lineage". *Weinstein International Cardiovascular conference* (Houston, TX, May 2008).
- "Transgenic lineage mapping and genetic ablation of the neural crest cell lineages". *Weinstein International Cardiovascular Conference* (Indianapolis, IN, May 2007).

Training and Mentoring Experience

Student trainees (IUPUI):

- Carla Mangum, Graduate Student, Cellular & Integrative Physiology, IUPUI — 2010
- Nathan VanDusen, Graduate Student, Medical & Molecular Genetics, IUPUI — 2010
- Olga Simmons, Graduate Student, Medical & Molecular Genetics, IUPUI — 2010
- Rachel Young, Visiting Undergraduate Student, University of Ulster, Ireland — 2009 - 2010
- Hyojin Kim, Graduate Student, Biochemistry & Molecular Biology, IUPUI — 2008

Graduate Student Ambassador / Mentor (IUPUI):

- Christopher Contreras, Graduate Student, Biochemistry & Molecular Biology, IUPUI — 2009
- Steven Messina-Graham, Graduate Student, Neuroscience, IUPUI — 2009
- Nicole Ashpole, Graduate Student, Neuroscience, IUPUI — 2007

Undergraduate Teaching and Laboratory Assistant (BC): 2004 - 2005
Department of Chemistry

- Trained one hundred and twenty (120) undergraduate students to become proficient in laboratory safety and protocols.

Training and Mentoring Experience (continued)

Computer Consultant / Trainer (BC): 2002 - 2004

Department of Information Systems & Services

- Led computer orientation and training sessions for campus community; Involved in the initiation and design of "Empowering a Dynamic Generation through Education" (EDGE) program aimed at distribution and technical support of laptops to every student and faculty on campus.

Personal

Volunteer and Service Experience:

- Student Associate, Center for the Business of Life Sciences, IU, Indianapolis, IN 2008 - present
- Volunteer/Fundraiser, American Heart Association 2008 - present
- Vice-President, African Students' Association, BC, Berea, KY 2003 - 2004
- Volunteer, Berea Buddies (Young Adolescent Mentor Program), BC, Berea, KY 2002 - 2004
- Volunteer, Habitat for Humanity, Madison County, KY 2002 - 2004
- Volunteer, Boys & Girls Club, Madison County, KY 2002

Extracurricular:

- *7th Gup* Ranking Member, "Choo Mok Kwan Tang Soo Do" School of Martial Arts, Indianapolis, IN 2009 - present
- Captain, Intramural Soccer Team, IUPUI, Indianapolis, IN 2006 - 2008
- Intercollegiate Soccer, BC, Berea, KY 2002 - 2005